



Pacific Northwest
NATIONAL LABORATORY

Proudly Operated by Battelle Since 1965

Material Property Correlations:

Comparisons between FRAPCON-4.0, FRAPTRAN-2.0, and MATPRO

September 2015

WG Luscher
KJ Geelhood
IE Porter

DISCLAIMER

This report was prepared as an account of work sponsored by an agency of the United States Government. Neither the United States Government nor any agency thereof, nor Battelle Memorial Institute, nor any of their employees, makes **any warranty, express or implied, or assumes any legal liability or responsibility for the accuracy, completeness, or usefulness of any information, apparatus, product, or process disclosed, or represents that its use would not infringe privately owned rights.** Reference herein to any specific commercial product, process, or service by trade name, trademark, manufacturer, or otherwise does not necessarily constitute or imply its endorsement, recommendation, or favoring by the United States Government or any agency thereof, or Battelle Memorial Institute. The views and opinions of authors expressed herein do not necessarily state or reflect those of the United States Government or any agency thereof.

PACIFIC NORTHWEST NATIONAL LABORATORY
operated by
BATTELLE
for the
UNITED STATES DEPARTMENT OF ENERGY
under Contract DE-AC05-76RL01830

Printed in the United States of America

Available to DOE and DOE contractors from the
Office of Scientific and Technical Information,
P.O. Box 62, Oak Ridge, TN 37831-0062;
ph: (865) 576-8401
fax: (865) 576-5728
email: reports@adonis.osti.gov

Available to the public from the National Technical Information Service
5301 Shawnee Rd., Alexandria, VA 22312
ph: (800) 553-NTIS (6847)
email: orders@ntis.gov <<http://www.ntis.gov/about/form.aspx>>
Online ordering: <http://www.ntis.gov>



This document was printed on recycled paper.

(8/2010)

Material Property Correlations:

Comparisons between FRAPCON-4.0, FRAPTRAN-2.0, and MATPRO

WG Lusher
KJ Geelhood
IE Porter

September 2015

Prepared for
Division of System Analysis
Office of Nuclear Regulatory Research
U.S. Nuclear Regulatory Commission
Washington DC 20555-0001
NRC Job Code V6917

Pacific Northwest National Laboratory
Richland, Washington 99352

Abstract

The U.S. Nuclear Regulatory Commission uses the computer codes FRAPCON and FRAPTRAN to model steady-state and transient fuel behavior, respectively, to support regulatory analyses. In this document, material property correlations for oxide fuels and cladding materials are presented and discussed. Comparisons are made between the material property correlations used in the most recent versions of the codes, FRAPCON-4.0 and FRAPTRAN-2.0. Comparisons are also made with MATPRO, which is a compilation of material property correlations with an extensive history of use with various fuel performance and severe accident codes. In addition to model-to-model comparisons, model-to-data comparisons and source codes for the FRAPCON-4.0 and FRAPTRAN-2.0 correlations are provided.

Foreword

The U.S. Nuclear Regulatory Commission uses the computer codes FRAPCON and FRAPTRAN to model steady-state and transient fuel behavior, respectively, to support regulatory analyses. To effectively model fuel behavior, material property correlations must be used for a wide range of operating conditions (e.g., temperature and burnup). In this sense, a “material property” is a physical characteristic of the material whose quantitative value is necessary in the analysis process.

The consolidated resource for “material properties” cited most often in the literature is MATPRO (as documented in Volume 4 of NUREG/CR-6150). MATPRO is a compilation of fuel and cladding material property correlations with an extensive history of use with fuel performance and severe accident codes. However, consistency among the material property correlations in FRAPCON-3, FRAPTRAN, and MATPRO has never been complete, as the material property correlations in the fuel performance codes have evolved to accommodate recent fuel design changes.

The primary purpose of this report is to consolidate the current material property correlations used in FRAPCON and FRAPTRAN into a single document. In addition to describing the material property correlations used in the subroutines of latest versions of the codes, FRAPCON-4.0 and FRAPTRAN-2.0, this report also provides a variety of comparisons to the material property correlations used in MATPRO.

Executive Summary

The U.S. Nuclear Regulatory Commission uses the computer codes FRAPCON and FRAPTRAN to model steady-state and transient fuel behavior, respectively, to support regulatory analyses. In this document, material property correlations for oxide fuels and cladding materials are presented and discussed. Comparisons are made between the material property correlations used in the most recent versions of the codes, FRAPCON-4.0 and FRAPTRAN-2.0.5. Comparisons are also made with MATPRO, which is a compilation of material property correlations with an extensive history of use with various fuel performance and severe accident codes. In addition to model-to-model comparisons, model-to-data comparisons and source codes for the FRAPCON-4.0 and FRAPTRAN-2.0 correlations are also provided.

This is one of three documents that describe the FRAPCON-4.0 and FRAPTRAN-2.0 fuel performance codes. The FRAPCON-4.0 code structure and behavioral models are described in the FRAPCON-4.0 code description document (Geelhood et al. 2015a). The FRAPTRAN-1.5 code structure and behavioral models are described in the FRAPTRAN-2.0 code description document (Geelhood et al. 2015b). Additional descriptions of mechanical models and model-to-data comparisons for mechanical property correlations are provided in the mechanical properties report (Geelhood et al. 2008).

Acronyms and Abbreviations

°C	degrees Celsius
°F	degrees Fahrenheit
µm	micrometer(s)
ANS	American Nuclear Society
Ar	argon
BWR	boiling-water reactor
CAGROW	Cladding Axial Growth
CCP	Cladding Specific Heat
CELMOD	Cladding Elastic Modulus
cm ²	square centimeter(s)
CMHARD	Cladding Meyer Hardness
CREPR	creep rate
crud	Chalk River Unidentified Deposit (generic term for various residues deposited on fuel rod surfaces, originally coined by Atomic Energy of Canada, Ltd. to describe deposits observed on fuel from the test reactor at Chalk River)
CSHEAR	Shear Modulus
CTHCON	Cladding Thermal Conductivity
CTHEXP	Cladding Thermal Expansion
FCP	Fuel Specific Heat Capacity
FCREEP	creep induced elongation
FEMISS	Fuel Emissivity
FENTHL	Fuel Enthalpy
FRAP	FRAPTRAN (Fuel Rod Analysis Program Transient)
FRAPCON	Fuel Rod Analysis Program, FRAPCON is a Fortran 90 computer code that calculates the steady-state response of light-water reactor fuel rods during long-term burnup.
FSWELL	fuel swelling
FTHCON	Fuel Thermal Conductivity
FTHEXP	Fuel Thermal Expansion
FUDENS	Fuel Densification
Gd ₂ O ₃	gadolinia
GPa	gigapascal(s)
GTHCON	Gas Thermal Conductivity
GWd/MTU	gigawatt-days per metric ton of uranium
H	hydrogen
He	helium
J	joule(s)

K	kelvin
kg	kilogram(s)
Kr	krypton
LWR	light-water reactor
m	meter(s)
m ²	square meter(s)
m ³	cubic meter(s)
MeV	megaelectron volt(s)
MH	Meyer hardness
mm	millimeter(s)
MOX	mixed oxide, (U, Pu)O ₂
MPa	megapascal(s)
MWd/kgU	megawatt-days per kilogram of uranium
MWd/MTU	megawatt-days per metric ton of uranium
MWs/kgU	megawatt-seconds per kilogram of uranium
n	neutron(s)
N	nitrogen
Nb	niobium
NFI	Nuclear Fuels Industries
NRC	U.S. Nuclear Regulatory Commission
O/M	oxygen-to-metal
Pa	pascal(s)
PNNL	Pacific Northwest National Laboratory
Pu	plutonium
PuO ₂	plutonium dioxide
PWR	pressurized-water reactor
RSNTR	resintered fuel density change
RXA	recrystallized annealed
s	second(s)
SRA	stress relief annealed
TD	theoretical density
tHM	tonne(s) of heavy metal
TSINT	sintering temperature
UO ₂	uranium dioxide
UO ₂ -Gd ₂ O ₃	urania-gadolinia
W	watt(s)
wt%	percent by weight
Xe	xenon

ZOTCON

ZrNb-1

ZrO₂

Cladding Oxide Thermal Conductivity

Russian zirconium alloy with 1 wt% of niobium

zirconium dioxide

Contents

Abstract	iii
Foreword	v
Executive Summary	vii
Acronyms and Abbreviations	ix
1.0 Introduction	1.1
1.1 Relation to Other Reports.....	1.2
2.0 Oxide Fuel Properties	2.1
2.1 Fuel Melting Temperature (PHYPRP).....	2.1
2.1.1 Model Development and Comparisons	2.1
2.1.2 Applicability and Uncertainty	2.3
2.2 Fuel Specific Heat Capacity (FCP) and Fuel Enthalpy (FENTHL).....	2.3
2.2.1 Model Development and Comparisons	2.4
2.2.2 Applicability and Uncertainty	2.7
2.3 Fuel Thermal Conductivity (FTHCON).....	2.7
2.3.1 Model Development and Comparisons	2.7
2.3.2 Applicability and Uncertainty	2.19
2.4 Fuel Emissivity (FEMISS).....	2.20
2.4.1 Model Development and Comparisons	2.20
2.4.2 Applicability and Uncertainty	2.21
2.5 Fuel Thermal Expansion (FTHEXP).....	2.21
2.5.1 Model Development and Comparisons	2.22
2.5.2 Applicability and Uncertainty	2.24
2.6 Fuel Densification (FUDENS).....	2.24
2.6.1 Model Development and Comparisons	2.25
2.6.2 Applicability and Uncertainty	2.28
2.7 Fuel Swelling (FSWELL)	2.28
2.7.1 Model Development and Comparisons	2.28
2.7.2 Applicability and Uncertainty	2.31
3.0 Cladding Material Properties.....	3.1
3.1 Cladding Specific Heat (CCP)	3.1
3.1.1 Model Development and Comparisons	3.1
3.1.2 Applicability and Uncertainty	3.3
3.2 Cladding Thermal Conductivity (CTHCON).....	3.4
3.2.1 Model Development and Comparisons	3.4
3.2.2 Applicability and Uncertainty	3.6
3.3 Cladding Oxide Thermal Conductivity (ZOTCON)	3.6

3.3.1	Model Development and Comparisons	3.7
3.3.2	Applicability and Uncertainty	3.10
3.4	Cladding Surface Emissivity (ZOEMIS)	3.10
3.4.1	Model Development and Comparisons	3.10
3.4.2	Applicability and Uncertainty	3.13
3.5	Cladding Thermal Expansion (CTHEXP).....	3.13
3.5.1	Model Development and Comparisons	3.13
3.5.2	Applicability and Uncertainty	3.17
3.6	Cladding Elastic Modulus (CELMOD) and Shear Modulus (CSHEAR)	3.17
3.6.1	Model Development and Comparisons	3.17
3.6.2	Applicability and Uncertainty	3.23
3.7	Cladding Axial Growth (CAGROW).....	3.23
3.7.1	Model Development and Comparisons	3.23
3.7.2	Applicability and Uncertainty	3.27
3.8	Creep Rate (CREPR).....	3.27
3.8.1	Model Development and Comparisons	3.27
3.8.2	Applicability and Uncertainty	3.31
3.9	Cladding Meyer Hardness (CMHARD).....	3.31
3.9.1	Model Development and Comparisons	3.31
3.9.2	Applicability and Uncertainty	3.32
4.0	Gas Material Properties	4.1
4.1	Gas Conductivity (GTHCON)	4.1
4.1.1	Model Development and Comparisons	4.1
4.1.2	Applicability and Uncertainty	4.7
4.2	Gas Molecular Weight (GASMWT).....	4.7
4.3	Gas Density (GASRHO).....	4.8
4.4	Gas Viscosity (GVISCO).....	4.8
4.5	Gas Specific Heat (GASCP)	4.10
5.0	References	5.1
	Appendix A Subroutine Source Codes	A.1

Figures

Figure 2.1. A Comparison Between Solidus Temperatures Calculated by MATPRO Using the FHYPRP Subroutine and FRAPCON/FRAPTRAN (FRAP) Using the PHYPRP Subroutine	2.2
Figure 2.2. A Comparison Between Liquidus Temperatures Calculated by MATPRO Using the FHYPRP Subroutine and FRAPCON/FRAPTRAN (FRAP) Using the PHYPRP Subroutine	2.3
Figure 2.3. Specific Heat Capacity of UO_2 from Three Experimenters Compared with the FRAPCON/FRAPTRAN/MATPRO (FRAP) Correlation (solid line) for UO_2	2.6
Figure 2.4. Specific Heat Capacity of $(U_{0.8}Pu_{0.2})O_2$ from Three Experimenters Compared with the FRAPCON/FRAPTRAN/MATPRO (FRAP) Correlations (solid line) for MOX.....	2.6
Figure 2.5. MATPRO and Modified NFI Thermal Conductivity Models for UO_2 as a Function of Temperature	2.13
Figure 2.6. MATPRO Model-to-Data Comparison for Thermal Conductivity of Unirradiated UO_2	2.14
Figure 2.7. Modified NFI Model-to-Data Comparison for Thermal Conductivity of Unirradiated UO_2	2.14
Figure 2.8. MATPRO Model-to-Data Comparison for Thermal Conductivity of Irradiated UO_2	2.15
Figure 2.9. Modified NFI Model-to-Data Comparison for Thermal Conductivity of Irradiated UO_2	2.16
Figure 2.10. MATPRO and Duriez/Modified NFI Conductivity Models as a Function of Temperature for MOX Fuel with 7 wt% Plutonium Content	2.17
Figure 2.11. MATPRO Model-to-Data Comparison for Thermal Conductivity of Unirradiated MOX Modeled with 7 wt% of Plutonium.....	2.18
Figure 2.12. Duriez/Modified NFI Model-to-Data Comparison for Thermal Conductivity of Unirradiated MOX Modeled with 7 wt% of Plutonium	2.18
Figure 2.13. Data to Model Comparison for FEMISS	2.21
Figure 2.14. Model-to-Data Comparison for UO_2 Correlation Used in MATPRO and FRAPCON/FRAPTRAN with Updated Constants.....	2.23
Figure 2.15. Model-to-Data Comparison for PuO_2 Correlation Used in MATPRO and FRAPCON/FRAPTRAN	2.24
Figure 2.16. Comparison of Densification Predictions Generated by the FUDENS Model and Experimental Densification Measurements Determined in Reactor	2.27
Figure 2.17. Data Comparison between MATPRO and FRAPCON Versions of FSWELL	2.30
Figure 2.18. Comparison between Swelling Rates Determined for Various Instrumented Fuel Assemblies Rests at Halden and Swelling Rates Predicted by FRAPCON.....	2.31
Figure 3.1. CTHCON Model and Data Used for Development.....	3.5
Figure 3.2. CTHCON Model and Data Collected Since Development	3.6
Figure 3.3. Oxide Thermal Conductivity Measurements as a Function of Temperature Compared with the MATPRO and FRAPCON-4.0/FRAPTRAN-2.0 (FRAP) Cladding Oxide Thermal Conductivity Models.....	3.9
Figure 3.4. Model-to-Data Comparison for Cladding Oxide Emissivity	3.12
Figure 3.5. Model-to-Data Comparison for FRAPCON-4.0/FRAPTRAN-2.0 (FRAP) and MATPRO Axial Thermal Expansion.....	3.16

Figure 3.6. Model-to-Data Comparison for FRAPCON-4.0/FRAPTRAN-2.0 (FRAP) and MATPRO Diametral Thermal Expansion.....	3.16
Figure 3.7. Predicted vs. Measured Values for Young’s Modulus for Various Data Sets.....	3.22
Figure 3.8. Model-to-Data Comparison for SRA Zircaloy-4 (PWR)	3.25
Figure 3.9. Model-to-Data Comparison for RXA Zircaloy-2 (BWR)	3.25
Figure 3.10. Model-to-Data Comparison for M5.....	3.26
Figure 3.11. Model-to-Data Comparison for ZIRLO.....	3.26
Figure 3.12. Predicted vs. Measured Hoop Strain for SRA Zircaloy Model.....	3.30
Figure 3.13. Predicted vs. Measured Hoop Strain for RXA Zircaloy Model	3.30
Figure 3.14. CMHARD Correlation as a Function of Temperature with Data from Peggs and Godin	3.32
Figure 4.1. Model-to-Data Comparison for He Thermal Conductivity	4.3
Figure 4.2. Model-to-Data Comparison for Ar Thermal Conductivity.....	4.4
Figure 4.3. Model-to-Data Comparison for Kr Thermal Conductivity.....	4.4
Figure 4.4. Model-to-Data Comparison for Xe Thermal Conductivity	4.5
Figure 4.5. Model-to-Data Comparison for H ₂ Thermal Conductivity.....	4.5
Figure 4.6. Model-to-Data Comparison for N ₂ Thermal Conductivity.....	4.6
Figure 4.7. Model-to-Data Comparison for Steam Thermal Conductivity	4.6
Figure 4.8. Fitting parameter (Ω) for calculating gas viscosity.....	4.9

Tables

Table 1.1. Roadmap to Documentation of Models and Properties in NRC Fuel Performance Codes, FRAPCON-4.0 and FRAPTRAN-2.0.....	1.2
Table 2.1. Constants Used in UO_2 , Gd_2O_3 , and PuO_2 Heat Capacity and Enthalpy Correlations	2.4
Table 2.2. Parameters Used in UO_2 and PuO_2 Solid-Phase Thermal Expansion Correlations	2.22
Table 3.1. Example Heat Treatments and Coldworked Conditions for Different Alloys	3.1
Table 3.2. Specific Heat Capacity Database for Zircaloy-2, Zircaloy-4, ZIRLO, Optimized ZIRLO, and M5	3.2
Table 3.3. Specific Heat Capacity Database for ZrNb-1 Alloys.....	3.3
Table 3.4. Parameters for FRAPCON-4.0 Creep Equation for SRA and RXA Cladding	3.28
Table 4.1. Constants Used in Gas Thermal Conductivity Correlations in MATPRO	4.1
Table 4.2. Constants Used in Gas Thermal Conductivity Correlations in FRAP	4.2
Table 4.3. Standard Deviation of Gas Thermal Conductivity Correlations	4.7
Table 4.4. Molecular Weight of Gas Species.....	4.7
Table 4.5. Ideal Gas Constant of Gas Species	4.8
Table 4.6. Viscosity Fits of Gas Species.....	4.9
Table 4.7. Fitting Parameters for Specific Heat of Gas Species	4.11
Table 4.8. Fitting Parameters for Specific Heat of steam	4.11

1.0 Introduction

The U.S. Nuclear Regulatory Commission (NRC) uses the computer codes FRAPCON and FRAPTRAN to model steady-state and transient fuel behavior, respectively, to support regulatory analyses. To effectively model fuel behavior, material property correlations must be used for a wide range of operating conditions (e.g., temperature and burnup). In this sense, a “material property” is a physical characteristic of the material whose quantitative value is necessary in the analysis process. Further, the property may be used to compare the benefits of one material with those of another. Generally speaking, the material properties of interest in regulatory analysis of nuclear fuel behavior are mechanical or thermodynamic.

The issue of what is and is not a “material property” will never be universally resolved. In this report, properties such as thermal conductivity are included. Other characteristics of the material (e.g., fission gas release) are considered “models” rather than properties and are discussed elsewhere. The material property correlations for the FRAPCON and FRAPTRAN computer codes were partially documented in NUREG/CR-6534 and NUREG/CR-6739, respectively (Lanning et al. 2005; Cunningham et al. 2001) as well as in NUREG/CR-6150 (Siefken et al. 2001). Some of these have been modified or updated since the original code documentation was published.

The primary purpose of this report is to consolidate the current material property correlations used in FRAPCON and FRAPTRAN into one document. Material property correlations for oxide fuels, including uranium dioxide (UO₂) and mixed oxide (MOX) fuels, are described in Section 2. Throughout this document, the term MOX is used to describe fuels that are blends of uranium and plutonium oxides, (U, Pu)O₂. The properties for UO₂ with other additives (e.g., gadolinia) are also discussed. Material property correlations for cladding materials and gases are described in Sections 3 and 4, respectively.

In addition to describing the material property correlations used in the subroutines of FRAPCON and FRAPTRAN, this report provides a variety of comparisons between material property correlations and data. Although they are frequently identical, comparisons are made between the material property correlations used in the FRAPCON and FRAPTRAN codes. Comparisons are also made between the material property correlations used in MATPRO, a compilation of fuel and cladding material property correlations with an extensive history of use with various fuel performance and severe accident codes. For several reasons, consistency among the material property correlations in FRAPCON, FRAPTRAN, and MATPRO has never been complete. However, the current versions of FRAPCON and FRAPTRAN use a relatively consistent set of correlations for the properties that are used by both codes. The material property correlations in the most recent version of MATPRO are documented in Volume 4 of NUREG/CR-6150 (Siefken et al. 2001). In addition to comparison of the various correlations, correlation-to-data comparisons are made with FRAPCON, FRAPTRAN, and MATPRO properties.

All comparisons in this report are based on the material property correlations used in the most recent version of the FRAPCON and FRAPTRAN codes, FRAPCON-4.0 and FRAPTRAN-2.0. The source code for each material property correlation discussed is provided for FRAPCON-4.0 and FRAPTRAN-2.0 (see Appendix A) as well as a range of applicability and an estimate of uncertainty, where possible.

1.1 Relation to Other Reports

The full documentation of the steady-state and transient fuel performance codes is described in three documents. The basic fuel, cladding, and gas material properties used in FRAPCON-4.0 and FRAPTRAN-2.0 are described in the material properties handbook (this report). The FRAPCON-4.0 code structure and behavioral models are described in the FRAPCON-4.0 code description document (Geelhood et al. 2015b). The FRAPTRAN-2.0 code structure and behavioral models are described in the FRAPTRAN-2.0 code description document (Geelhood et al. 2015b). Additional descriptions of mechanical models and model-to-data comparisons for mechanical property correlations are provided in the mechanical properties report (Geelhood et al. 2008).

Table 1.1 shows where each specific material property and model used in the NRC fuel performance codes are documented.

Table 1.1. Roadmap to Documentation of Models and Properties in NRC Fuel Performance Codes, FRAPCON-4.0 and FRAPTRAN-2.0

Model/Property	FRAPCON-4.0	FRAPTRAN-2.0
Fuel thermal conductivity	Material properties handbook	Material properties handbook
Fuel thermal expansion	Material properties handbook	Material properties handbook
Fuel melting temperature	Material properties handbook	Material properties handbook
Fuel specific heat	Material properties handbook	Material properties handbook
Fuel enthalpy	Material properties handbook	Material properties handbook
Fuel emissivity	Material properties handbook	Material properties handbook
Fuel densification	Material properties handbook	NA
Fuel swelling – solid	Material properties handbook	NA
Fuel swelling – gaseous	Material properties handbook	NA
Fission gas release	FRAPCON code description	FRAPTRAN code description
Fuel relocation	FRAPCON code description	FRAPTRAN code description
Fuel grain growth	FRAPCON code description	NA
High burnup rim model	FRAPCON code description	NA
Nitrogen release	FRAPCON code description	NA
Helium release	FRAPCON code description	NA
Radial power profile	FRAPCON code description	NA (input parameter)
Stored energy	FRAPCON code description	FRAPTRAN code description
Decay heat model	NA	FRAPTRAN code description
Fuel and cladding temperature solution	FRAPCON code description	FRAPTRAN code description
Cladding thermal conductivity	Material properties handbook	Material properties handbook
Cladding thermal expansion	Material properties handbook	Material properties handbook
Cladding elastic modulus	Material properties handbook	Material properties handbook
Cladding creep model	Material properties handbook	NA
Cladding specific heat	Material properties handbook	Material properties handbook

Table 1.1. Continued

Model/Property	FRAPCON-4.0	FRAPTRAN-2.0
Cladding emissivity	Material properties handbook	Material properties handbook
Cladding axial growth	Material properties handbook	NA
Cladding Meyer hardness	Material properties handbook	Material properties handbook
Cladding annealing	FRAPCON code description	FRAPTRAN code description
Cladding yield stress, ultimate stress, and plastic deformation	FRAPCON code description	FRAPTRAN code description
Cladding failure criteria	NA	FRAPTRAN code description
Cladding waterside corrosion	FRAPCON code description	NA (input parameter)
Cladding hydrogen pickup	FRAPCON code description	NA (input parameter)
Cladding high temperature oxidation	NA	FRAPTRAN code description
Cladding ballooning model	NA	FRAPTRAN code description
Cladding mechanical deformation	FRAPCON code description	FRAPTRAN code description
Oxide thermal conductivity	Material properties handbook	Material properties handbook
Crud thermal conductivity	FRAPCON code description	NA
Gas conductivity	Material properties handbook	Material properties handbook
Gap conductance	FRAPCON code description	FRAPTRAN code description
Plenum gas temperature	FRAPCON code description	FRAPTRAN code description
Rod internal pressure	FRAPCON code description	FRAPTRAN code description
Coolant temperature and heat transfer coefficients	FRAPCON code description	FRAPTRAN code description
Optional models and properties not developed at PNNL		
Water-cooled, water-moderated energy reactor fuel and cladding models	NA	NUREG/IA-0164 (Shestopalov et al. 1999)
Cladding finite element analysis model	VTT-R-11337-06 (Knuutila 2006)	VTT-R-11337-06 (Knuutila 2006)
NA	=	not applicable

2.0 Oxide Fuel Properties

Material property correlations for UO₂ and MOX fuel pellets are described in the following subsections. These correlations include the melting temperature, specific heat capacity and enthalpy, thermal conductivity, emissivity, thermal expansion, densification, and swelling of the fuel pellets. When indicated, some correlations account for gadolinia (Gd₂O₃) additions in UO₂ fuel pellets. The subroutine containing the material correlation in the FRAPCON/FRAPTRAN codes is given in parentheses in the heading of each subsection.

2.1 Fuel Melting Temperature (PHYPRP)

The subroutine Fuel Melting Temperature (PHYPRP) is used to calculate the temperature of the first appearance of liquid phase (solidus) and the temperature of the melting point of the last solid phase (liquidus) of UO₂ and MOX. These temperatures are calculated as a function of burnup and plutonia content. The same subroutine is used in both FRAPCON-4.0 and FRAPTRAN-2.0 and exhibits smaller burnup dependence than the corresponding MATPRO correlation, FHYPRP.

2.1.1 Model Development and Comparisons

The equations used to calculate the UO₂ and MOX melting points were derived by using 3113.15K as the melting temperature of urania, which was determined experimentally by Brassfield (1968), and a least squares fit to parabolic equations for the solidus and liquidus boundaries from the Lyon and Baily (1967) phase diagram for the stoichiometric (U, Pu)O₂ mixed oxide. These correlations are presented in Equations 2.1 through 2.5.

$$\text{sldus}(c) = 2840 - 5.41395c + 7.468390 \times 10^{-3} c^2 \quad (2.1)$$

$$\text{liqdu}(c) = 2840 - 3.21860c + 1.448518 \times 10^{-2} c^2 \quad (2.2)$$

For $c = 0$

$$\text{ftmelt} = 3113.15 - 5\text{FBu}/10000 \quad (2.3)$$

For $c > 0$

$$\text{ftmelt} = \text{sldus}(c) + 273.15 - 5\text{FBu}/10000 \quad (2.4)$$

$$\text{fdelta} = \text{liqdu}(c) - \text{sldus}(c) - 5\text{FBu}/10000 \quad (2.5)$$

where

- c = Pu content (wt%)
- $\text{sldus}(c)$ = solidus temperature as a function of Pu content (°C)
- $\text{liqdu}(c)$ = liquidus temperature as a function of Pu content (°C)
- ftmelt = fuel melting temperature (K)
- FBu = burnup (MWd/MTU)
- fdelta = temperature range between solidus and liquidus (K)

The correlations defined above for the subroutine PHYPRP are almost identical to those used in the subroutine FHYPRP documented in MATPRO. However, the burnup dependence of the PHYPRP subroutine differs from the FHYPRP subroutine. A burnup dependence of 3.2 K/GWd/MTU is used in FHYPRP, while a burnup dependence of 0.5 K/GWd/MTU is used in PHYPRP. This change was suggested by Popov et al. (2000) and is based on data from Adamson et al. (1985) and Komatsu et al. (1988).

The burnup-dependent term in Equations 2.3 through 2.5 reflects this change in burnup dependence. Also, the term 3.21860 c in Equation 2.2 is slightly different from the term used in FHYPRP. The coefficient was changed from 3.21660 in FHYPRP to 3.21860 in PHYPRP. However, this change does not appreciably affect the liquidus temperature.

Comparisons between solidus and liquidus temperature calculated by PHYPRP and FHYPRP are presented in Figure 2.1 and Figure 2.2. Both subroutines predict solidus and liquidus temperatures that decrease with increasing burnup and plutonium concentration. However, these figures reveal a smaller decline in solidus and liquidus temperatures for the FRAPCON and FRAPTRAN subroutine (PHYPRP) than the MATPRO subroutine (FHYPRP). This is a result of reducing the burnup dependence from 3.2 to 0.5 K/GWd/MTU between the FHYPRP and PHYPRP subroutines, respectively.

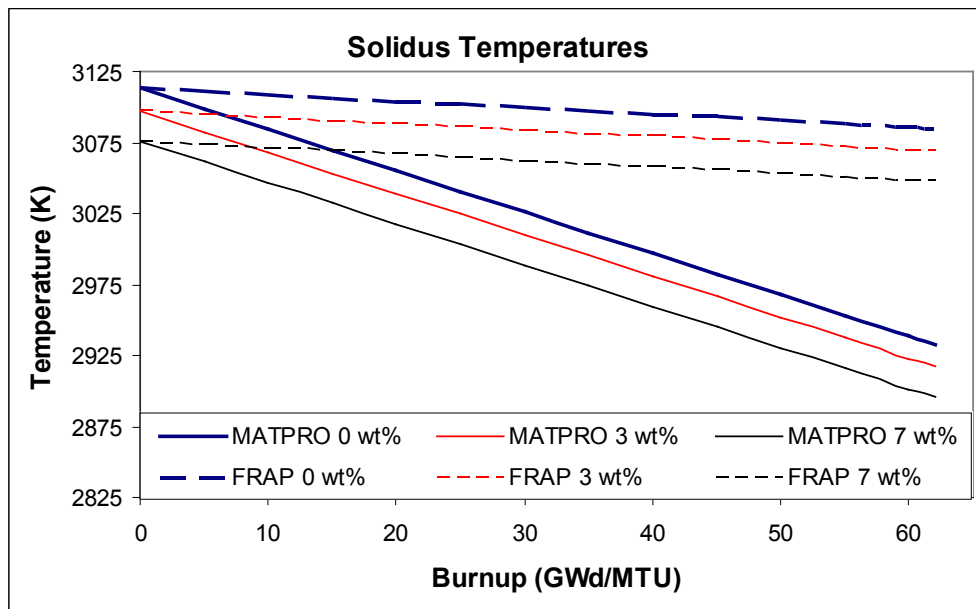


Figure 2.1. A Comparison Between Solidus Temperatures Calculated by MATPRO Using the FHYPRP Subroutine and FRAPCON/FRAPTRAN (FRAP) Using the PHYPRP Subroutine. Results for burnup varying from 0 to 62 GWd/MTU and Pu contents of 0, 3, and 7 wt% are presented.

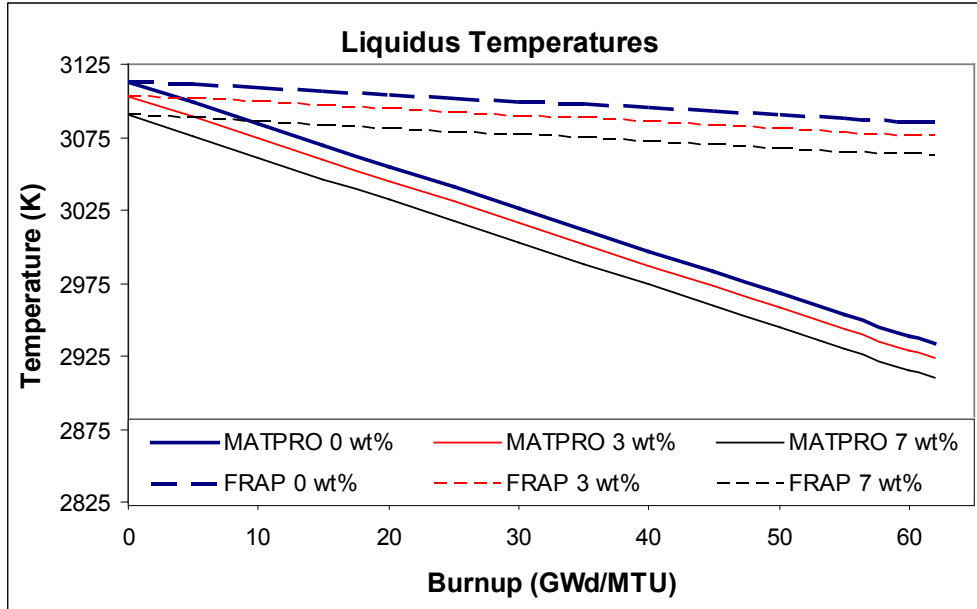


Figure 2.2. A Comparison Between Liquidus Temperatures Calculated by MATPRO Using the FHYPRP Subroutine and FRAPCON/FRAPTRAN (FRAP) Using the PHYPRP Subroutine. Results for burnup varying from 0 to 62 GWd/MTU and Pu contents of 0, 3, and 7 wt% are presented.

The fuel melting correlation in FRAPCON-4.0 has been revised to account for gadolinia additions within the fuel. Based on available literature regarding gadolinia-doped urania (Toyoaki 1999), the melting point is estimated with the correlation presented in Equation 2.6.

$$T_{melt} = 3115 - 4.8 * X_{Gd_2O_3} \quad (2.6)$$

Equation 2.6 relates the melting temperature (T_{melt} in K) to the concentration of gadolinia ($X_{Gd_2O_3}$ in wt%).

2.1.2 Applicability and Uncertainty

The correlation used in PHYPRP is valid through the melting temperature of UO_2 and MOX for burnups up to 62 GWd/MTU. Due to the limited experimental data and data interpretations on which these temperature correlations are based, it is difficult to express a quantitative measure of uncertainty. A conservative estimate of uncertainty based on engineering judgment is $\pm 50K$.

2.2 Fuel Specific Heat Capacity (FCP) and Fuel Enthalpy (FENTHL)

The subroutines Fuel Specific Heat Capacity (FCP) and Fuel Enthalpy (FENTHL) are used to calculate the specific heat capacity and enthalpy of the fuel pellet, respectively. The specific heat capacity and enthalpy of nuclear fuel are modeled empirically as functions of four parameters: temperature, composition, molten fraction, and oxygen-to-metal (O/M) ratio. The same subroutine is used in FRAPCON-4.0, FRAPTRAN-2.0, and MATPRO.

2.2.1 Model Development and Comparisons

Equations for the specific heat capacity and enthalpy of solid UO₂ and plutonium dioxide (PuO₂) are assumed to have the same form, but with different constants. The basic relationships are presented in Equations 2.7 and 2.8, respectively.

$$FCP = \frac{K_1 \theta^2 \exp(\theta / T)}{T^2 [\exp(\theta / T) - 1]^2} + K_2 T + \frac{Y K_3 E_D}{2RT^2} \exp(-E_D / RT) \quad (2.7)$$

$$FENTHL = \frac{K_1 \theta}{\exp(\theta / T) - 1} + \frac{K_2 T^2}{2} + \frac{Y}{2} [K_3 \exp(-E_D / RT)] \quad (2.8)$$

where

- FCP = specific heat capacity (J/kg*K)
- FENTHL = fuel enthalpy (J/kg)
- T = temperature (K)
- Y = oxygen-to-metal ratio
- R = universal gas constant = 8.3143 (J/mol*K)
- θ = the Einstein temperature (K)
- E_D = activation energy for Frenkel defects (J/mol)

and the constants are given in Table 2.1.

Table 2.1. Constants Used in UO₂, Gd₂O₃, and PuO₂ Heat Capacity and Enthalpy Correlations

Constant	UO ₂	PuO ₂	GdO ₂ *	Units
K ₁	296.7	347.4	315.86	J/kg*K
K ₂	2.43 x 10 ⁻²	3.95 x 10 ⁻⁴	4.044 x 10 ⁻²	J/kg*K ²
K ₃	8.745 x 10 ⁷	3.860 x 10 ⁷	0.0	J/kg
θ	535.285	571.000	348.0	K
E _D	1.577 x 10 ⁵	1.967 x 10 ⁵	0.0	J/mol

* Gadolinia additions are only accounted for in FRAPCON-4.0.

The constants in Table 2.1 were determined by Kerrisk and Clifton (1972) for UO₂ and Kruger and Savage (1968) for PuO₂. The specific heat capacity of UO₂ in the liquid state (see Equation 2.9) was determined by Leibowitz et al. (1971) and assumed to be valid for PuO₂ in the liquid state.

$$FCP_{Liquid} = 503 \text{ J/kg*K} \quad (2.9)$$

Inspection of Equations 2.7 and 2.8 reveals that fuel enthalpy, or stored energy, is calculated by integrating the fuel specific heat capacity correlation from 0 to T in kelvin. Stored energy is important in reactor transient analysis because the severity of the transient is significantly affected by the initial stored energy of the fuel. Since UO_2 and PuO_2 are the principal oxides in light-water reactor (LWR) fuels, they are the constituents considered.

The correlations for specific heat and enthalpy in both UO_2 and MOX fuel pellets are identical in FRAPCON-4.0, FRAPTRAN-2.0, and MATPRO. However, FRAPCON-4.0 can accommodate gadolinia additions whereas FRAPTRAN cannot. For a mixture of UO_2 , Gd_2O_3 , and PuO_2 , the specific heat capacity of the solid is determined by combining the contribution from each constituent in proportion to its weight fraction. When the material is partially molten, the heat capacity is determined similarly with a weighted sum of the solid and molten fractions.

Since the specific heat correlation is only valid above a fuel temperature of about 300K, the fuel enthalpy correlation is not valid below a temperature of about 300K. In addition, it is necessary to calculate fuel enthalpy with respect to a reference temperature $\geq 300\text{K}$. Thus, the fuel enthalpy at any desired temperature, T, is calculated by evaluating Equation 2.8 at T and a reference temperature, T_{ref} , of 300K and taking the difference $[\text{FENTHL}(T) - \text{FENTHL}(T_{\text{ref}})]$. For temperatures greater than 2K below melting, the molten fraction and heat of fusion are used to interpolate between the enthalpy of unmelted fuel and just-melted fuel at the melting temperature.

Specific heat correlations are compared with independent experimental data in Figure 2.3 and Figure 2.4 for UO_2 and PuO_2 , respectively. Comparison between the UO_2 model and experimental data from Hein et al. (1968), Leibowitz et al. (1969), and Gronvold et al. (1970) in Figure 2.3 reveals agreement between predicted and measured values up to high temperatures (a few hundred kelvin below melting). At this point the data begin to fall lower than the model. This is attributed to partial melting due to a non-uniform temperature distribution within the sample. With the exception of the Affortit and Marcon (1970) data, relatively good agreement is observed in Figure 2.4, which compares the values measured by Gibby et al. (1974), Leibowitz et al. (1972), and Affortit with predicted heat capacities for a MOX fuel, $(\text{U}_{0.8}, \text{Pu}_{0.2})\text{O}_2$. Since the Affortit results are known to be generally low in comparison to results from other investigators, the correlation is considered to be in good agreement with the experimental data.

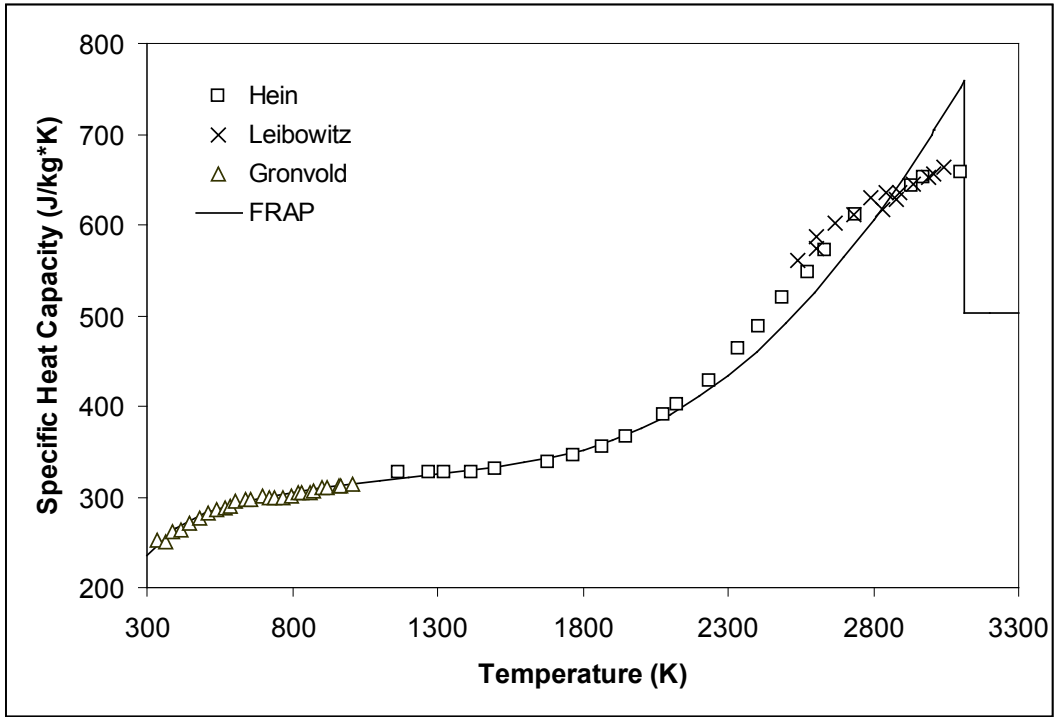


Figure 2.3. Specific Heat Capacity of UO_2 from Three Experimenters Compared with the FRAPCON/FRAPTRAN/MATPRO (FRAP) Correlation (solid line) for UO_2

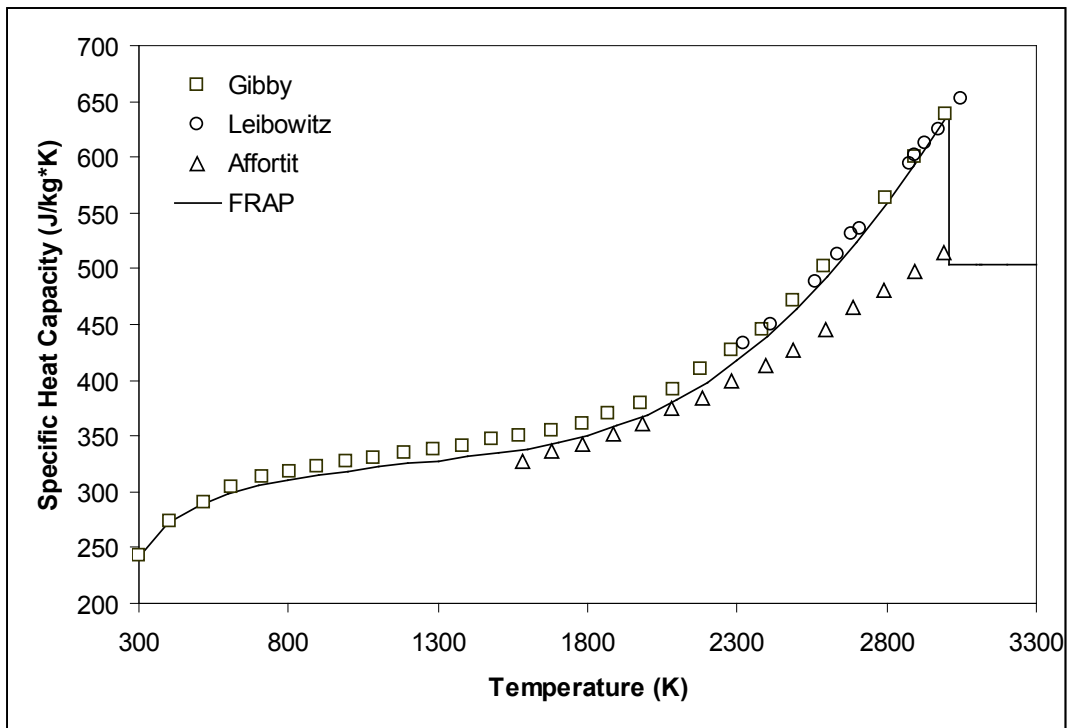


Figure 2.4. Specific Heat Capacity of $(U_{0.8}Pu_{0.2})O_2$ from Three Experimenters Compared with the FRAPCON/FRAPTRAN/MATPRO (FRAP) Correlations (solid line) for MOX

2.2.2 Applicability and Uncertainty

The correlations for fuel specific heat and enthalpy are valid for temperatures from 300K to more than 4000K. The standard error of the UO_2 specific heat capacity correlation is $\pm 3 \text{ J/kg}\cdot\text{K}$. However, this error increases at temperatures above 2300K, as seen in Figure 2.3, and may lead to underpredictions and overpredictions of 59 and 66 $\text{J/kg}\cdot\text{K}$, respectively. As for the mixed-oxide-specific heat capacity correlation, it is 6 to 10 $\text{J/kg}\cdot\text{K}$, depending on the fraction of PuO_2 . For nonstoichiometric fuels, these uncertainties are approximately double.

2.3 Fuel Thermal Conductivity (FTHCON)

The subroutine Fuel Thermal Conductivity (FTHCON) is used to calculate the thermal conductivity of the fuel pellet. Since accurate predictions of fuel rod behavior are strongly dependent on temperature, the calculation of fuel thermal conductivity is critical. The FTHCON subroutine is used in FRAPCON-4.0, FRAPTRAN-2.0, and MATPRO. However, the calculation of fuel thermal conductivity has evolved from the model originally proposed in MATPRO to the modified Nuclear Fuels Industries (NFI) and Duriez/modified NFI models adopted by Pacific Northwest National Laboratory (PNNL) and used in the FRAPCON-4.0 and FRAPTRAN-2.0 codes for UO_2 , $\text{UO}_2\text{-Gd}_2\text{O}_3$, and MOX, respectively. An additional fuel thermal conductivity model for MOX developed at Halden is included as an option in FRAPCON-4.0 (Wiesenack and Tverberg 2000). Each of the models is discussed in detail in the following sections along with the evolution of the MATPRO model and the applicability and uncertainty of the models.

Following the initial description of the MATPRO fuel thermal conductivity model, an overview of subsequent thermal conductivity models is given. This historical summary of how thermal conductivity modeling has evolved provides insight to model development and previous motivations for change. For example, the MATPRO model was followed by a model by Lucuta that accounted for burnup degradation and was incorporated in FRAPCON. However, there were several issues with the Lucuta model, including its non-standard form and weak burnup degradation term, that led to its replacement by a modified model developed at NFI. Further refinements of this model were implemented by PNNL to provide a better fit to UO_2 data. In addition, PNNL added refinements to include the Duriez-derived modifications to the NFI model, which permit MOX fuels to be modeled. These updates were incorporated in FRAPCON-3.3 (Lanning et al. 2005) and continue to be used in FRAPCON-4.0.

2.3.1 Model Development and Comparisons

The original MATPRO model for fuel thermal conductivity is based on a mechanistic description of thermal conductivity, including lattice vibration (i.e., phonon) and electron-hole pair (i.e., electronic) contributions (Hagman et al. 1981). The MATPRO thermal conductivity model is a function of temperature, density, O/M ratio, and plutonium content. Burnup is also included; however, it is only used to calculate the melt temperature. Unlike the models used in FRAPCON 4.0 and FRAPTRAN-2.0, MATPRO does not account for the degradation of thermal conductivity with increasing burnup.

The dominant contributor to thermal conductivity (i.e., phonon or electron) is dependent on temperature. Phonon contributions to thermal conductivity are dominant below 1500K, whereas electronic contributions are dominant above 2000K. In general, thermal conductivity decreases with increasing porosity, but this effect is significantly decreased above 1600K due to radiation effects and gas

conductivity within the pores at these temperatures. At higher temperatures (> 3000K), estimates of liquid fuel thermal conductivity are made from physical considerations because data for molten fuel have not been found.

The MATPRO model used to express thermal conductivity of solid fuel is described with Equation 2.10.

$$k = \left(\frac{D}{1 + (6.5 - 0.00469T')(1 - D)} \right) \left(\frac{C_v}{(A + BT'')(1 + 3e_{th})} \right) \dots \dots \dots \quad (2.10)$$

$$\dots \dots \dots + 5.2997 \times 10^{-3} T \left[\exp(-13358/T) \right] \left\{ 1 + 0.169 \left[(13358/T) + 2 \right]^2 \right\}$$

where

- k = thermal conductivity (W/m*K).
- D = fraction of theoretical density (unitless).
- CV = phonon contribution to the specific heat at constant volume (J/kg*K). The first term of the correlation for fuel specific heat capacity is used for this factor.
- e_{th} = linear strain caused by thermal expansion when temperature is > 300K (unitless); the MATPRO correlation for fuel thermal expansion is used for this factor
- T = fuel temperature (K).
- T' = porosity correction for temperature, for temperature < 1364, T' = 6.50 - T*(4.69x10⁻³), for temperature > 1834, T' = -1, and for temperatures in the range from 1364 to 1834K, T' is found by interpolation.
- T'' = fuel temperature if < 1800K. For temperatures > 2300K, T'' is equal to 2050K; for temperature in the range 1800 to 2300K, T'' is found by interpolation.
- A = a factor proportional to the point defect contribution to the phonon mean free path (m*s/kg*K); the correlation used for this factor is 0.339 + 12.6 x absolute value (2.0 - O/M ratio).
- B = a factor proportional to the phonon-phonon scattering contribution to the phonon mean free path (m*s/kg*K); the correlation used for this factor is 0.06867 x (1 + 0.6238 x plutonium content of the fuel).

The first term of Equation 2.10 represents the phonon contribution to specific heat. The temperature and density dependence of this term can be seen in Equation 2.10. Although not as evident, the dependence of the first term on O/M ratio and plutonium content is also included. The specific heat capacity of the fuel (CV) and the phonon scattering factor (B) are dependent on the plutonium content, while the point defect contribution factor (A) is dependent on the O/M ratio. Temperature dependence can also be observed in the second term of Equation 2.10, which represents the electronic contribution.

This MATPRO model (Hagrman et al. 1981) was initially replaced in FRAPCON and FRAPTRAN with a model from Lucuta (Lucuta et al. 1996) which accounts for the degradation of thermal conductivity due to burnup. The Lucuta model for fuel thermal conductivity, K, is presented in Equation 2.11

$$K = K_o \bullet FD \bullet FP \bullet FM \bullet FR \quad (2.11)$$

where

- K_o = thermal conductivity of unirradiated, fully dense urania
- FD = factor for dissolved fission products
- FP = factor for precipitated fission products
- FM = factor to correct for the Maxwell porosity effect
- FR = factor for the radiation effect

Thermal conductivity of unirradiated, fully dense urania and factors included in the Lucuta model are described by the Equations 2.12 through 2.16.

$$K_o = \frac{1}{0.0375 + 2.165 \times 10^{-4} T} + \left[\frac{4.715 \times 10^9}{T^2} \right] \exp \left[-\frac{16361}{T} \right] \quad (2.12)$$

$$FD = \left[\frac{1.09}{B^{3.265}} + \frac{0.0643}{\sqrt{B}} \sqrt{T} \right] \arctan \left[\frac{1}{\frac{1.09}{B^{3.265}} + \frac{0.0643}{\sqrt{B}} \sqrt{T}} \right] \quad (2.13)$$

$$FP = 1 + \left[\frac{0.019B}{3 - 0.019B} \right] \left[\frac{1}{1 + \exp\left(-\frac{T - 1200}{100}\right)} \right] \quad (2.14)$$

$$FM = \frac{1 - p}{1 + (s - 1)p} \quad (2.15)$$

$$FR = 1 - \frac{0.2}{1 + \exp\left(\frac{T - 900}{80}\right)} \quad (2.16)$$

where

- K_o = conductivity of unirradiated, fully dense urania (W/m-K)
- T = temperature (K)
- B = burnup in atom% (1 atom% = 9.383 GWd/MTU at 200 MeV/fission)
- p = porosity fraction (as-fabricated plus swelling)
- s = shape factor (= 1.5 for spherical pores)

Although the Lucuta model for thermal conductivity accounted for burnup degradation, this model tended to overpredict thermal conductivity values at high temperature (> 2200K). Furthermore, the model had too little burnup degradation, making it non-conservative above 30 GWd/MTU. In addition, the form of the Lucuta model is non-standard, which does not facilitate comparison between models. As a result, the Lucuta model was later replaced with a modified version of a thermal conductivity model proposed by NFI (Ohira and Itagaki 1997) (Lanning et al. 2005).

Both FRAPCON-4.0 and FRAPTRAN-2.0 currently model uranium fuel pellet thermal conductivity with the modified version of the pellet thermal conductivity model proposed by NFI (Ohira and Itagaki 1997). The original NFI model was modified to alter the temperature-dependent portion of the burnup function in the phonon terms and change the electronic term (Lanning et al. 2005). The original (unmodified) and modified versions of the NFI thermal conductivity model are presented in Equations 2.17 and 2.18, respectively.

$$K_{95} = \frac{1}{A + BT + f(Bu) + g(Bu)h(T)} - CT^2 + DT^4 \quad (2.17)$$

$$K_{95} = \frac{1}{A + BT + f(Bu) + (1 - 0.9 \exp(-0.04Bu))g(Bu)h(T)} + \frac{E}{T^2} \exp(-F/T) \quad (2.18)$$

where

- K = thermal conductivity, W/m-K
- T = temperature, K
- Bu = burnup, GWd/MTU
- f(Bu) = effect of fission products in crystal matrix (solution)
= 0.00187 * Bu
- g(Bu) = effect of irradiation defects
= 0.038 * Bu^{0.28}
- h(T) = temperature dependence of annealing on irradiation defects
= $\frac{1}{1 + 396 \exp(-Q/T)}$
- Q = temperature-dependent parameter ("Q/R") = 6380K
- A = 0.0452 m-K/W
- B = 2.46 x 10⁻⁴ m-K/W/K
- C = 5.47 x 10⁻⁹ W/m-K³
- D = 2.29 x 10¹⁴ W/m-K⁵
- E = 3.5 x 10⁹ W-K/m
- F = 16,361K

The NFI model was further modified in FRAPCON-4.0 with a data correlation presented by Massih (Massih et al. 1992) to include gadolinia content (Lanning et al. 2005). The modified NFI with gadolinia dependency used in FRAPCON-4.0 is presented in Equation 2.19.

$$K = \frac{1}{A + a \cdot \text{gad} + BT + f(Bu) + (1 - 0.9 \exp(-0.04Bu))g(Bu)h(T)} + \dots \quad (2.19)$$

$$\dots \frac{E}{T^2} \exp(-F/T)$$

where

- a = constant = 1.1599
- gad = weight fraction of gadolinia

As applied in FRACON-4.0 and FRAPTRAN-2.0, the above models are adjusted for as-fabricated fuel density (in fraction of theoretical density [TD]) using the Lucuta recommendation for spherical-shaped pores (Lucuta et al. 1996), as follows:

$$K_d = 1.0789 * K_{95} * [d / \{1.0 + 0.5(1 - d)\}] \quad (2.20)$$

where

- K_d = thermal conductivity adjusted for as-fabricated fuel density, d
- K_{95} = thermal conductivity for 95 percent dense fuel
- d = as-fabricated fuel density

The phonon-term modification by PNNL in the modified NFI model reduces defect annealing at low burnup from that by Ohira and Itagaki (NFI). However, the original temperature-dependent annealing is restored at higher burnups such that, for burnups greater than 40 GWd/MTU, the phonon term is equivalent to that in the original NFI model. The electronic terms (which in either case become significant above 1500K) are altered in the modified NFI model to a more theoretically based equation. The magnitude is slightly lower than the original NFI model at high temperature. This adjustment by PNNL was based on the Institute for Transuranium Elements data from unirradiated pressurized-water reactor (PWR) pellet material at temperatures approaching fuel melting (Ronchi et al. 1999).

At low burnups (< 20 GWd/MTU) and low temperatures (< 1000K), the PNNL modified model is higher than the unmodified NFI model and roughly equivalent to the Lucuta model without its radiation term. At higher burnup (> 30 GWd/MTU), the modified model is equivalent to the original NFI model with the exception of the small reduction at very high temperatures.

Fuel thermal conductivity modeling was extended by PNNL (Lanning et al. 2005) to include MOX in FRAPCON and FRAPTRAN by adopting a model that was a combination of the Duriez stoichiometry-dependent correlation, which is derived from diffusivity measurements on unirradiated fuel pellets, and the modified version of the NFI model, which includes burnup degradation effects. The Duriez data places greater dependence of MOX thermal conductivity on stoichiometry, but only a minor dependence on plutonia content (Duriez et al. 2000). The Duriez/modified NFI model is presented in Equation 2.21.

$$K_{95} = \frac{1}{A(x) + a \cdot gad + B(x)T + f(Bu) + (1 - 0.9 \exp(-0.4Bu)) g(Bu) h(T)} \dots \quad (2.21)$$

$$\dots + \frac{C_{\text{mod}}}{T^2} \exp\left(-\frac{D}{T}\right)$$

where

- K_{95} = conductivity at 95 percent TD, W/m-K
- x = 2.00 – O/M (i.e., oxygen-to-metal ratio)
- T = temperature, K
- A(x) = 2.85x + 0.035, m-K/W
- B(x) = (2.86 – 7.15x)*1E-4 m/W
- C = 1.689x10⁹, W-K/m
- D = 13,520K

$$\begin{aligned}
a &= 1.1599 \\
gad &= \text{weight fraction gadolinia (not expected in MOX)} \\
Bu &= \text{burnup in GWd/THM} \\
f(Bu) &= \text{effect of fission products in crystal matrix (solution)} \\
&= 0.00187 \cdot Bu \\
g(Bu) &= \text{effect of irradiation defects} \\
&= 0.038 \cdot Bu^{0.28} \\
h(T) &= \text{temperature dependence of annealing on irradiation defects} \\
&= \frac{1}{1 + 396 \exp(-Q/T)} \\
Q &= \text{temperature dependent parameter ("Q/R") = 6380K} \\
C_{\text{mod}} &= 1.5 \times 10^9 \text{ W-K/m}
\end{aligned}$$

FRAPCON provides an option to use a fuel thermal conductivity model derived at Halden. The Halden correlation does not include dependency on stoichiometry, but does emphasize burnup effects. The Halden correlation tends to overpredict thermal conductivity data at high temperatures (> 2500K) (Lanning et al. 2005).

$$K_{95} = \frac{0.92}{0.1148 + a \cdot gad + 1.1599x + 0.0040B + 2.475 \times 10^{-4} (1 - 0.00333B)\Phi \dots} \dots \quad (2.22)$$

$$\dots + 0.0132 \exp(0.00188T)$$

where

$$\begin{aligned}
K_{95} &= \text{conductivity at 95 percent TD, W/m-K} \\
T &= \text{temperature, } ^\circ\text{C} \\
a &= 1.1599 \\
gad &= \text{weight fraction gadolinia (not expected in MOX)} \\
B &= \text{burnup in MWd/kg UO}_2 \\
\Phi &= \text{minimum of } 1650^\circ\text{C or current temperature in } ^\circ\text{C}
\end{aligned}$$

To summarize, the modified NFI model is used for UO₂, whereas the Duriez/NFI model is used for MOX. The modified NFI model used in FRAPCON-4.0 accounts for gad additions, but the modified NFI model in FRAPTRAN-2.0 does not. The Duriez/NFI models account for gad in both codes, although no gad additions are included in MOX at this time. Finally, FRAPCON-4.0 has the option for Halden thermal conductivity correlation, but FRAPTRAN does not.

A comparison between the MATPRO model and the modified NFI model is presented in Figure 2.5. The MATPRO model predicts lower thermal conductivities than the modified NFI model across the applicable temperature range (i.e., 500 to 3000K) for unirradiated UO₂. However, unlike the MATPRO model, the modified NFI model can account for degradation of thermal conductivity with increasing burnup. The modified NFI model at a burnup level of 30 GWd/MTU is shown for comparison and reveals significant degradation of thermal conductivity. This represents an improvement relative to the MATPRO model, which does not account for burnup degradation of thermal conductivity.

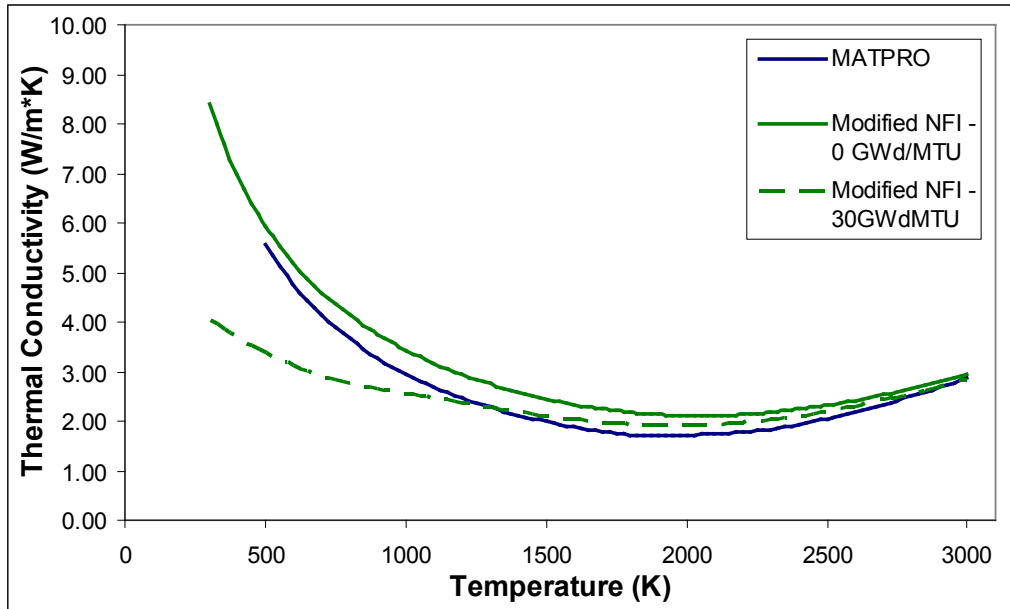


Figure 2.5. MATPRO and Modified NFI Thermal Conductivity Models for UO_2 as a Function of Temperature. Unlike the MATPRO model, the modified NFI model can account for burnup and is presented at burnup levels of 0 and 30 GWd/MTU for comparison.

Model-to-data comparisons for the MATPRO and modified NFI models and data collected from unirradiated UO_2 are made in Figure 2.6 and Figure 2.7. In addition to Ronchi (1999), the unirradiated UO_2 data sets that were used to derive the MATPRO model are also included. Based on Figure 2.6, it can be seen that the MATPRO model tends to underpredict the thermal conductivity of the unirradiated UO_2 . The average bias in Figure 2.6 underpredicts thermal conductivity by about 9.5 percent, with a standard deviation of about 11 percent. The modified NFI model also underpredicts the unirradiated data, but only by about 2.4 percent and with a standard deviation of 8 percent (see Figure 2.7). Based on the smaller bias and standard deviation, it can be seen that the modified NFI model predicts the thermal conductivity of UO_2 much better than the MATPRO model.

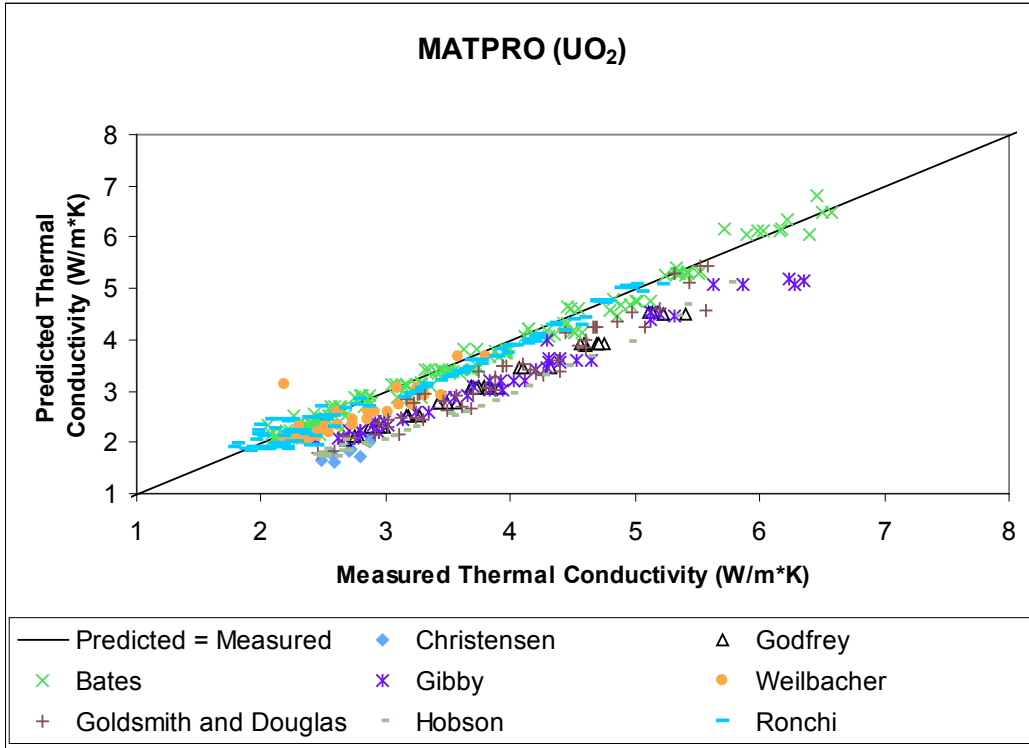


Figure 2.6. MATPRO Model-to-Data Comparison for Thermal Conductivity of Unirradiated UO₂

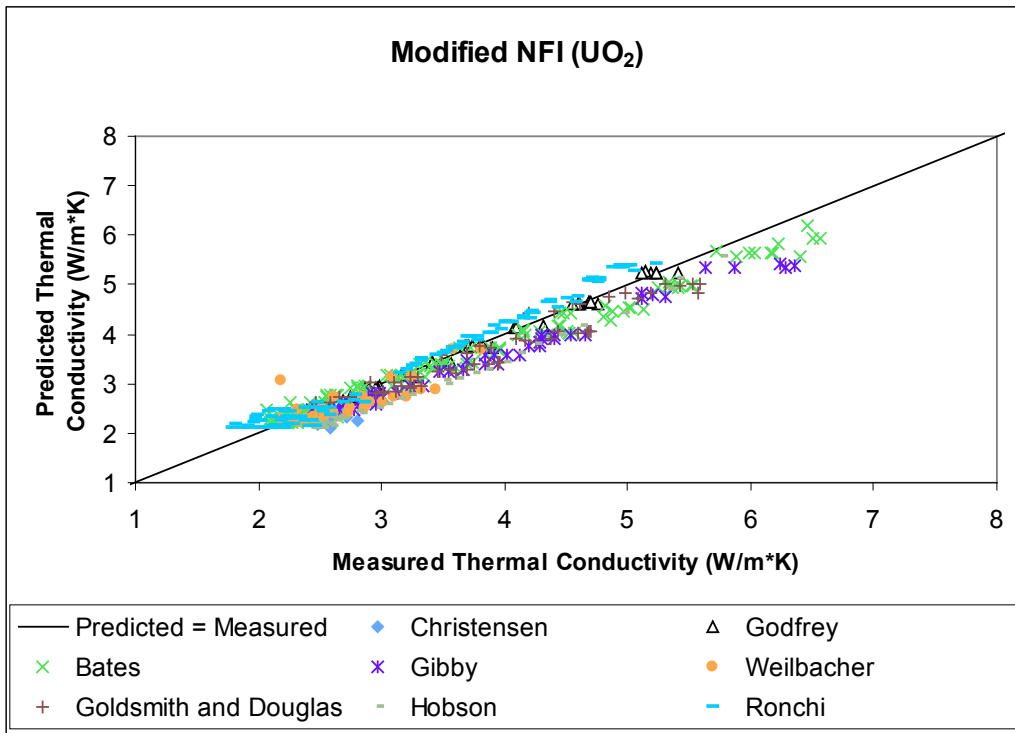


Figure 2.7. Modified NFI Model-to-Data Comparison for Thermal Conductivity of Unirradiated UO₂

Model-to-data comparisons for the MATPRO and modified NFI models and data collected from irradiated UO_2 are made in Figure 2.8 and Figure 2.9. The thermal conductivity values are measured ex-reactor from small portions of fuel irradiated at various temperatures and burnup levels. Based on Figure 2.8, it can be seen that the MATPRO model predicts significantly higher values for thermal conductivity than the measured values obtained from irradiated UO_2 . The average bias in Figure 2.8 indicates that the thermal conductivity is overpredicted by about 40 percent, with a standard deviation of about 31 percent. The modified NFI model also tends to overpredict the small amount of irradiated data on average, but only by about 5 percent and with a standard deviation of about 8 percent (see Figure 2.9). Based on the significantly smaller bias and standard deviation, it can be seen that the modified NFI model predicts the thermal conductivity of irradiated UO_2 better than the MATPRO model. The disparity between models is attributed to the degradation of thermal conductivity with increasing burnup, which is accounted for in the modified NFI model but not the MATPRO model.

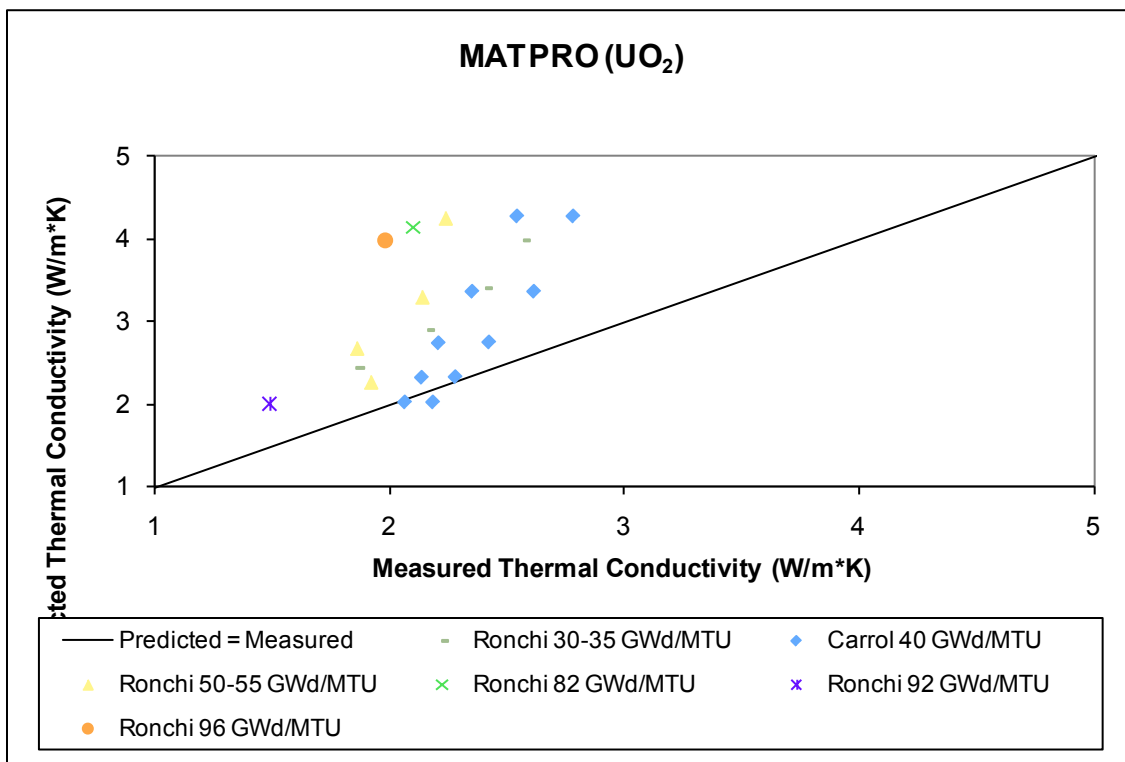


Figure 2.8. MATPRO Model-to-Data Comparison for Thermal Conductivity of Irradiated UO_2

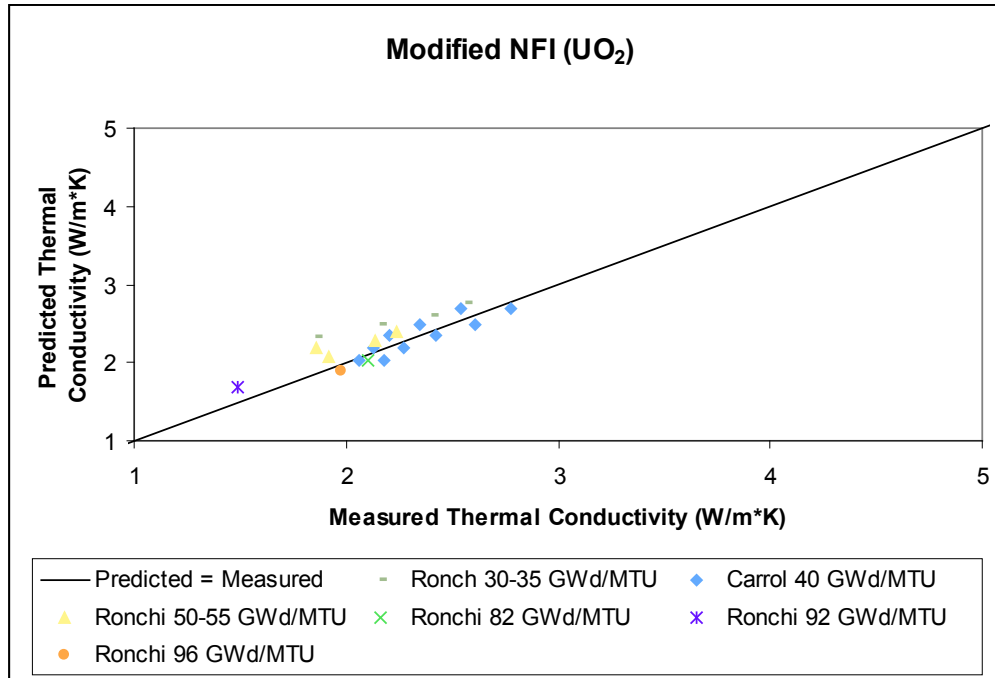


Figure 2.9. Modified NFI Model-to-Data Comparison for Thermal Conductivity of Irradiated UO₂

A comparison between the MATPRO model and the Duriez/modified NFI model is presented in Figure 2.10 for MOX fuel with a plutonium concentration of 7 wt%. The MATPRO model predicts lower thermal conductivities than the Duriez/modified NFI model across the applicable temperature range (i.e., 500 to 3000K). However, unlike the MATPRO model, the Duriez/modified NFI model can account for degradation of thermal conductivity with increasing burnup. The Duriez/modified NFI model at a burnup level of 30 GWd/MTU is shown for comparison and reveals significant degradation of thermal conductivity. This represents an improvement relative to the MATPRO model, which does not account for burnup degradation of thermal conductivity.

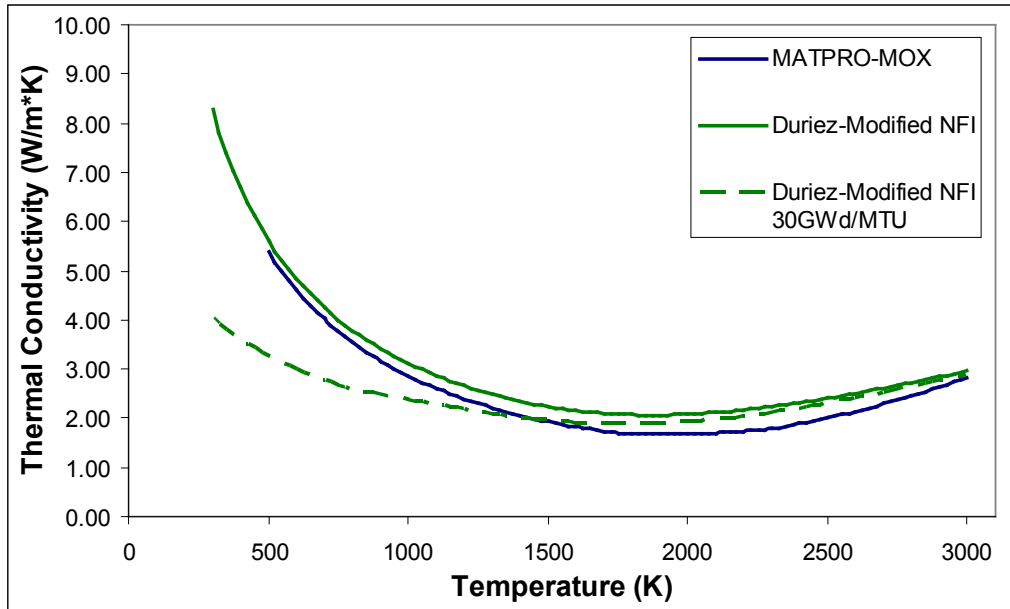


Figure 2.10. MATPRO and Duriez/Modified NFI Conductivity Models as a Function of Temperature for MOX Fuel with 7 wt% Plutonium Content. Unlike the MATPRO model, the Duriez/modified NFI model can account for burnup and is presented at burnup levels of 0 and 30 GWd/MTU for comparison.

Model-to-data comparisons for the MATPRO and Duriez/modified NFI models and unirradiated MOX fuel are made in Figure 2.11 and Figure 2.12. The comparisons utilize the data used to derive the Duriez/modified NFI model. Data collected from MOX with plutonium concentrations of 3 and 15 wt% were used (Duriez et al. 2000). Based on Figure 2.11, it can be seen that the MATPRO model tends to underpredict thermal conductivity. The average bias in Figure 2.11 underpredicts thermal conductivity by about 9 percent at both 3 and 15 wt% plutonium concentrations. The standard deviation of the MATPRO predictive bias at both plutonium concentrations is under 6 percent. As expected, the Duriez/modified NFI model exhibits better agreement with the limited experimental data from which it was derived. The average bias indicates that the MOX model overpredicts by less than 2 percent and the standard deviation between the model and the data is less than 3 percent. Based on the smaller bias and standard deviation, it can be seen that the Duriez/modified NFI model fits this MOX thermal conductivity data better than the MATPRO model.

It should be noted that the MOX fuel thermal conductivity is strongly influenced by O/M ratio, with conductivity decreasing with a deviation from stoichiometry (2.0). Based on Figure 2.12, it can be seen that plutonium content has a relatively minor effect at concentrations less than 15 wt%. The current MOX fuel is fabricated closer to being stoichiometric than fuel typically fabricated more than 25 years ago. The older data from which the MATPRO model was developed were not as close to being stoichiometric as the more recent data.

Verification of UO_2 , $\text{UO}_2\text{-Gd}_2\text{O}_3$, and MOX thermal conductivity models are further demonstrated by the comparisons to measured in-reactor fuel temperatures as a function of burnup presented in the FRAPCON-4.0 assessment documentation (Geelhood and Luscher 2014).

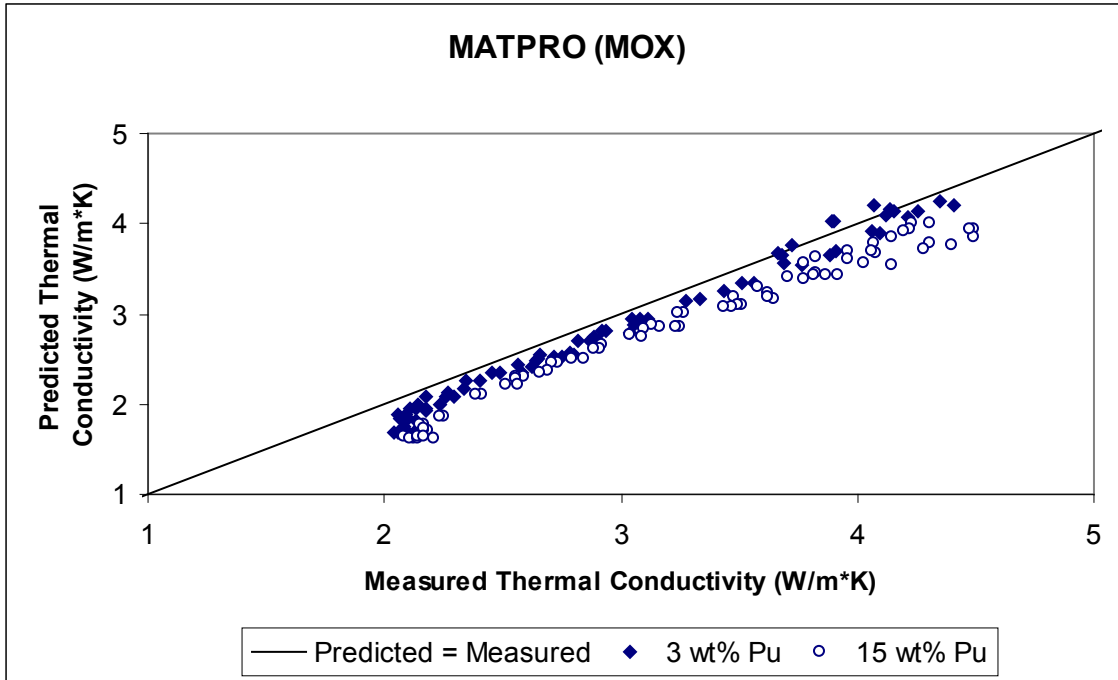


Figure 2.11. MATPRO Model-to-Data Comparison for Thermal Conductivity of Unirradiated MOX Modeled with 7 wt% of Plutonium

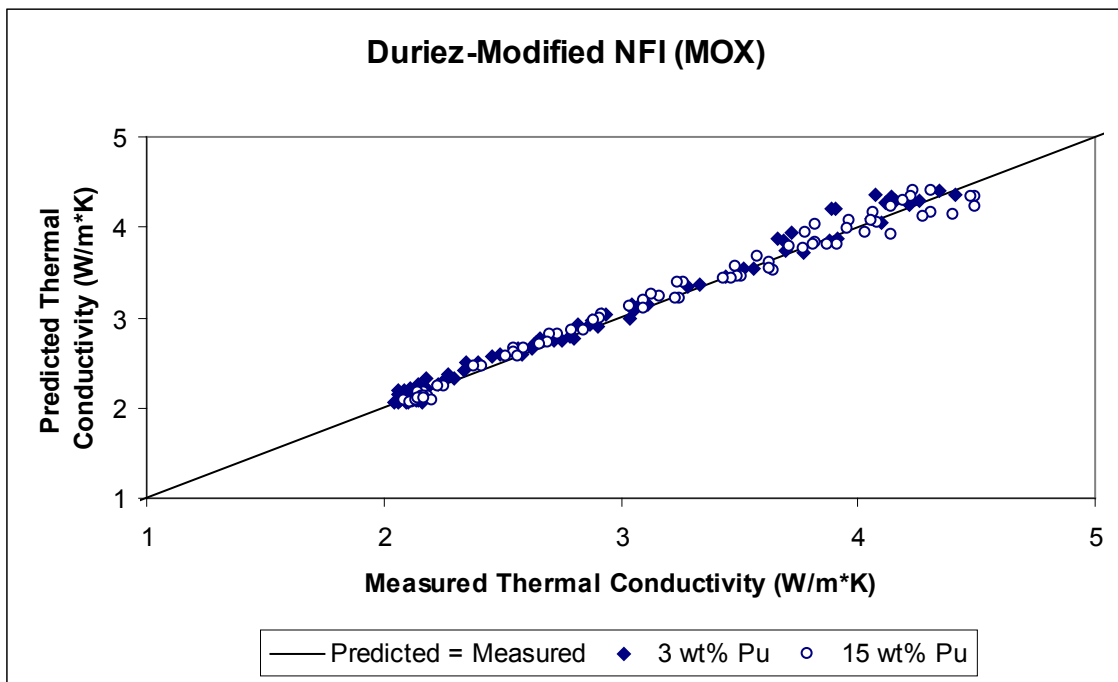


Figure 2.12. Duriez/Modified NFI Model-to-Data Comparison for Thermal Conductivity of Unirradiated MOX Modeled with 7 wt% of Plutonium

2.3.2 Applicability and Uncertainty

The following are limits that restrict the applicability of the MATPRO fuel thermal conductivity model (Equation 2.10):

- Theoretical density must range between 90 and 100 percent.
- Temperature must range between 500 (the Debye temperature) and 3000K.
- Above 3000K, it is assumed that the fuel becomes molten and the uncertainties on predictions made above this temperature are large.
- Only applicable to low burnup fuel (<5 GWd/MTU) because thermal conductivity degradation is not included in the model.

In addition, several assumptions have been made to provide an approximate model for effects of variation in the plutonium content and O/M ratio of ceramic fuels:

- The effect of variation in theoretical density for MOX fuels has been assumed to be described by the porosity correction derived with UO₂ data.
- The high-temperature electronic contribution to thermal conductivity has been assumed to be the same for PuO₂, UO₂, and nonstoichiometric fuels.
- Variations in plutonium content have been assumed to affect only the phonon-phonon scattering factor.
- Variation in O/M ratio has been assumed to affect only the defect term.

The bias and relative error of the MATPRO fuel thermal conductivity model was assessed based on the model-to-data comparisons previously presented for unirradiated UO₂, irradiated UO₂, and MOX. The average and standard deviations of the bias for unirradiated UO₂ are approximately 9.5 and 11 percent, respectively, while the relative error is approximately 19 percent. For irradiated UO₂, which has a limited number of data points for comparison, the average and standard deviations of the bias are 40 and 31 percent, respectively. The relative error for the limited number of irradiated UO₂ data points is approximately 51 percent. Finally, for MOX, the average and standard deviations of the bias are -9 and 6 percent, respectively, while the relative error is approximately 13 percent. For reference, a negative bias indicates that the model underpredicts the data, whereas a positive bias indicates that the model overpredicts the data.

For the modified NFI and the Duriez/modified NFI models, the recommended ranges for application for modeling the thermal conductivity of UO₂ are as follows:

- Temperature: 300 to 3000K
- Rod-average burnup: 0 to 62 GWd/MTU
- As-fabricated density: 92 to 97 percent TD
- Gadolinia content: 0 to 10 wt%

For the Duriez/modified NFI model, the thermal conductivity model is applicable for plutonia particle sizes of less than 20 microns.

The bias and relative error of the modified NFI and the Duriez/modified NFI fuel thermal conductivity models were assessed based on the model-to-data comparisons previously presented for unirradiated UO₂, irradiated UO₂, and MOX. The average and standard deviations of the bias for unirradiated UO₂ are approximately -2.4 and 8 percent, respectively, while the relative error is approximately 9 percent. For irradiated UO₂, which has a limited number of data points for comparison, the average and standard deviations of the bias are approximately 5 and 8 percent, respectively, while the relative error is approximately 10 percent. Finally, for the Duriez/modified NFI fuel thermal conductivity model for MOX, the average and standard deviations of the bias are less than 2 and 3 percent, respectively, while the relative error is approximately 3 percent. These values are based on comparisons to the small amount of near-stoichiometric MOX data. For reference, a negative bias indicates that the model underpredicts the data, whereas a positive bias indicates that the model overpredicts the data.

2.4 Fuel Emissivity (FEMISS)

The subroutine Fuel Emissivity (FEMISS) is used to calculate the total hemispherical fuel emissivity (emissivity integrated over all wavelengths) as a function of temperature. Fuel emissivity is defined as the ratio of radiant energy emitted from a material to that emitted by a black body at the same temperature. The subroutine FEMISS is used to calculate radiant energy transfer from fuel to cladding in conjunction with thermal conduction. Radiant energy transfer can be a significant heat transfer mechanism, depending on the gap size, temperature gradient across the gap, and plenum gas. The FEMISS subroutine used by FRAPCON and FRAPTRAN is the same as the subroutine documented in MATPRO.

2.4.1 Model Development and Comparisons

According to the Stefan-Boltzmann law, the total radiant power per unit area emitted by a body at temperature T is

$$P = e \sigma T^4 \quad (2.22)$$

where

- P = radiant power per unit area (W/m²)
- e = total hemispherical emissivity (unitless)
- σ = the Stefan-Boltzmann constant (5.672 x 10⁻⁸ W/m²-K)
- T = temperature (K)

The expression used in the FEMISS subroutine to describe total emissivity is

$$e = 0.78557 + 1.5263 \times 10^{-5} T \quad (2.23)$$

The first term of Equation 2.23 is slightly less than the value used in MATPRO, 0.7856. The standard error of Equation 2.23 with respect to its database is ± 8.9 percent, while the error reported in MATPRO is ± 6.8 percent.

The emissivity data were measured at temperatures up to approximately 2400K, and use of FEMISS above this temperature is speculative because of possible high-temperature effects that are not modeled. At the time of model development, there were no data to develop a MOX emissivity equation, so Equation 2.23 is also recommended for MOX.

The hemispherical spectral data of Held and Wilder (1969) and the emissivity data of Cabannes (1967) and Jones and Murchison (1965) were used in developing the FEMISS model. The emissivity data used to model comparison for FEMISS are presented in Figure 2.13.

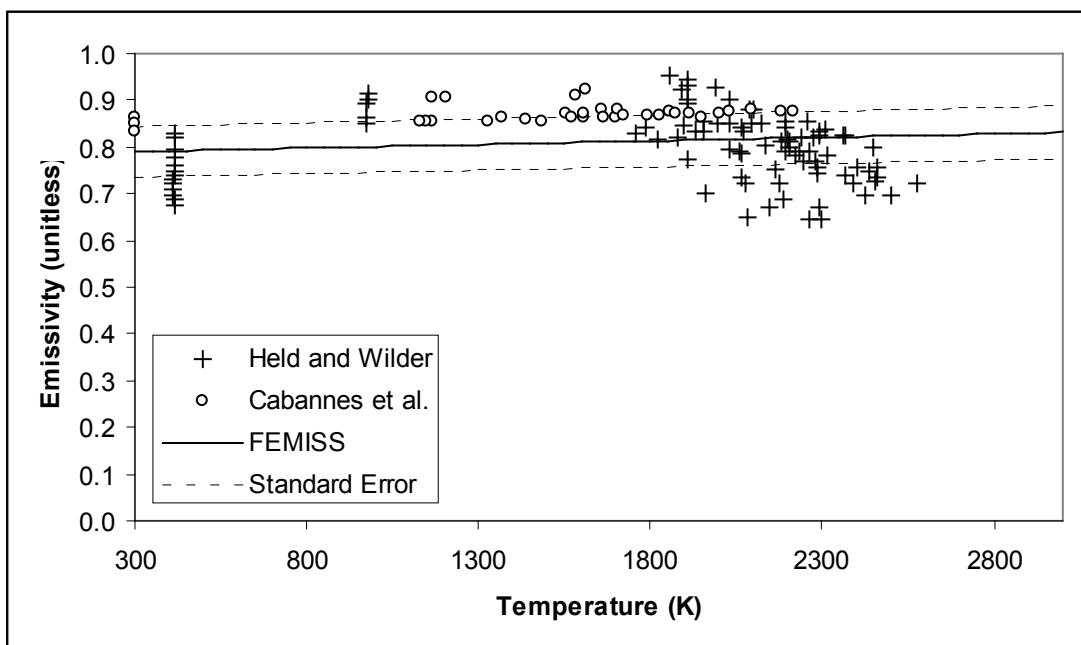


Figure 2.13. Data to Model Comparison for FEMISS

2.4.2 Applicability and Uncertainty

The correlation used in the FEMISS subroutine to calculate fuel emissivity is applicable at temperatures up to 2400K. The standard error of this correlation with respect to the database from which it was derived is approximately ± 6.8 percent.

2.5 Fuel Thermal Expansion (FTHEXP)

The subroutine Fuel Thermal Expansion (FTHEXP) models dimensional changes in unirradiated fuel pellets caused by thermal expansion. It can handle any combination of UO_2 , UO_2 - Gd_2O_3 , or PuO_2 in solid, liquid, or solid-liquid states and includes expansion due to the solid-liquid phase change. Dimensional changes in the fuel affect the pellet-to-cladding gap size, which is a major factor in determining gap heat transfer and thus the stored energy, an important quantity for safety analysis. The subroutine FTHEXP is used in FRAPCON-4.0, FRAPTRAN-2.0, and MATPRO. However, the FRAPCON and FRAPTRAN codes use updated fitting coefficients based on more recent data.

2.5.1 Model Development and Comparisons

The FTHEXP subcode models fuel thermal expansion as a function of temperature, fraction of PuO₂, and the fraction of fuel which is molten. The O/M ratio is not included. When the departure from stoichiometry (O/M – 2.0) is greater than 0.2, there is clearly an effect. However, this effect is ignored in modeling thermal expansion, since typical reactor fuels only deviate less than a tenth this much from the stoichiometric composition.

The equations for thermal expansion of UO₂, UO₂-Gd₂O₃, and PuO₂ have the same form. In the solid phase, Equation 2.24 is used.

$$\Delta L / L_0 = K_1 T - K_2 + K_3 \exp(-E_D / kT) \quad (2.24)$$

where

- $\Delta L/L$ = linear strain caused by thermal expansion (equal to zero at 300K) (unitless)
- T = temperature (K)
- E_D = energy of formation of a defect (J)
- k = Boltzmann's constant (1.38×10^{-23} J/K)

and K₁, K₂, and K₃ are constants to be determined.

The correlation given in Equation 2.24 was originally used in MATPRO and was incorporated into both the FRAPCON and FRAPTRAN codes. Data collected by Baldock et al. (1966), Burdick and Paker (1956), Gronvold (1955), Christensen (1963), and Kempeter and Elliott (1958) were used to determine the correlation constants for UO₂ used in MATPRO. However, newer data provided by Martin (1988) and Momin et al. (1991) required the constants to be updated to improve the fit between the correlation and high-temperature data (Luscher and Geelhood 2011). These updated constants are included in FRAPCON-4.0/FRAPTRAN-2.0 (FRAP). Table 2.2 presents the original MATPRO constants and the updated constants for UO₂, as well as the constants for PuO₂.

Table 2.2. Parameters Used in UO₂ and PuO₂ Solid-Phase Thermal Expansion Correlations

Constant	MATPRO	FRAP	PuO ₂	Units
	UO ₂	UO ₂		
K ₁	1.0×10^{-5}	9.80×10^{-6}	9.0×10^{-6}	K ⁻¹
K ₂	3.0×10^{-3}	2.61×10^{-3}	2.7×10^{-3}	Unitless
K ₃	4.0×10^{-2}	3.16×10^{-1}	7.0×10^{-2}	Unitless
E _D	6.9×10^{-20}	1.32×10^{-19}	7.0×10^{-20}	J

For mixed UO₂ and PuO₂, the thermal expansion of the solid is found by combining the contribution from each constituent in proportion to its weight fraction.

During melting, an expansion equal to a linear strain of 0.043 occurs. If the fuel is partially molten, the strain due to thermal expansion is given by Equation 2.25.

$$\Delta L / L_0 = \Delta L / L_0(T_m) + 0.043 \cdot FACMOT \quad (2.25)$$

where

- $\Delta L/L_0(T_m)$ = thermal expansion strain of solid fuel from equations with $T = T_m$
- T_m = melting temperature of the fuel (K)
- FACMOT = fraction of the fuel which is molten (unitless)
 If FACMOT = 0.0, the fuel is all solid;
 If FACMOT = 1.0, the fuel is all molten

The correlation used to describe the expansion of entirely molten fuel is given by Equation 2.26.

$$\Delta L / L_0 = \Delta L / L_0(T_m) + 0.043 + 3.6 \times 10^{-5} [T - (T_m + \Delta T_m)] \quad (2.26)$$

The solid-to-liquid phase transition is isothermal only for pure UO_2 or pure PuO_2 . For MOX, the transition occurs over a finite temperature range, denoted in Equation 2.26 by ΔT_m .

Comparisons between the databases for UO_2 and PuO_2 with their respective correlations are presented in Figure 2.14 and Figure 2.15, respectively. In Figure 2.14, it can be seen that the updated constants used in FRAPCON-4.0/FRAPTRAN-2.0 (FRAP) for UO_2 provide a better fit to the high-temperature data than the previous constants used in MATPRO. The comparison in Figure 2.15 reveals good agreement between the correlation and the database.

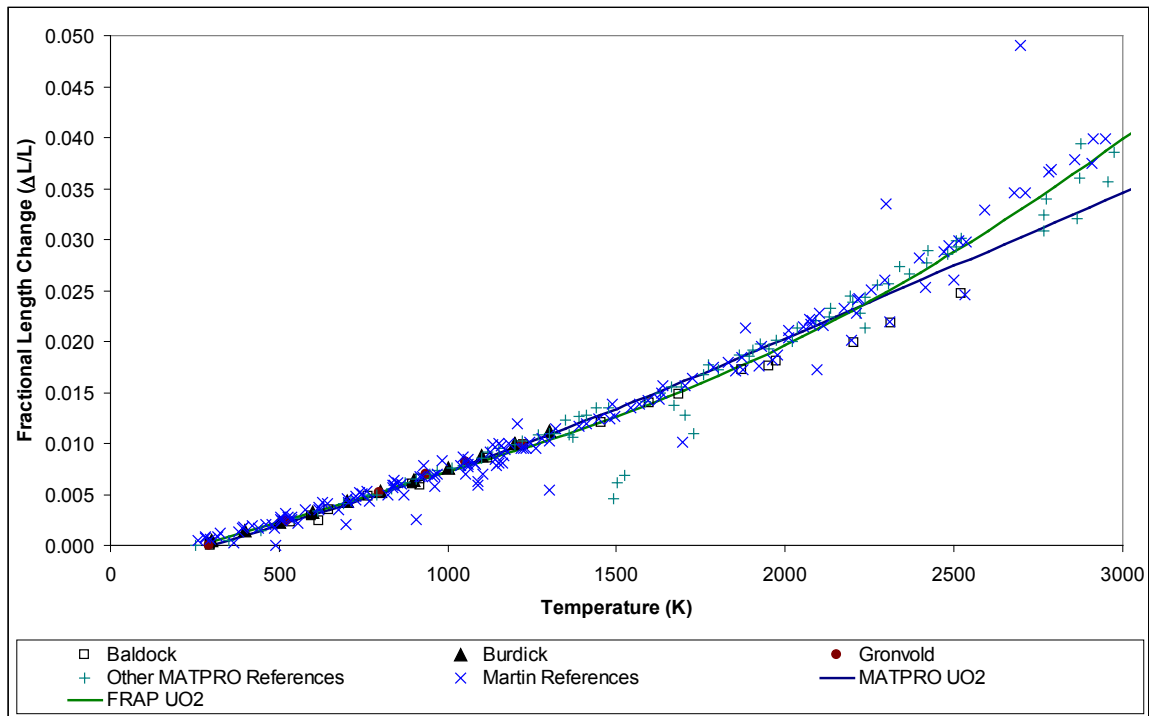


Figure 2.14. Model-to-Data Comparison for UO_2 Correlation Used in MATPRO and FRAPCON/FRAPTRAN with Updated Constants

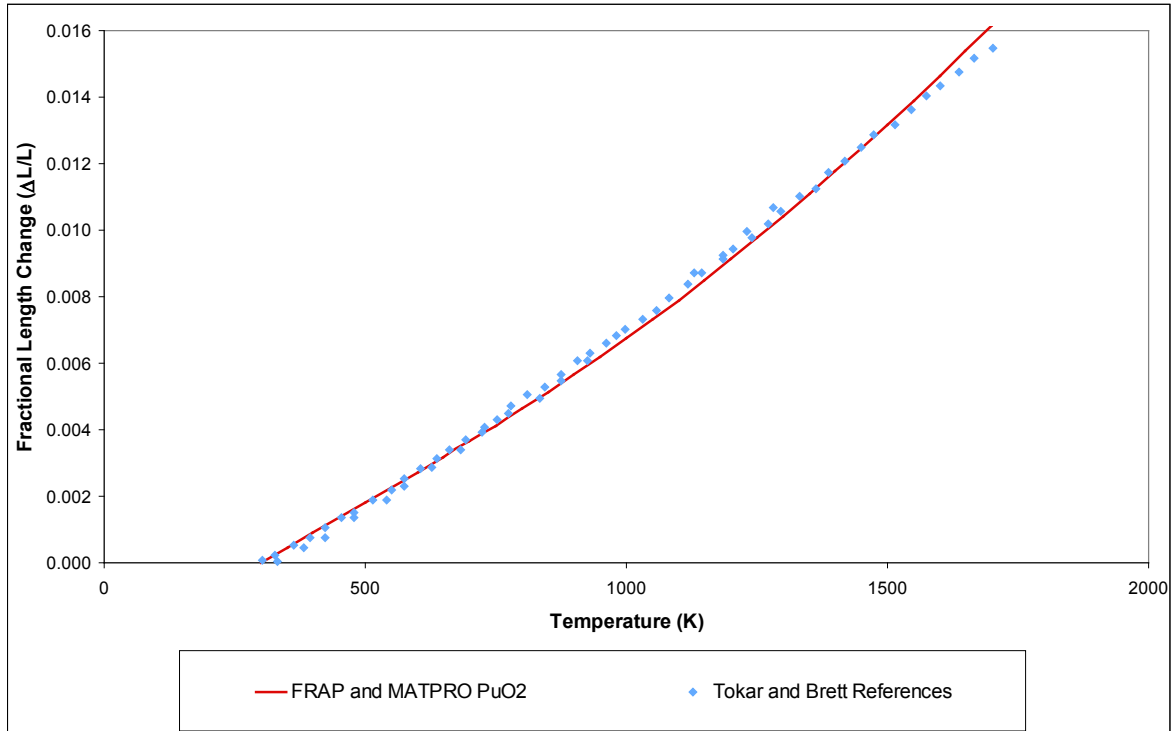


Figure 2.15. Model-to-Data Comparison for PuO₂ Correlation Used in MATPRO and FRAPCON/FRAPTRAN

2.5.2 Applicability and Uncertainty

The fuel thermal expansion correlation used in the FTHEXP subroutine is applicable through the melting temperature of the fuel (3111.15K for UO₂). The uncertainty of the pooled data was found to be temperature dependent, increasing approximately linearly with temperature. Therefore, a percentage error is given rather than a fixed number. The $\pm \sigma$ limits were found to be within ± 10 percent of the calculated value. Due to the limited amount of data, the same standard deviation is applied to the PuO₂ data.

2.6 Fuel Densification (FUDENS)

The subroutine Fuel Densification (FUDENS) calculates fuel dimensional changes due to densification of UO₂ and MOX during the first few thousand hours of water reactor operation. If available, data from resintering tests should be input by the user to determine densification (Regulatory Guide 1.126 [NRC 1978]). Otherwise, the subcode FUDENS calculates densification as a function of fuel burnup, temperature, and initial density.

The data used to develop FUDENS were taken from irradiated fuel which also included swelling (Rolstad 1974). If fuel densification is much greater than swelling during the first 1000 hours of irradiation, then, to a first approximation, swelling can be neglected during this period. This was done during the development of the FUDENS model.

The FUDENS subroutine is used in FRAPCON-4.0 and is similar to the correlation described by MATPRO. However, FUDENS is not included in FRAPTRAN because FRAPTRAN is intended for transient events occurring over a short time scale. Since densification occurs over longer time scales, it is not included in FRAPTRAN.

2.6.1 Model Development and Comparisons

The subroutine FUDENS uses one of two methods to calculate the maximum density change during irradiation. The RSNTR method uses the density change observed during resintering tests (1973K for 24 hours based on Regulatory Guide 1.126 [NRC 1978]) in a laboratory furnace and is the preferred input for the calculation. When RSNTR > 0, MATPRO uses either Equation 2.27 or 2.28 and 2.32 while FRAPCON-4.0 uses Equations 2.29 and 2.32. If a resintering density change is not input (i.e., RSNTR = 0), the TSINT method uses the initial unirradiated density of the fuel and the fuel fabrication sintering temperature and burnup for density calculations. For TSINT calculations, both MATPRO and FRAPCON-4.0 use either Equation 2.30 or 2.31 and 2.32. Both the RSNTR and TSINT methods for MATPRO and FRAPCON-4.0 are described by the following equations to calculate the maximum densification length change during irradiation.

In the MATPRO version of FUDENS, if a nonzero value for the resintering density change is input, then either Equation 2.27 or Equation 2.28 is used, depending on the fuel temperature, FTEMP (Siefken et al. 2001).

$$\text{For } FTEMP < 1000K \quad \left(\frac{\Delta L}{L} \right)_m = -(0.0015) RSNTR \quad (2.27)$$

$$\text{For } FTEMP \geq 1000K \quad \left(\frac{\Delta L}{L} \right)_m = -(0.00285) RSNTR \quad (2.28)$$

In FRAPCON-4.0, if the resintering density is a nonzero input, then the following equation is used to calculate the maximum dimensional change.

$$\left(\frac{\Delta L}{L} \right)_m = 100 * RSNTR / (3.0 * FDENS) \quad (2.29)$$

If zero is input for the resintering density change, then the MATPRO and FRAPCON-4.0 models use either Equation 2.30 or Equation 2.31, depending on the fuel temperature, FTEMP (Rolstad et al. 1974).

$$\text{For } FTEMP < 1000K \quad \left(\frac{\Delta L}{L} \right)_m = \frac{-22.2(100 - DENS)}{(TSINT - 1453)} \quad (2.30)$$

$$\text{For } FTEMP \geq 1000K \quad \left(\frac{\Delta L}{L} \right)_m = \frac{-66.6(100 - DENS)}{(TSINT - 1453)} \quad (2.31)$$

where

$$\begin{aligned} \left(\frac{\Delta L}{L}\right)_m &= \text{maximum possible dimension change of fuel due to irradiation (percent)} \\ \text{RSNTR} &= \text{resintered fuel density change (kg/m}^3\text{)} \\ \text{FTEMP} &= \text{fuel temperature (K)} \\ \text{DENS} &= \text{initial density (percent theoretical)} \\ \text{TSINT} &= \text{sintering temperature (K)} \\ \text{FDENS} &= \text{starting density (kg/m}^3\text{)} \end{aligned}$$

Densification as a function of burnup is calculated using

$$\frac{\Delta L}{L} = \left(\frac{\Delta L}{L}\right)_m + e^{[-3(FBU+B)]} + \left(2.0 e^{[-35(FBU+B)]}\right) \quad (2.32)$$

where

$$\begin{aligned} \left(\frac{\Delta L}{L}\right) &= \text{dimension change (percent)} \\ \text{FBU} &= \text{fuel burnup (MWd/kgU)} \\ \text{B} &= \text{a constant determined by the subcode to fit the boundary condition: } \Delta L/L \\ &= 0 \text{ when FBU} = 0 \end{aligned}$$

The FUDENS subcode presented in Equation 2.32 is used to calculate total densification, and then the densification from the previous time step is subtracted to obtain the incremental densification. The incremental densification for the time step being considered is the output of the subcode FUDENS and is determined by Newton's method (Hamming 1971).

The relationship between densification and burnup in Equation 2.32 was originally suggested by Rolstad et al. (1974). This relationship was adopted for use in the FUDENS subroutine because it successfully describes the burnup dependence of both the original data (Rolstad et al. 1974) and Electric Power Research Institute data (Freshley et al. 1976) that was collected shortly thereafter. Since these initial studies, there have been additional in-reactor densification data collected for UO₂ and MOX fuels irradiated in thermal reactors.

Banks (1974) reported densification data on solid and annular UO₂ pellets irradiated in the Winfrith Steam Generating Heavy Water Reactor and the Halden Boiling Water Reactor. The solid pellets experienced centerline temperatures of 733 to 2443K over the burnup range 0.37 to 23.7 MWd/kgU. They concluded that pellets with centerline temperatures less than 1423K densified during irradiation, but at higher temperatures dimensional change was affected by intergranular fission gas swelling. Therefore, only data for temperatures less than 1423K were included in comparison with the FUDENS model (Equations 2.30, 2.31, and 2.32). The mechanism for densification was determined to be the loss of pores with initial diameters less than 2 μm.

Freshley et al. (1978) reported densification data on MOX pellets irradiated in the radially adjustable facility tubes of the General Electric Test Reactor. Two pins were irradiated with fuel centerline temperatures up to 2048K and burnup to 4.6 MWd/kgM. The pellets were fabricated with sintering

temperatures from 1748 to 2008K and had starting density values ranging from 91 to 95 percent TD. They concluded that dilute additions of PuO₂ in UO₂ (up to 6 wt% PuO₂) do not change the densification behavior of the fuel. The mechanism of densification was observed to be sintering of pores with initial diameters of 0.5 μm or smaller.

Small (1987) irradiated four types of UO₂ pellets in the Harwell Materials Test Reactor. Pellet centerline temperatures ranged from 623 to 1823K and burnup ranged from 0.0025 to 2.6 MWd/kgU. Three of the four types of pellets were fabricated with pores smaller than 2 μm in diameter to more carefully examine the mechanisms behind densification. For reference, fuel currently fabricated has very few pores less than 2 μm in diameter. Densification was determined by measuring porosity before and after irradiation. At centerline temperatures above 1273K, densification was caused by sintering of pores less than 1 μm in diameter.

Figure 2.16 compares measured and predicted values of densification using the TSNTNTR correlation, which is used in both FRAPCON-4.0 and MATPRO and incorporates Equations 2.30, 2.31, and 2.32.

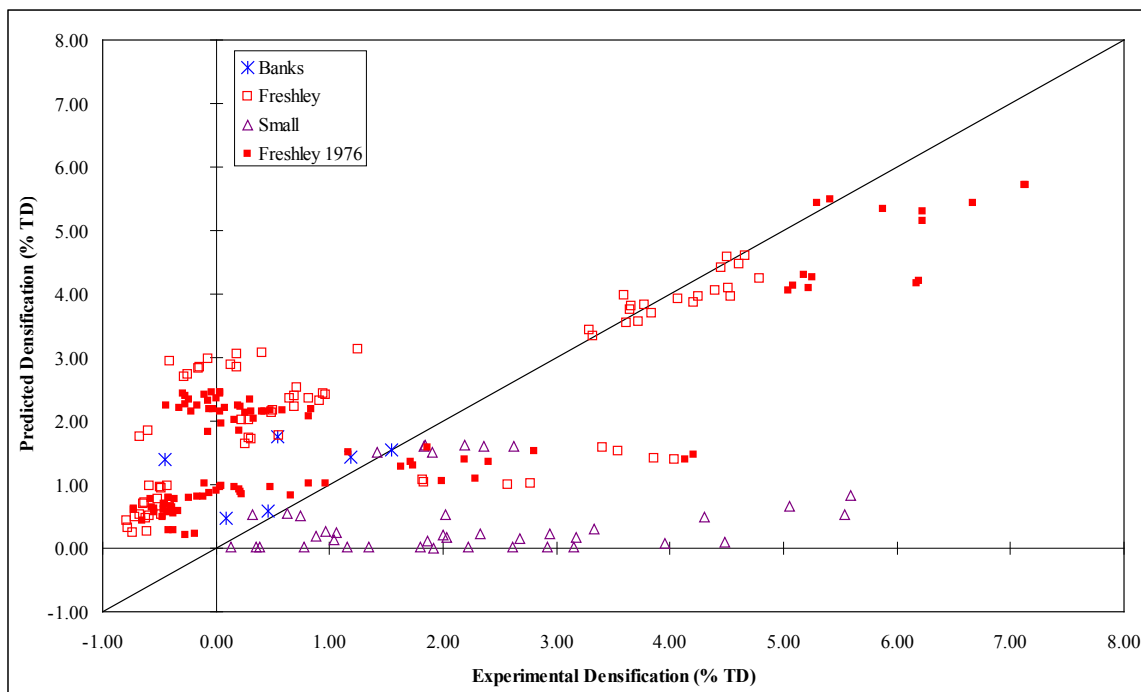


Figure 2.16. Comparison of Densification Predictions Generated by the FUDENS Model and Experimental Densification Measurements Determined in Reactor

This data comparison demonstrates that basing densification on the sintering temperature provides a large degree of uncertainty. However, it should be noted that the Small (1987) data, which exhibited very high densification at very low burnup (less than 0.07 MWd/kgU), possessed a non-prototypic pore size distribution that was heavily weighted toward smaller diameters. Three of the four fuel types had 100 percent of their porosity in pores smaller than 2 μm diameter, which is atypical of current fuel fabrication.

Since in-reactor densification is strongly influenced by fuel fabrication, ex-reactor re-sintering tests are the preferred method for predicting in-reactor fuel densification (NRC 1978). Ex-reactor resintering tests conducted by Freshly et al. (1976 and 1978) at 1600 and 1700°C provided reasonable estimate of in-reactor densification tests with standard deviations of 0.5 to 0.6 percent of the theoretical density.

2.6.2 Applicability and Uncertainty

The densification correlation used in the subroutine FUDENS is applicable to fuels with pore size distributions that are similar to those included in the Freshley et al. (1976) study. Due to the scatter in the experimental data, it is difficult to establish a meaningful measure of uncertainty.

2.7 Fuel Swelling (FSWELL)

The subroutine Fuel Swelling (FSWELL) calculates fuel swelling, which is caused by the buildup of solid and gaseous fission products during irradiation. FSWELL is combined with creep induced elongation (FCREEP) and densification due to pressured sintering (FHOTPS) and irradiation (FUDENS) to calculate the overall dimensional changes in fuel.

The gaseous swelling correlation in FSWELL was not used in previous versions of FRAPCON because it significantly overpredicts swelling. However, a new gaseous swelling model was devised for FRAPCON-4.0 after ramp tests suggested gaseous swelling may contribute to permanent cladding deformation in high burnup rods. As for solid swelling, a modified version of the solid swelling correlation presented in the MATPRO FSWELL subroutine was adopted for FRAPCON. Although this solid swelling model is still used in FRAPCON-4.0, an additional model and recommendations for modeling solid swelling in gadolinia-doped fuels is also provided. The FSWELL subroutine is only applicable to time scales on the order of minutes to hours and, therefore, not used in FRAPTRAN-2.0.

2.7.1 Model Development and Comparisons

In MATPRO, the correlation used by FSWELL to calculate swelling due to the buildup of solid fission products is give by Equation 2.33.

$$S_g = 2.5 \times 10^{-29} B_s \quad (2.33)$$

where

$$\begin{aligned} S_s &= \text{fractional volume change due to solid fission products} \\ &\quad (\text{m}^3 \text{ volume change}/\text{m}^3 \text{ fuel}) \\ B_s &= \text{burnup during a time step (fissions}/\text{m}^3) \end{aligned}$$

At temperatures below 2800K, swelling due to the buildup of gaseous fission products is given by Equation 2.34.

$$S_g = 8.8 \times 10^{-56} (2800 - T)^{11.73} e^{[-0.0162(2800 - T)]} e^{[-8.0 \times 10^{-27} B]} B_s \quad (2.34)$$

where

$$\begin{aligned}
 S_g &= \text{fractional volume change due to gas fission products (m}^3 \text{ volume change/m}^3 \text{ fuel)} \\
 T &= \text{temperature (K)} \\
 B &= \text{total burnup of fuel (fissions/m}^3\text{)}
 \end{aligned}$$

For temperatures greater than 2800K, S_g is zero because it is assumed that the gas that causes swelling is released. The correlations presented in Equations 2.33 and 2.34 are used to determine swelling due to solid and gaseous fission product buildup, respectively, in the FSWELL subcode described by MATPRO.

Although previous releases of FRAPCON have considered solid swelling, the effects of gaseous swelling have been ignored based on available model-to-data comparisons. Comparison between FRAPCON predictions and NRC-sponsored test rod results revealed that the MATPRO swelling model that included gaseous fission product buildup overpredicted test results at burnup levels up to 10GWd/MTU (Lanning and Bradley 1984; Lanning et al. 1997). Consequently, it was determined that swelling could be modeled better by eliminating the contribution from gaseous fission products and increasing the contributions of solid fission products from 0.669 percent (MATPRO and FRAPCON-2) to 0.77 percent (FRAPCON) per 10 GWd/MTU.

However, a gaseous swelling model has been introduced in FRAPCON-4.0. The FRAPCON-4.0 model is based on data from Mogensen (Mogensen et al. 1985) and was developed after ramp test results suggested gaseous swelling may influence permanent cladding hoop strain in high burnup rods. The linear strain is given as a function of temperature over the ranges given in equations 2.35 and 2.36. These models are phased in between 40 and 50 GWd/MTU by applying a factor that varies linearly between 0 and 1 at 40 and 50 GWd/MTU, respectively.

$$\frac{\Delta l}{l} = 4.55 \times 10^{-5} T - 4.37 \times 10^{-2} \quad (960^\circ < T < 1370^\circ\text{C}) \quad (2.35)$$

$$\frac{\Delta l}{l} = -4.05 \times 10^{-5} T + 7.40 \times 10^{-2} \quad (1370^\circ < T < 1832^\circ\text{C}) \quad (2.36)$$

As of FRAPCON-3.4, the solid swelling was decreased to 0.62 percent per 10 GWd/MTU for burnup less than 80 GWd/MTU and increased to 0.86 percent per 10 GWd/MTU for burnup greater than 80 GWd/MTU. This is the same assumption for solid swelling that is used in FRAPCON-4.0. The correlations used to calculate fuel swelling under these conditions are given in Equations 2.37 and 2.38, respectively.

For burnup < 80 GWd/MTU

$$\text{soldsw} = \text{bus} * (2.315 \times 10^{-23} + \text{sigswell} * 2.987 \times 10^{-24}) \quad (2.37)$$

For burnup > 80 GWd/MTU

$$\text{soldsw} = \text{bus} * (3.211 \times 10^{-23} + \text{sigswell} * 5.974 \times 10^{-24}) \quad (2.38)$$

where

- soldsw = fractional volume change due to solid fission products (m^3 volume change/ m^3 fuel)
- sigswell = user-defined parameter that incrementally changes error
- bus = fuel burnup during time step (analogous to B_S in MATPRO model)
- fdens = initial pellet density (kg/m^3)
- bu = burnup at end of time step (MWs/kgU)
- bul = burnup at end of previous time step (MWs/kgU)

and

$$bus = fdens * 2.974 \times 10^{10} * (bu - bul)$$

The variable “bus” in Equations 2.37 and 2.38 is analogous to the variable “ B_S ” in Equation 2.33. However, “bus” permits the fractional volume change due to solid fission products to be determined as a function of burnup in MWs/kgU as opposed to fissions/ m^3 .

A comparison between the MATPRO and the FRAPCON-4.0 versions of FSWELL is presented in Figure 2.17 along with experimental data from immersion density measurements. Based on this figure, it can be seen that the FRAPCON-4.0 model predicts less swelling than the MATPRO model, which tends to overpredict the experimentally determined data points.

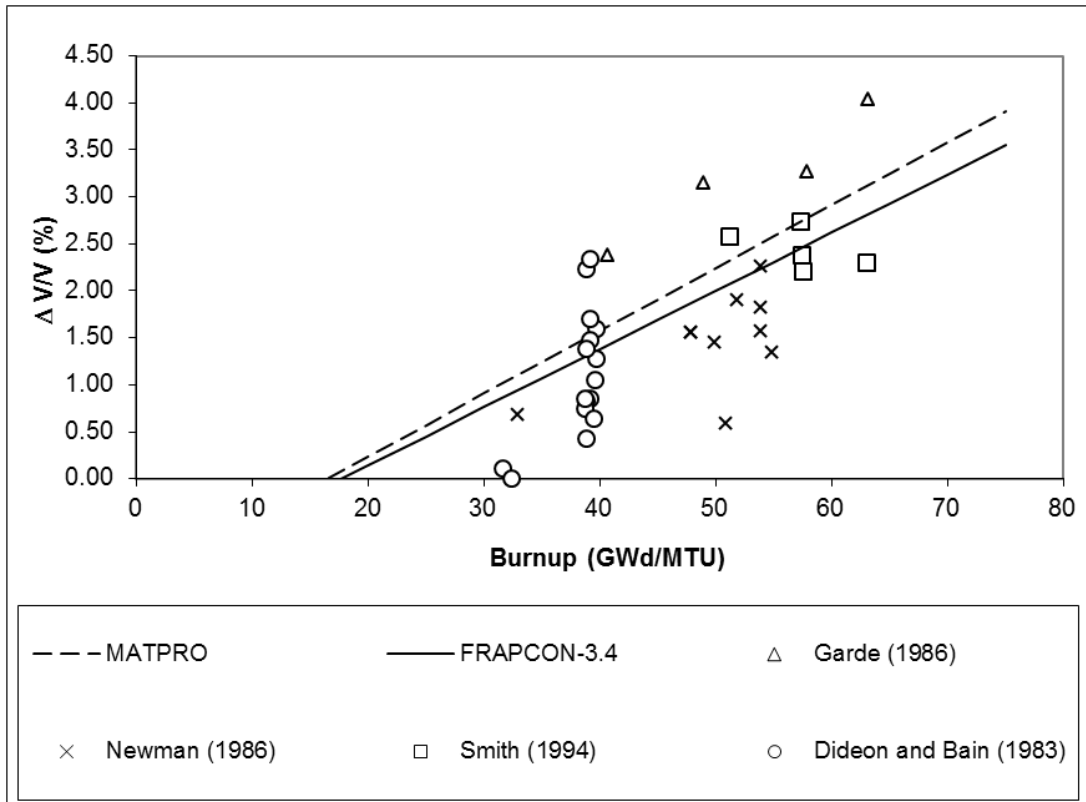


Figure 2.17. Data Comparison between MATPRO and FRAPCON Versions of FSWELL

For burnup > 80 GWd/MTU, a higher swelling rate is used in the FRAPCON-4.0 version of FSHELL. Data comparisons between FRAPCON-4.0 predictions and data from instrumented fuel assemblies tested at Halden are presented in Figure 2.18 for varying levels of burnup. These Halden swelling data are based on measurements of fuel stack length and cladding diameter change with burnup and converted to volume swelling assuming isotropic swelling. The diametral cladding change data versus burnup is particularly valuable because it implicitly includes the effects of cladding restraint on fuel swelling.

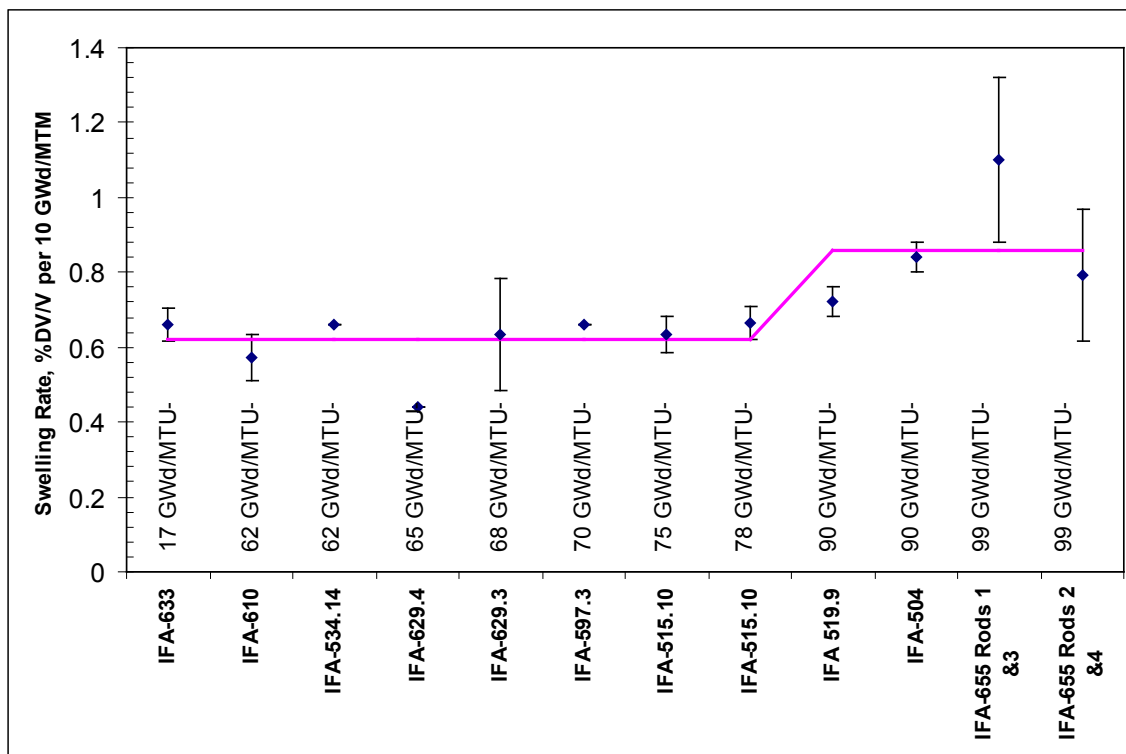


Figure 2.18. Comparison between Swelling Rates Determined for Various Instrumented Fuel Assemblies Rests at Halden and Swelling Rates Predicted by FRAPCON

The solid swelling model in FRAPCON-4.0 was also revised to model gadolinia-doped fuels. For gadolinia-doped fuels, the swelling rate was reduced from 0.62 to 0.50% per 10 GWd/MTU based on swelling data from several integrated fuel assemblies irradiated in Halden (Colombier et al. 2010). This lower swelling rate for gadolinia-doped fuels is extended to higher burnups rather than modified to reflect any assumed changes in swelling behavior. It is also recommended that “zero” densification be assumed for gadolinia-doped fuels to reproduce experimentally observed swelling behavior.

2.7.2 Applicability and Uncertainty

Based on the data from which it is derived, the correlation used in FSHELL is applicable to fuels with burnups up to 100 GWd/MTU. Below 80 GWd/MTU, a 1-sigma uncertainty of 0.08 percent $\Delta V/V$ per 10 GWd/MTU has been calculated. Above 80 GWd/MTU, a 1-sigma uncertainty of 0.16 percent $\Delta V/V$ per 10 GWd/MTU has been calculated.

3.0 Cladding Material Properties

Material property correlations for fuel claddings are described in the following subsections. Unless otherwise specified, the correlations below are applicable to Zircaloy-2, -4, ZIRLO, Optimized ZIRLO, and M5. Various heat treatments can be accommodated by specifying the coldworked condition of the alloy. Examples of coldworked conditions for the different alloys are provided in Table 3.1.

Table 3.1. Example Heat Treatments and Coldworked Conditions for Different Alloys

Alloy	Heat Treatment	Cold Worked Condition
Zr-4	Cold Worked, Stress Relief Annealed	50%
Zirlo	Cold Worked, Stress Relief Annealed	50%
Optimized Zirlo	Partially Recrystallized Annealed	< 50%
M5	Recrystallized Annealed	0%
Zr-2	Recrystallized Annealed (typical Zr-2 condition)	0%

In addition, several FRAPTRAN-2.0 subroutines include additional correlations to describe a Russian zirconium alloy containing 1 wt% niobium (ZrNb-1). The subroutine used to determine the material correlation in either the FRAPCON or FRAPTRAN codes is given in parentheses.

3.1 Cladding Specific Heat (CCP)

The specific heat subcode, Cladding Specific Heat (CCP), determines the true specific heat at constant pressures for cladding. Specific heat calculations are based on interpolation of measured data. The correlation in FRAPCON-4.0, FRAPTRAN-2.0, and MATPRO is applicable to Zircaloy-2, Zircaloy-4, ZIRLO, Optimized ZIRLO, and M5 alloys. However, FRAPTRAN-2.0 contains correlations to calculate the specific heat of ZrNb-1. This calculation can be based on data collected at either fast or slow heating rates and the user can designate the appropriate data set.

3.1.1 Model Development and Comparisons

The CCP subcode requires temperature as an input to calculate specific heat. For the alpha phase of the Zircaloy alloys (temperature less than 1090K), CCP returns linear interpolations for the points listed in Table 3.2. These data points are based on precise data taken by Brooks and Stansbury (1966) with a Zircaloy-2 sample that had been vacuum-annealed at 1075K to remove hydrogen, which would have otherwise affected the measurement.

The standard errors associated with this interpolation technique differ between MATPRO and FRAPCON-4.0/FRAPTRAN-2.0. In MATPRO, the standard error of the CCP interpolation was based on 90 points in the Brooks and Stansbury (1966) database and was found to be temperature dependent. For the 57 data points between 300 and 800K, the standard error is 1.1 J/kg*K. Between 800 and 1090K, it is 2.8 J/kg*K. The FRAPCON-4.0/FRAPTRAN-2.0 codes assume a standard error of 10 J/kg*K below 1090K.

For temperatures from 1090 to 1300K (where Brooks and Stansbury do not report results), values of specific heat proposed by Deem and Eldridge (1967) are adopted. The Deem and Eldridge (1967) values are based on measurements of enthalpy and temperature which provide considerably less precise specific heat data than the results of Brooks and Stansbury (1966).

As a result, the MATPRO standard error estimated from the Deem and Eldridge (1967) data in the region of 1090 through 1310K is 10.7 J/kg*K. This standard error is a measure only of the precision of the fit, since only a single data source is used. The standard error in FRAPCON 4.0/FRAPTRAN-2.0 is assumed to be 25 J/kg*K between 1090 and 1300K.

Above the alpha + beta to beta transformation temperature (about 1250K) and up to about 1320K, a constant value of 355.7 J/kg*K was reported by Deem and Eldridge (1967). This value agrees well with a value of 365.3 reported by Coughlin and King (1950) for pure beta zirconium. The standard error of specific heat calculations made above 1300K is assumed to be 100 J/kg*K in the FRAPCON-4.0/FRAPTRAN-2.0 codes.

Table 3.2. Specific Heat Capacity Database for Zircaloy-2, Zircaloy-4, ZIRLO, Optimized ZIRLO, and M5

Temperature (K)	Specific Heat Capacity (J/kg*K)	Source	Standard Error	
			MATPRO (J/kg*K)	FRAPCON / FRAPTRAN (J/kg*K)
-----Alpha Phase-----				
300	281	Brooks and Stansbury	1.1	10
400	302	Brooks and Stansbury	1.1	10
640	331	Brooks and Stansbury	1.1	10
1090	375	Brooks and Stansbury	2.8	10
-----Beta Phase-----				
1093	502	Deem and Eldridge	10.7	25
1113	590	Deem and Eldridge	10.7	25
1133	615	Deem and Eldridge	10.7	25
1153	719	Deem and Eldridge	10.7	25
1173	816	Deem and Eldridge	10.7	25
1193	770	Deem and Eldridge	10.7	25
1213	619	Deem and Eldridge	10.7	25
1233	469	Deem and Eldridge	10.7	25
1248	356	Deem and Eldridge	10.7	25
2098	356	Coughlin and King	100	100
2099	356	Coughlin and King	100	100

In addition to Zircaloy alloys, FRAPTRAN-2.0 has been modified to include specific heat calculations for ZrNb-1. These calculations are based on data collected at two different heating rates. Depending on the user input, specific heat calculations can be based on either the fast or the slow heating rate data. The data used to interpolate specific heat values for the ZrNb-1 alloy are presented in Table 3.3. There is no standard error described for specific heat calculations based on these data sets.

Table 3.3. Specific Heat Capacity Database for ZrNb-1 Alloys

Temperature (K)	Specific Heat Capacity (J/kg*K)	Source
----- Low Heating Rate (< 1000 K/s) -----		
280	345	Volkov BYu et al.
473	360	Volkov BYu et al.
573	370	Volkov BYu et al.
673	380	Volkov BYu et al.
773	383	Volkov BYu et al.
873	385	Volkov BYu et al.
883	448	Volkov BYu et al.
973	680	Volkov BYu et al.
1025	816	Volkov BYu et al.
1073	770	Volkov BYu et al.
1153	400	Volkov BYu et al.
1173	392	Volkov BYu et al.
1248	356	Volkov BYu et al.
----- High Heating Rate (> 1000 K/s) -----		
1100	412	Ljusternik VE et al.
1110	420	Ljusternik VE et al.
1120	480	Ljusternik VE et al.
1134	600	Ljusternik VE et al.
1142	1000	Ljusternik VE et al.
1150	1400	Ljusternik VE et al.
1155	1600	Ljusternik VE et al.
1161	1400	Ljusternik VE et al.

3.1.2 Applicability and Uncertainty

The CCP subroutine is valid over the temperature range from which the data sets have been collected on zirconium alloys (300 to 2099K). This correlation is applied to Zircaloy-2, -4, ZIRLO, Optimized ZIRLO, and M5. However the standard error increases with increasing temperature as indicated in Table 3.2.

3.2 Cladding Thermal Conductivity (CTHCON)

The subroutine Cladding Thermal Conductivity (CTHCON) is used to calculate cladding thermal conductivity, which is required for accurate predictions of fuel temperature. The thermal conductivity of the cladding is primarily a function of temperature. Other characteristics, such as residual stress levels, crystal orientation, and minor composition differences, may have secondary effects on thermal conductivity. The correlation used in CTHCON to calculate cladding thermal conductivity is the same in MATPRO, FRAPCON-4.0, and FRAPTRAN-2.0. This correlation is applied to Zircaloy-2, -4, ZIRLO, Optimized ZIRLO, and M5. In addition, FRAPTRAN 1.4 includes a correlation to calculate the cladding thermal conductivity of ZrNb-1.

3.2.1 Model Development and Comparisons

Considering only temperature as the defining parameter, the thermal conductivity of Zircaloy for temperatures less than 2098K is described by CTHCON in Equation 3.1. The uncertainty of the conductivity calculations is given in Equation 3.2.

$$k = 7.51 + 2.09 \times 10^{-2} T - 1.45 \times 10^{-5} T^2 + 7.67 \times 10^{-9} T^3 \quad (3.1)$$

$$\sigma_k = 1.01 \quad (3.2)$$

For temperatures greater than or equal to 2098K, the thermal conductivity and uncertainty are given in Equations 3.3 and 3.4, respectively.

$$k = 36 \quad (3.3)$$

$$\sigma_k = 5 \quad (3.4)$$

where

- k = thermal conductivity of Zircaloy (W/m* K)
- T = temperature (K)
- σ_k = standard deviation (W/m*K)

Equation 3.1 predicts k very well from room temperature to the data limit of about 1800K (Figure 3.1) and may be extrapolated with some confidence to the melting point. The standard deviation (σ_k) of the data with respect to this correlation appears to be temperature independent over the data range.

The standard deviation of the constants in Equation 3.1 is 20 to 30 percent of the value of the constant. Jensen (1969) performed a parametric analysis of several variables involved in the estimation of fuel and cladding temperatures. Both steady-state and transient analysis showed that variations of ± 20 percent resulted in calculated cladding temperature variations of about 2.8K. Fuel centerline temperatures are more sensitive to cladding thermal conductivity and showed variations of 28K. Similar findings were reported by Korber and Unger (1974).

For temperatures less than 2133K, the thermal conductivity of the ZrNb-1 alloy is calculated by FRAPTRAN-2.0 with the correlation presented in Equation 3.5.

$$k = 15.0636 e^{0.000461843 * T} \quad (3.5)$$

For temperatures above 2133K, the thermal conductivity of the ZrNb-1 cladding is assumed to be 36 W/m*K.

Figure 3.1 compares the CTHCON model as incorporated in MATPRO, FRAPCON-4.0, and FRAPTRAN-2.0 with the data on which it is based, extrapolated to the melting point of Zircaloy (2098K).

Figure 3.2 compares the CTHCON model with the Zircaloy thermal conductivity and diffusivity data that were not included in development of the model. Thermal diffusivity data, such as that provided by Peggs and Bunnell et al. (1983), were converted to thermal conductivity using the recommended models in Fink (2000) for specific heat and density, respectively. Although different alloys were examined, there were no discernable differences between the alloys. The scatter in the data due to differences in alloy, form, or measurement direction is comparable to the variation between individual data sets. The scatter in the data is distributed relatively uniformly around the curve representing the CTHCON model, except for anomalously high Peggs data below 1000K and the anomalously low Bunnell et al. (1983) data above 1300K. The relative error determined by comparison between the data presented in both Figure 3.1 and Figure 3.2, respectively, and the CTHCON model described in Equation 3.1 is approximately 9%.

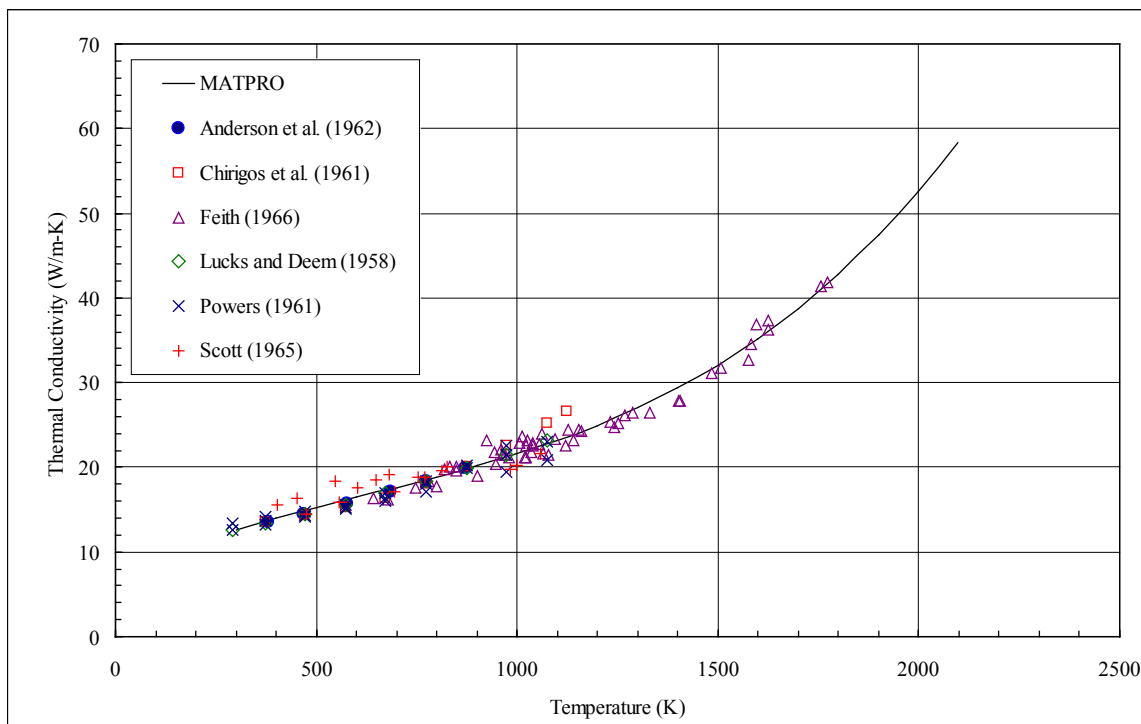


Figure 3.1. CTHCON Model and Data Used for Development

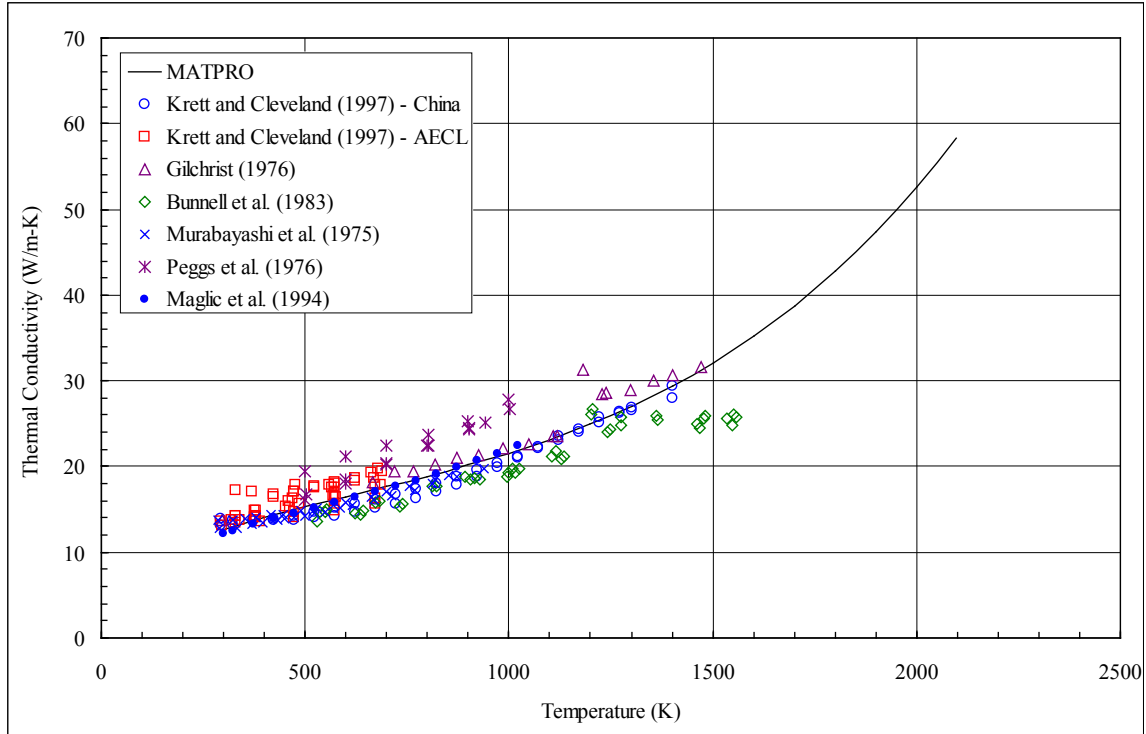


Figure 3.2. CTHCON Model and Data Collected Since Development

3.2.2 Applicability and Uncertainty

The correlation used in CTHCON to calculate the cladding thermal conductivity may be applied to temperatures up to the melting temperature of Zircaloy (2098K). The uncertainty through this range of temperature is given by Equation 3.2. Above the melting temperature, the uncertainty increases to the value given by Equation 3.4.

3.3 Cladding Oxide Thermal Conductivity (ZOTCON)

The Cladding Oxide Thermal Conductivity (ZOTCON) subroutine calculates the thermal conductivity of the zirconium oxide layer that forms on zirconium alloys. Cladding temperature is the only parameter used to calculate zirconium oxide thermal conductivity. The correlation used in the ZOTCON subroutine differs between MATPRO (2001) and the FRAPCON-4.0/FRAPTRAN-2.0 codes. The MATPRO (2001) correlation is based on an arbitrary correction to an earlier correlation that was fit to a large database of oxide thermal conductivity measurements. This database contained measurements from a variety of zirconium oxide materials and test methods. The correction was applied to better fit data that was more representative of the oxide layer that forms on zirconium alloys. The correlation used in FRAPCON-4.0 and FRAPTRAN-2.0 is based on measurements obtained by Kingery (1954) from fully dense and porous (87 percent TD) zirconium oxides.

3.3.1 Model Development and Comparisons

Oxide thermal conductivity models in MATPRO and FRAPCON-4.0/FRAPTRAN-2.0 are only a function of temperature. After the cladding temperature is established, the thermal conductivity of the oxide layer can be calculated using the correlation determined from either the MATPRO or the FRAPCON-4.0/FRAPTRAN-2.0 databases.

The MATPRO (2001) correlation is derived from a database that includes data collected by Adams (1954), Maki (1973), Lapshov and Bashkatov (1973), and Gilchrist (1976). The correlation used in FRAPCON-4.0/FRAPTRAN-2.0 is derived from data collected by Kingery (1954). The FRAPCON-4.0/FRAPTRAN-2.0 correlation and database was adopted from an earlier version of MATPRO (Hagrman et al. 1981).

The database for the MATPRO (2001) model includes data from a variety of zirconium oxide materials and test conditions. The Maki (1973) data include two samples oxidized in steam over a small temperature range and show a sharp increase in conductivity between 400 and 500K. The principal recommendation for the data is that they were taken with black oxide from Zircaloy tubes. Two sets of data attributed to Waldman by Maki are also shown in the table. The data of Lapshov and Bashkatov (1973) are from films formed by plasma sputtering of zirconium dioxide on tungsten substrates. However, these data may not be representative of Zircaloy cladding oxide thermal conductivity because sputtered coatings are quite porous. In addition, these films do not have the same O/M ratio as cladding oxide and may not adhere well to the substrate. The Gilchrist (1976) data includes two types of oxide films. One is a nodular oxide and the other a black oxide characteristic of the kinds of layers usually reported in high-temperature tests with cladding. The nodular oxide thermal conductivities are much lower than the black oxide thermal conductivities, and both kinds of oxide have conductivities that are significantly lower than the stabilized Zircaloy dioxide conductivities reported by Adams (1954). Considerable uncertainty is reported by Gilchrist (1976) because of difficulty in measuring oxide film thickness.

The database for the FRAPCON-4.0 and FRAPTRAN-2.0 model is based on data from Kingery (1954). The data are from two different samples; one was a bulk sample of 100 percent dense ZrO₂ and the other with approximately 13 percent porosity.

Each database was fit with a different model to relate the thermal conductivity of the cladding oxide layer to temperature. The equations used to describe these models are presented in Equations 3.6 and 3.7 for MATPRO and FRAPCON-4.0/FRAPTRAN-2.0 (i.e., FRAP), respectively. These models relate the thermal conductivity of the cladding oxide layer, K (W/m*K), to cladding temperature, T (K).

$$K_{MATPRO} = 0.835 + 1.81 \times 10^{-4} T \quad (3.6)$$

$$K_{FRAP} = 1.9599 - T * (2.41 \times 10^{-4} - T * (6.43 \times 10^{-7} - T * 1.946 \times 10^{-10})) \quad (3.7)$$

Both databases are presented in Figure 3.3 along with both cladding oxide thermal conductivity models. In addition, a more recent data set from Gilchrist (1979) is included. Figure 3.3 reveals that the FRAP model fits the Kingery data from which it was derived and agrees well with the measurements performed by Adams (1954). The FRAP model tends to overestimate both the Gilchrist data sets and the data from Lapshov and Bashkatov (1973). However, as stated earlier, the earlier Gilchrist (1976) data is associated

with considerable uncertainty and the data from Lapshov and Bashkatov (1973) is likely to be low due to different O/M ratios and high porosity in the sputtered films.

The MATPRO model was initially fit to the data collected by Adams (1954), but it was adjusted to the form presented in Equation 3.6 to better fit the Gilchrist (1976) data for black oxide. The rationale for this correction was that the black oxide was more prototypic of the cladding oxide layer and was achieved by dividing the original equation by two.

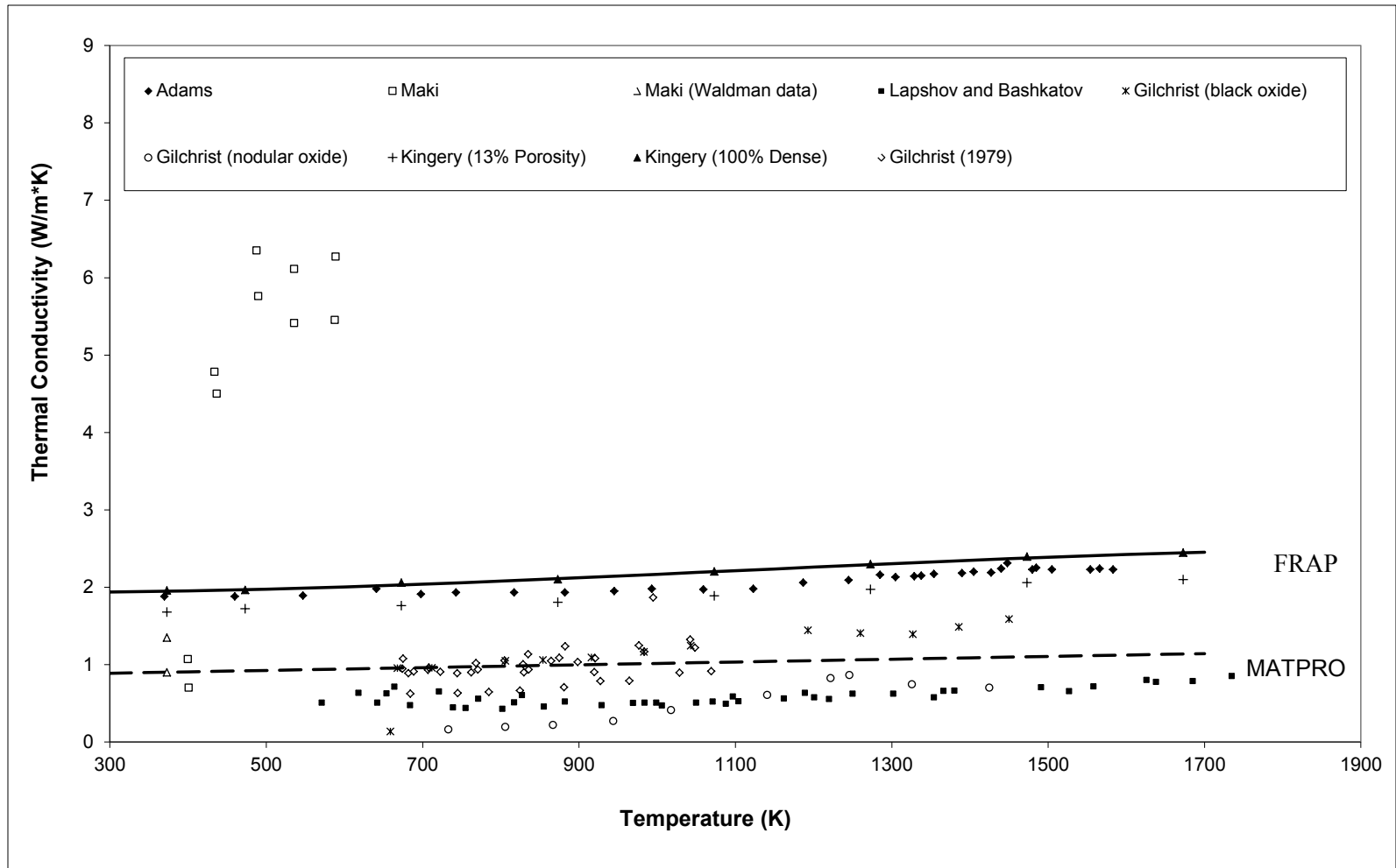


Figure 3.3. Oxide Thermal Conductivity Measurements as a Function of Temperature Compared with the MATPRO and FRAPCON-4.0/FRAPTRAN-2.0 (FRAP) Cladding Oxide Thermal Conductivity Models

3.3.2 Applicability and Uncertainty

The subroutine ZOTCON in FRAPCON-4.0/FRAPTRAN-1.4 is applicable over the temperature range for which the data was collected, 375 to 1673K. Since the relatively high density of the bulk ZrO₂ materials bias the thermal conductivity measurements high, it is difficult to establish a meaningful measurement of uncertainty.

The MATPRO model is applicable from 300K to the melting temperature (2973K). Upon melting the thermal conductivity, K_{Liquid} (W/m*K), is assumed to be described by Equation 3.8 (Hagrman et al. 1981).

$$K_{Liquid} = 1.4 \quad (3.38)$$

The standard error for the MATPRO model is approximately ± 0.75 W/m*K, but is assumed to be within 10 percent for materials that are known to be dense (>87%TD) ZrO₂.

3.4 Cladding Surface Emissivity (ZOEMIS)

The subcode Cladding Surface Emissivity (ZOEMIS) returns the cladding surface emissivity, which is directly proportional to the radiant heat transfer from the cladding surface during an abnormal transient. The ZOEMIS model described in MATPRO is the same as the model used in FRAPCON-4.0 and FRAPTRAN-2.0.

3.4.1 Model Development and Comparisons

Surface emissivities are significantly affected by surface layers on the cladding. For cladding with thin oxide coatings, the oxide surface thickness is only a few wavelengths of near infrared radiation and is partly transparent. Oxide thickness is an important parameter for these thin coatings. Thicker oxide layers are opaque, so the oxide thickness is not as important as the nature of the outer oxide surface, which is affected by temperature and by chemical environment. The effect of temperature has been modeled, but variations in crud on the external cladding surface and chemical reaction products on the inside surface are not modeled explicitly.

The model for emissivity was constructed by considering measured emissivities reported by several investigators. Expressions used to predict the emissivity of Zircaloy cladding surfaces are summarized below.

When the cladding surface temperature has not exceeded 1500K, emissivities are modeled by Equations 3.9 and 3.10. Equation 3.9 is used for oxide layers less than 3.88×10^{-6} m thick and Equation 3.10 is used for oxide layers equal to or greater than 3.88×10^{-6} m thick. Both equations relate the hemispherical emissivity, ϵ_1 (unitless), to the oxide layer thickness, d (m).

$$\epsilon_1 = 0.325 + 0.1246 \times 10^6 d \quad d < 3.88 \times 10^{-6} \quad (3.9)$$

$$\epsilon_1 = 0.808642 - 50.0 d \quad d > 3.88 \times 10^{-6} \quad (3.10)$$

When the maximum cladding temperature has exceeded 1500K, emissivity is taken to be the larger of 0.325 and the result of Equation 3.11. Equation 3.11 relates the emissivity above 1500K, ε_2 (unitless), to ε_1 and the maximum cladding temperature, T (K).

$$\varepsilon_2 = \varepsilon_1 \exp\left[\frac{1500 - T}{300}\right] \quad (3.11)$$

Comparisons between data and the high and low temperature models are presented in Figure 3.4.

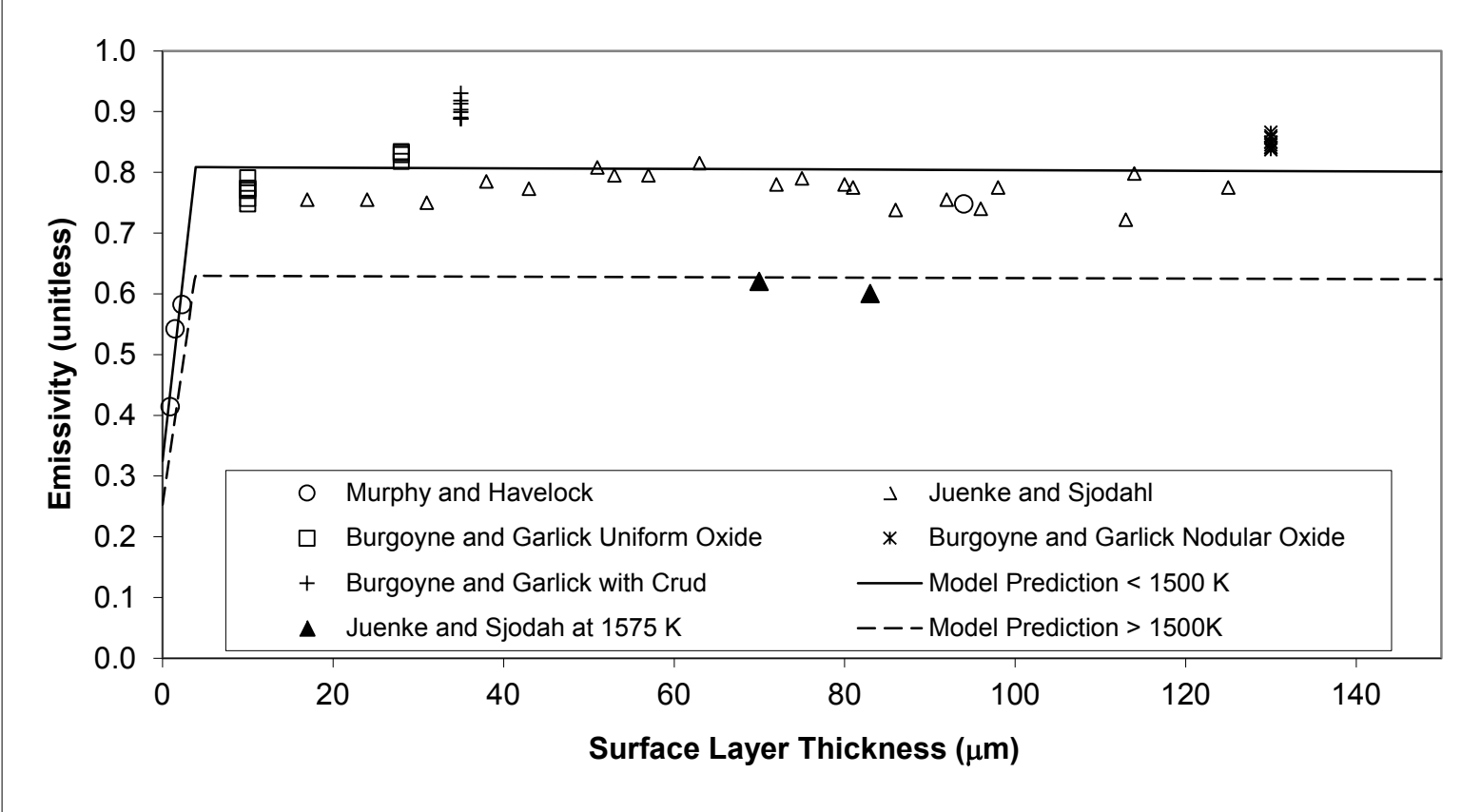


Figure 3.4. Model-to-Data Comparison for Cladding Oxide Emissivity

3.4.2 Applicability and Uncertainty

The absolute standard error, σ_1 , expected from the use for Equation 3.9 to predict emissivity in a reactor when cladding surface temperature has never exceeded 1500K is given by Equation 3.12.

$$\sigma_1 = \pm 0.1 \quad (3.12)$$

When the maximum cladding temperature exceeds 1500K, the expected standard error is estimated by σ_2 , which is described by Equation 3.13.

$$\sigma_2 = \pm 0.1 \exp\left[\frac{T-1500}{300}\right] \quad (3.13)$$

If Equations 3.11 and 3.13 predict values of ε_2 and σ_2 that fall inside the range of physically possible values of emissivity (0.0 – 1.0), the value σ_2 is returned as the expected standard error. If the prediction $\varepsilon_2 + \sigma_2$ is greater than 1 or if $\varepsilon_2 - \sigma_2$ is less than 0, the standard error of Equation 3.13 is modified to limit $\varepsilon_2 + \sigma_2$ at 1 and/or $\varepsilon_2 - \sigma_2$ at 0.

3.5 Cladding Thermal Expansion (CTHEXP)

The subroutine Cladding Thermal Expansion (CTHEXP) returns the axial and diametral components of thermal expansion in the cladding as a function of temperature. The MATPRO model calculates these strain components for single crystal Zircaloy and applies these to polycrystalline cladding materials through the use of pole figures collected over a cladding section. The FRAPCON-4.0/FRAPTRAN-2.0 models use the correlation from Mehan and Wiesinger (1961) for temperatures below 1073K and a constant value of thermal expansion above 1273K. Values of thermal expansion between 1073 and 1273K are determined in the FRAPCON-4.0/FRAPTRAN-2.0 codes by linear interpolation. In addition, the FRAPTAN-2.0 model includes a calculation of the thermal expansion for ZrNb-1.

3.5.1 Model Development and Comparisons

In the MATPRO model, a total of six correlations that are functions of temperature only are used to find single crystal thermal strains. In addition, basal plane symmetry ($\varepsilon_{11} = \varepsilon_{22}$) is assumed. The model was developed for as fabricated Zircaloy-4, but comparisons with Zircaloy-2 and zirconium data also show good agreement for these materials.

The correlations for single crystal thermal strains are:

For $300 < T < 1083\text{K}$

$$\varepsilon_{11} = 4.95 \times 10^{-6} T - 1.485 \times 10^{-3} \quad (3.14)$$

$$\varepsilon_{33} = 1.26 \times 10^{-5} T - 3.78 \times 10^{-3} \quad (3.15)$$

where

$$\begin{aligned}\varepsilon_{11} &= \text{circumferential thermal expansion (m/m)} \\ \varepsilon_{33} &= \text{axial thermal expansion (m/m)}\end{aligned}$$

For $1083 \leq T < 1244\text{K}$

$$\varepsilon_{11} = \left[2.77763 + 1.09822 \cos\left(\frac{T-1083}{161} \pi\right) \right] \times 10^{-3} \quad (3.16)$$

$$\varepsilon_{33} = \left[2.77763 + 1.09822 \cos\left(\frac{T-1083}{161} \pi\right) \right] \times 10^{-3} \quad (3.17)$$

where the arguments of the cosines are in radians.

For $1244 \leq T < 2098\text{K}$

$$\varepsilon_{11} = 9.7 \times 10^{-6} T - 1.04 \times 10^{-2} \quad (3.18)$$

$$\varepsilon_{33} = 9.76 \times 10^{-6} T - 4.4 \times 10^{-3} \quad (3.19)$$

For temperatures $\geq 2098\text{K}$, consideration of the volume change associated with melting is required. Since no data were found for the MATPRO model, a typical 2 percent volume increase at melt was assumed (Siefken et al. 2001). The expressions used for the thermal strain in liquid zirconium (temperatures $\geq 2098\text{K}$) are thus:

$$\varepsilon_p = \frac{2}{3} \varepsilon_{11} + \frac{1}{3} \varepsilon_{33} + 0.0067 \quad (3.20)$$

$$\begin{aligned}\varepsilon_p &= \text{thermal expansion strain in liquid Zircaloy (m/m)} \\ \varepsilon_{11} &= \text{circumferential thermal expansion strain of a single crystal of Zircaloy at 2098K} \\ &\quad \text{(m/m)} \\ \varepsilon_{33} &= \text{axial thermal expansion strain of a single crystal of Zircaloy at 2098K (m/m)}\end{aligned}$$

where the ε_{11} and ε_{33} are calculated by Equations 3.3.16 and 3.17, respectively.

To obtain cladding strains from these single crystal strains, it is necessary to do a volume weighted averaging of crystalline orientation over the entire cladding section. Such an averaging requires the collection of pole figures and is described in greater detail in the MATPRO (2001) handbook. The input parameters for typical cladding are not readily available.

The model for cladding thermal expansion in the FRAPCON-4.0/FRAPTRAN-2.0 (FRAP) codes is different from the MATPRO model but provides similar predictions of expansion (< 6 percent). The data for the FRAP correlation used from room temperature to 1273K was taken from Mehan and Wiesinger (1961), Scott (1965), and Kearns (1965). Above 1273K , the coefficient of thermal expansion is the

constant value of 9.7×10^{-6} , as recommended by Lustman and Kerze (1955). Between 1073 and 1273K (approximately the alpha-beta transition range for Zircaloy), the thermal expansion components are determined by linear interpolation.

The correlations used to calculate the axial and diametral components of thermal expansion in the cladding between room temperature and 1073K are presented in Equations 3.21 and 3.22, respectively. Strain is given a function of temperature, T ($^{\circ}\text{C}$).

$$\varepsilon_{axial} = -2.5060 \times 10^{-5} + 4.4410 \times 10^{-6} T \quad (3.21)$$

$$\varepsilon_{diametral} = -2.3730 \times 10^{-5} + 6.7210 \times 10^{-6} T \quad (3.22)$$

The correlations used to calculate the axial and diametral components of thermal expansion in the cladding above 1273K are presented in Equations 3.23 and 3.24, respectively. Strain is given a function of temperature, T ($^{\circ}\text{C}$).

$$\varepsilon_{axial} = -8.300 \times 10^{-3} + 9.70 \times 10^{-6} T \quad (3.23)$$

$$\varepsilon_{diametral} = -6.800 \times 10^{-3} + 9.70 \times 10^{-6} T \quad (3.24)$$

Model-to-data comparisons for the MATPRO and FRAPCON-4.0/FRAPTRAN-2.0 models are presented in Figure 3.5 and Figure 3.6 for axial and diametral thermal expansion, respectively. These comparisons illustrate that the axial and diametral components of cladding thermal expansions are being underpredicted. These correlations will be examined further and possibly revised in a future revision of FRAPCON-4.0/FRAPTRAN-2.0.

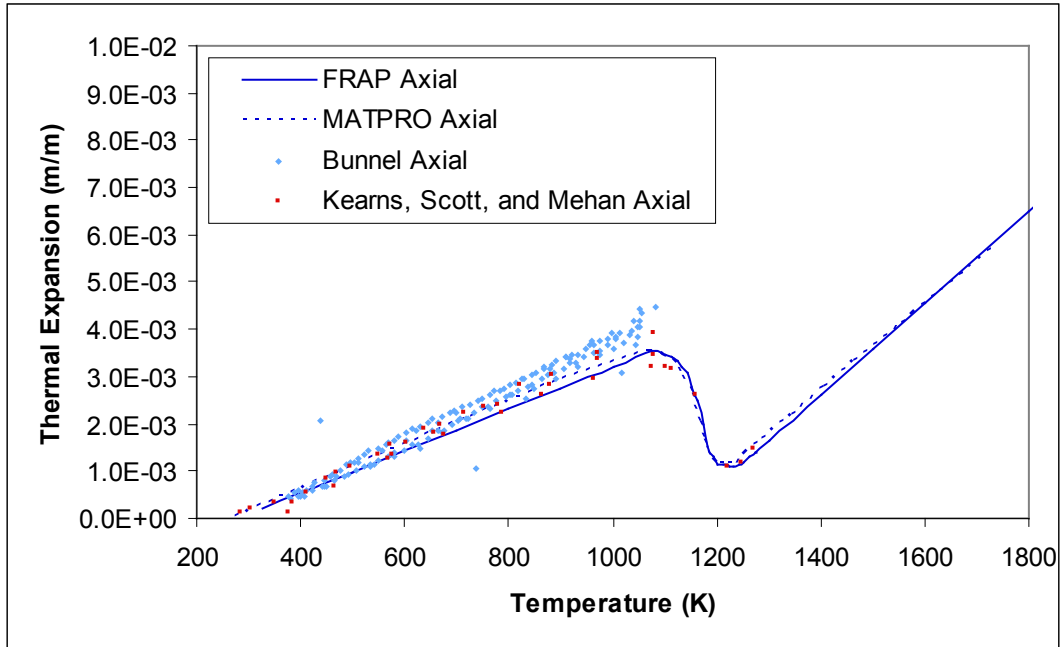


Figure 3.5. Model-to-Data Comparison for FRAPCON-4.0/FRAPTRAN-2.0 (FRAP) and MATPRO Axial Thermal Expansion. Data from cladding tubes.

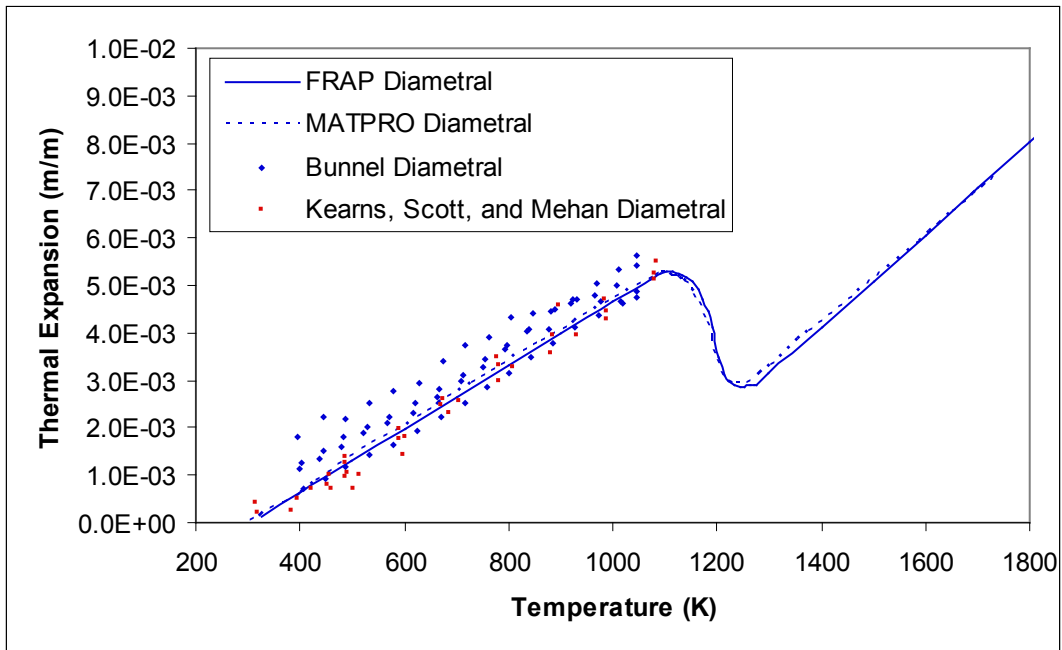


Figure 3.6. Model-to-Data Comparison for FRAPCON-4.0/FRAPTRAN-2.0 (FRAP) and MATPRO Diametral Thermal Expansion. Data from cladding tubes.

3.5.2 Applicability and Uncertainty

The subroutine CTHEXP is applicable over the temperature range for which the experimental data was collected, which included temperatures up to 1100K. The uncertainty of the axial and diametral thermal expansion correlations has not been quantified.

3.6 Cladding Elastic Modulus (CELMOD) and Shear Modulus (CSHEAR)

Elastic moduli are required to relate stresses to strains. The elastic moduli are defined by the generalized form of Hooke's law as elements of the fourth rank tensor that relates the second rank stress and strain tensors below the yield point. In practice, cladding is frequently assumed to be an isotropic material. In such a case, only two independent elastic moduli are needed to describe the relation between elastic stress and strain: the Young's modulus and the shear modulus.

The subcodes Cladding Elastic Modulus (CELMOD) and Shear Modulus (CSHEAR) are used in the MATPRO and the FRAPCON-4.0/FRAPTRAN-2.0 (FRAP) codes to determine the Young's modulus and the shear modulus, respectively. The tensor from which these moduli are derived is calculated by CELAST, which is included in MATPRO and determines the compliance matrix for isotropic cladding. However, CELAST is not used in the FRAP codes. The subcode CELAST would only be required if the Young's modulus and shear modulus for an anisotropic cladding is desired and, as stated previously, the cladding is assumed to be isotropic.

Elastic moduli are affected primarily by temperature and oxygen content. Fast neutron fluence, cold work, and texture effects are also included in the models described herein, but they are not as important as temperature and oxygen content for typical LWR fuel rod cladding. The models are based primarily on data published by Bunnell et al. (1977), Fisher and Renken (1964), Armstrong and Brown (1964), and Padel and Groff (1976), since these data include the best description of texture for the temperature range in which they were used. Data from several other sources are used to evaluate the expected standard error of the CELMOD and CSHEAR codes and to estimate the effect of fast neutron fluence (Shober et al. 1957; Whitmarsh 1962). To calculate Zircaloy elastic moduli at temperatures greater than the melting temperature of Zircaloy (2098K), the moduli are set to zero (actually, 1.0×10^{-10} is used to avoid dividing by zero).

3.6.1 Model Development and Comparisons

CELMOD

The CELMOD subcode used in MATPRO uses different forms of the same equations as those used in FRAPCON-4.0/FRAPTRAN-2.0 (FRAP). The differences in equations between the codes will be discussed in this subsection.

MATPRO uses Equations 3.25 and 3.26 to describe the Young's modulus in the alpha phase and the beta phase, respectively.

$$Y = (1.088 \times 10^{11} - 5.475 \times 10^7 T + K_1 + K_2) / K_3 \quad (3.25)$$

$$Y = 9.21 \times 10^{10} - 4.05 \times 10^7 T \quad (3.26)$$

where

- Y = Young's modulus for Zircaloy-2 and -4 with random texture (Pa)
- T = cladding temperature (K)
- K₁ = modification to account for the effect of oxidation (Pa)
- K₂ = modification to account for the effect of cold work (Pa)
- K₃ = modification to account for the effect of fast neutron fluence (unitless)

In the alpha plus beta phase, MATPRO determines Y by linearly interpolating between values calculated at the alpha to alpha plus beta and the alpha plus beta to beta phase boundaries.

The MATPRO expressions used to model the effects of oxidation, cold work, and fast neutron fluence are presented in Equations 3.27 through 3.29.

$$K_1 = (6.61 \times 10^{11} + 5.912 \times 10^8 T) \Delta \quad (3.27)$$

$$K_2 = -2.6 \times 10^{10} C \quad (3.28)$$

$$K_3 = 0.88 + 0.12 \exp\left(-\frac{\Phi}{10^{25}}\right) \quad (3.29)$$

where

- Δ = average oxygen concentration minus oxygen concentration of as-received cladding (kg oxygen/kg Zircaloy). As-received oxygen concentrations are so small (0.0012 kg oxygen/kg Zircaloy) that the exact magnitude of the as-received concentration will not affect the correlation predictions.
- C = cold work (unitless ratio of areas).
- Φ = fast neutron fluence (n/m²).

The standard error of CELMOD is 6.4x10⁹ Pa. Although FRAPCON-4.0 is coded to include this error, this value is not used. This standard error is not included in FRAPTRAN-2.0.

The CELMOD subcode included in the FRAP codes differs only in form from the MATPRO version. For instance, the expression for Young's modulus in the alpha phase is presented in Equation 3.30.

$$cel \text{ mod} = (1.088 \times 10^{11} - 5.475 \times 10^7 * ctemp + c_1 * deloxy + c_3 * cwkf) / c_2 \quad (3.30)$$

where

- celmod = Young's modulus (Pa)
- ctemp = cladding temperature (K)
- deloxy = input average oxygen concentration excluding oxide layer (kg oxygen/kg Zircaloy)(hardwired to zero in FRAPCON-4.0/FRAPTRAN-2.0)
- cwkwf = input effective cold work (unitless ratio of areas)

In Equation 3.30, c_1 , c_3 , and c_2 are expressions that account for oxygen content, cold work, and fast neutron fluence respectively.

Equations 3.31 through 3.33 describe the constants c_1 , c_2 , and c_3 , respectively.

$$c_1 = (1.16 \times 10^{11} + ctemp * 1.037 \times 10^8) * 5.7015 \quad (3.31)$$

$$c_2 = 1.0 \quad (3.32)$$

$$c_3 = -2.6 \times 10^{10} \quad (3.33)$$

For neutron fluences greater than 1×10^{22} , c_2 is given by Equation 3.34.

$$c_2 = 0.88 * (1 - \exp(-fnck / 1 \times 10^{25})) + \exp(-fnck / 1 \times 10^{25}) \quad (3.34)$$

where

- fnck = input effective fast fluence (n/m²)

Both FRAPCON-4.0 and FRAPTRAN-2.0 use the same correlations to determine Young's modulus in the subcode CELMOD. Although FRAPCON-4.0 includes the coding to return the standard error of the model, neither FRAPCON-4.0 nor FRAPTRAN-2.0 uses these errors. FRAPTRAN-2.0 includes additional coding to determine Young's modulus for ZrNb-1.

CSHEAR

In MATPRO, the expressions used to determine shear modulus in the alpha and beta phases are given in Equations 3.35 and 3.36, respectively.

$$G = \frac{(4.04 \times 10^{10} - 2.168 \times 10^7 T + K_1 + K_2)}{K_3} \quad (3.35)$$

$$G = 3.49 \times 10^{10} - 1.66 \times 10^7 T \quad (3.36)$$

In the alpha plus beta phase, MATPRO determines G by linearly interpolating between values calculated at the alpha to alpha plus beta and the alpha plus beta to beta phase boundaries.

The constants K_1 , K_2 , and K_3 have the same definitions as stated before in CELMOD. However, the expression used to model the effect of oxidation for shear modulus is given in Equation 3.37.

$$K_1 = (7.07 \times 10^{11} + 2.315 \times 10^8 T) \Delta \quad (3.37)$$

The standard error of the CSHEAR code is 9×10^9 Pa.

The CSHEAR subcode included in the FRAP codes differs slightly from the MATPRO version. For instance, the expression for shear modulus in the alpha phase is presented in Equation 3.38.

$$c_{shear} = (4.04 \times 10^{10} - 2.168 \times 10^7 * ctemp + c_1 * deloxy + c_3 * cwkf) / c_2 \quad (3.38)$$

where

<i>c_{shear}</i>	=	shear modulus (Pa)
<i>ctemp</i>	=	cladding temperature (K)
<i>deloxy</i>	=	input average oxygen concentration excluding oxide layer
<i>cw_{kf}</i>	=	input effective cold work (unitless ratio of areas)

In Equation 3.38, c_1 , c_3 , and c_2 are expressions that account for oxygen content, cold work, and fast neutron fluence, respectively.

Equations 3.39 through 3.41 describe the constants c_1 , c_2 , and c_3 , respectively.

$$c_1 = 7.07 \times 10^{11} - ctemp * 2.315 \times 10^8 \quad (3.39)$$

$$c_2 = 1.0 \quad (3.40)$$

$$c_3 = -0.867 \times 10^{10} \quad (3.41)$$

For neutron fluences greater than 1×10^{22} , c_2 is given by Equation 3.42.

$$c_2 = 0.88 * (1 - \exp(-fnck / 1 \times 10^{25})) + \exp(-fnck / 1 \times 10^{25}) \quad (3.42)$$

where

$$fnck = \text{input effective fast fluence (n/m}^2\text{)}$$

Both FRAPCON-4.0 and FRAPTRAN-2.0 use the same correlations to determine shear modulus in the subcode CSHEAR. Although FRAPCON-4.0 includes the coding to return the standard error of the model, neither FRAPCON-4.0 nor FRAPTRAN-2.0 returns the error. FRAPTRAN-2.0 includes additional coding to determine Young's modulus, shear modulus, and Poisson's ratio as a function of temperature for ZrNb-1.

Since there is limited data available from shear modulus measurements, a model-to-data comparison for Young's modulus is presented. Figure 3.7 presents predicted vs. measured Young's modulus values for data sets used in the development of the CELMOD models as well as more recent data.

The upper and lower bounds of Figure 3.7 represent an interval of ± 6.4 GPa. It may be noted that the data fit is slightly better below 80 GPa ($\sim < 4$ percent) than above 80 GPa ($\sim > 5$ percent). This is attributed to the relatively low temperatures that were used to collect these data above 80 GPa (e.g., a quarter of Bolmaro's data is collected at $< 250^\circ\text{F}$). It should also be noted that, with exception to several data points near the lower bound from Busby (1966), the majority of data is from material in a recrystallized or annealed condition (i.e., zero coldwork). Nevertheless the CELMOD model, in general, provides a satisfactory fit to the data within the temperature range it will be applied for predicting in-reactor performance ($> 250^\circ\text{F}$).

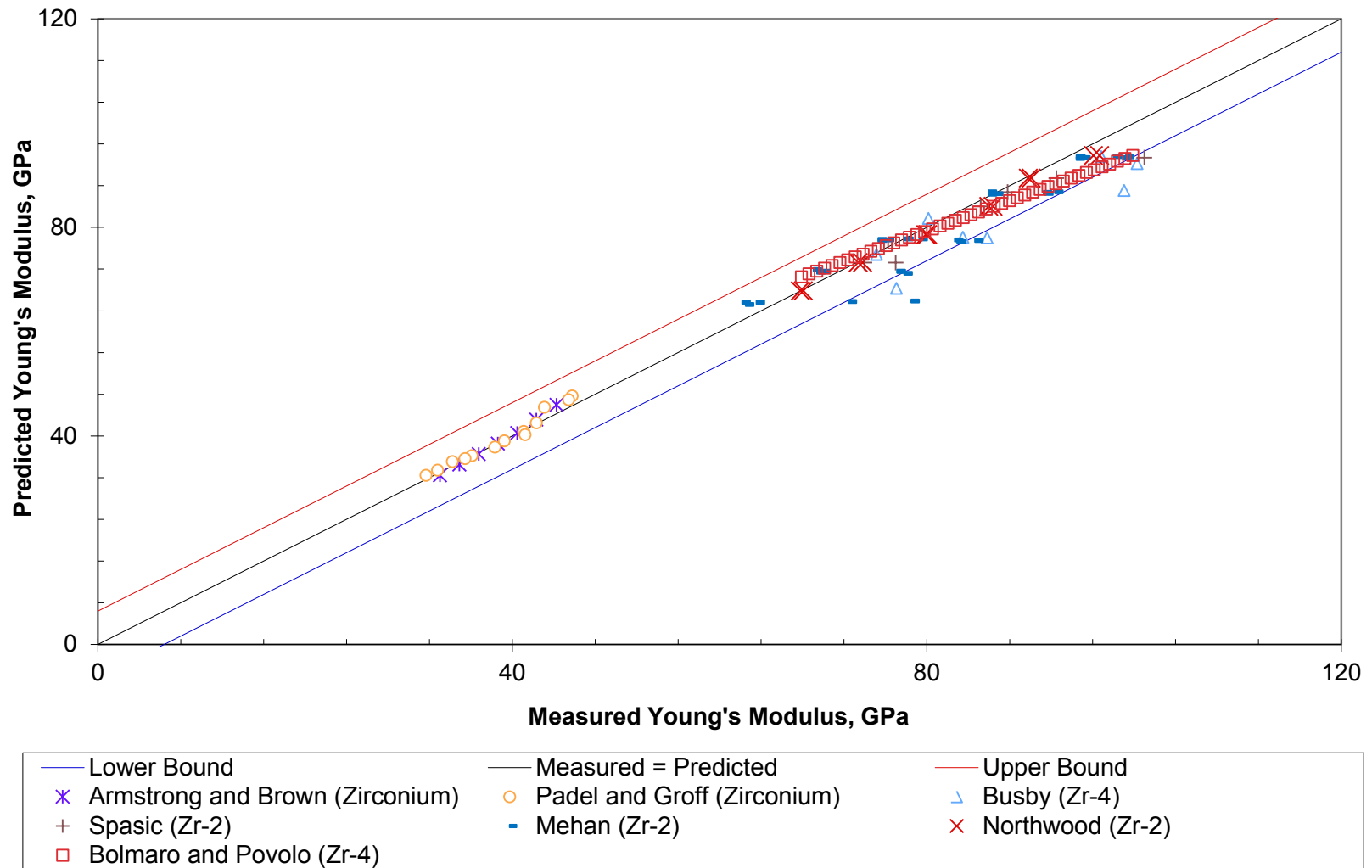


Figure 3.7. Predicted vs. Measured Values for Young's Modulus for Various Data Sets

3.6.2 Applicability and Uncertainty

The CELMOD and CSHEAR correlations are applicable below the melting temperature of the cladding (2098K). Above this temperature, the moduli are assumed to be zero (but actually set at 1×10^{-10} to avoid dividing by zero). The CELMOD and CSHEAR correlations are similar between MATPRO and the FRAPCON-4.0/FRAPTRAN-2.0. The uncertainty of the predictions for CELMOD are within 6.4 GPa (the upper and lower bounds), and typically < 5 percent below 80 GWd/MTU. The uncertainty of the CSHEAR predictions is estimated to be within 9 GPa.

3.7 Cladding Axial Growth (CAGROW)

The subcode Cladding Axial Growth (CAGROW) calculates the fractional change in length of Zircaloy tubes due to irradiation-induced growth. The change in length of commercial fuel rods due to irradiation growth is small. However, growth can be a significant fraction of the clearance between the rod and the top and bottom assembly nozzles. Contact with the nozzles can cause rods to bow and possibly fail at points where the rods contact each other. In addition, rod growth increases the internal void volume that impacts the rod internal pressure calculation.

A modified version of the CAGROW correlation is used in FRAPCON-4.0 to better describe the cladding axial growth at higher fluence. The MATPRO version of CAGROW was applied to both Zircaloy-2 and -4. The FRAPCON-4.0 version includes correlations for Zircaloy 2 and -4, M5, and ZIRLO. These correlations may be applied to either PWR or boiling water reactor (BWR) conditions. The CAGROW subroutine is not used in FRAPTRAN-2.0 because significant irradiation axial growth is not expected under the short time scales considered by FRAPTRAN-2.0.

3.7.1 Model Development and Comparisons

The MATPRO correlation used to describe cladding axial growth is presented in Equation 3.43. This equation has been developed to model the irradiation growth of Zircaloy tubes at temperature between 40 and 360°C (the normal range of cladding temperatures in LWRs).

$$\Delta L / L = A \left[\exp(240.8 / T) \right] (\Phi t)^{1/2} (1 - f_z) (1 + 0.02 CW) \quad (3.43)$$

where

- $\Delta L / L$ = fractional change in length due to growth.
- A = $1.407 \times 10^{-16} \text{ (n/m}^2\text{)}^{1/2}$.
- T = cladding temperature (K).
- Φ = fast neutron flux ($\text{n/m}^2\text{s}$) ($E > 1.0 \text{ MeV}$).
- t = time (s).
- f_z = texture factor for the tubing. The variable f_z is the effective fraction of cells aligned with their <0001> axis parallel to the tubing axis, as determined by X-ray diffraction analysis. A value of $f_z = 0.05$ is typical.
- CW = cold work (fraction of cross-sectional area reduction).

Axial growth for temperature below 40°C is approximated by using $T = 40^\circ\text{C}$ in Equation 3.43 and growth above 360°C is approximated by using $T = 360^\circ\text{C}$.

The MATPRO subroutine CAGROW was based on low-burnup, low-fluence data found in Harbottle (1970) and Daniel (1971, 1972). Consequently, the CAGROW model was updated in FRAPCON-4.0 to better model axial growth under greater fluences ($> 1 \times 10^{25} \text{ n/m}^2$). A model proposed by Franklin (1982) that was based on high fluence PWR data was adopted for FRAPCON-4.0. This model is presented in Equation 3.44 and relates the axial growth, ax (m/m), of stress relief annealed (SRA) Zircaloy-4 in a PWR to fluence (n/cm^2).

$$ax = 2.18 \times 10^{-21} * \Phi^{0.845} \quad (3.44)$$

where

$$\begin{aligned} ax &= \text{axial growth increment (m/m)} \\ \Phi &= \text{fast neutron fluence (n/cm}^2\text{) (E > 1.0 MeV)} \end{aligned}$$

The expression in Equation 3.44 is used to determine the axial growth at the beginning and the end of a time increment. The difference is used to determine the axial growth for the time increment, which is the value returned by the CAGROW subroutine. The expression in Equation 3.44 can be used to describe the axial growth of fully recrystallized annealed (RXA) Zircaloy-2 cladding in a BWR by multiplying by a factor of 0.5.

In addition to updating the cladding axial growth model for SRA Zircaloy-4 and RXA Zircaloy-2, new correlations have been added to describe the cladding axial growth of M5 and ZIRLO. The cladding axial growth correlations for M5 and ZIRLO are presented in Equations 3.45 and 3.46, respectively. These equations relate the cladding axial growth, ax (m/m), to fluence (n/cm^2). The variables have the same definitions as those described in Equation 3.44 and the time difference is used to determine the axial growth during the time increment, which is the value returned by the CAGROW subroutine.

For M5 cladding:

$$ax = 7.013 \times 10^{-21} \Phi^{0.81787} \quad (3.45)$$

For ZIRLO cladding:

$$ax = 9.7893 \times 10^{-25} \Phi^{0.98239} \quad (3.46)$$

Model-to-data comparisons are presented in Figure 3.8 through Figure 3.11 for SRA Zircaloy-4, RXA Zircaloy-2, M5, and ZIRLO, respectively. Based on these figures, it appears that the cladding axial growth of these alloys can be predicted well with the CAGROW subroutine.

It should be noted that these growth correlations should not be applied above the fluence levels of the data from which they are derived as different growth behavior may occur (e.g., accelerated growth at high fluence). Furthermore, it should be noted that the growth models are only applicable to fuel rods and should not be applied to other components that may be under an applied stress (e.g., PWR guide tubes or BWR tie rods).

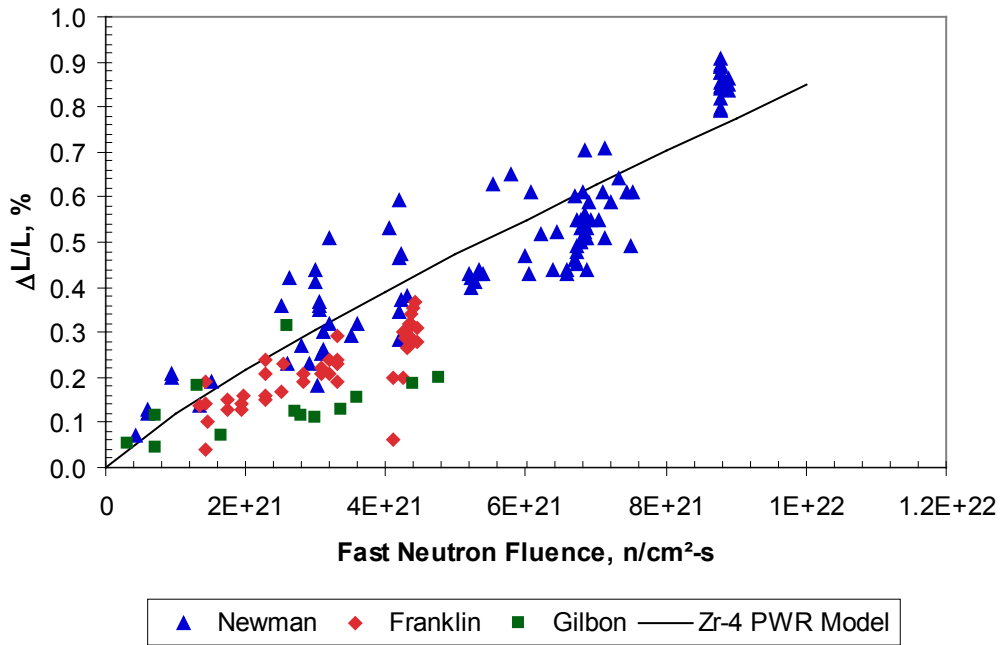


Figure 3.8. Model-to-Data Comparison for SRA Zircaloy-4 (PWR). The standard error of $\Delta L/L$ (%) is 0.11.

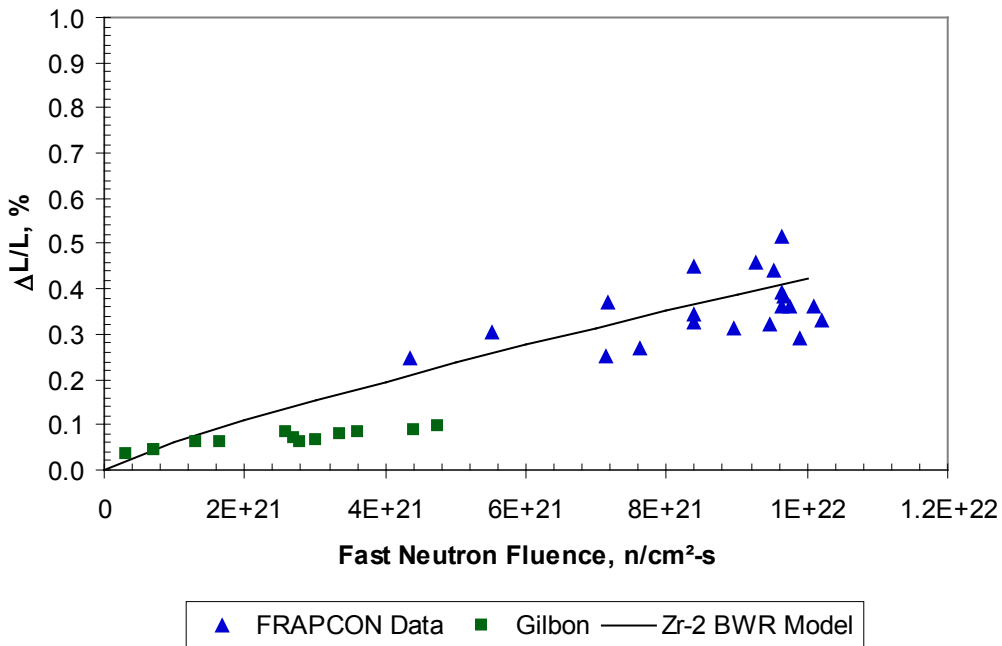


Figure 3.9. Model-to-Data Comparison for RXA Zircaloy-2 (BWR). The standard error of $\Delta L/L$ (%) is 0.07.

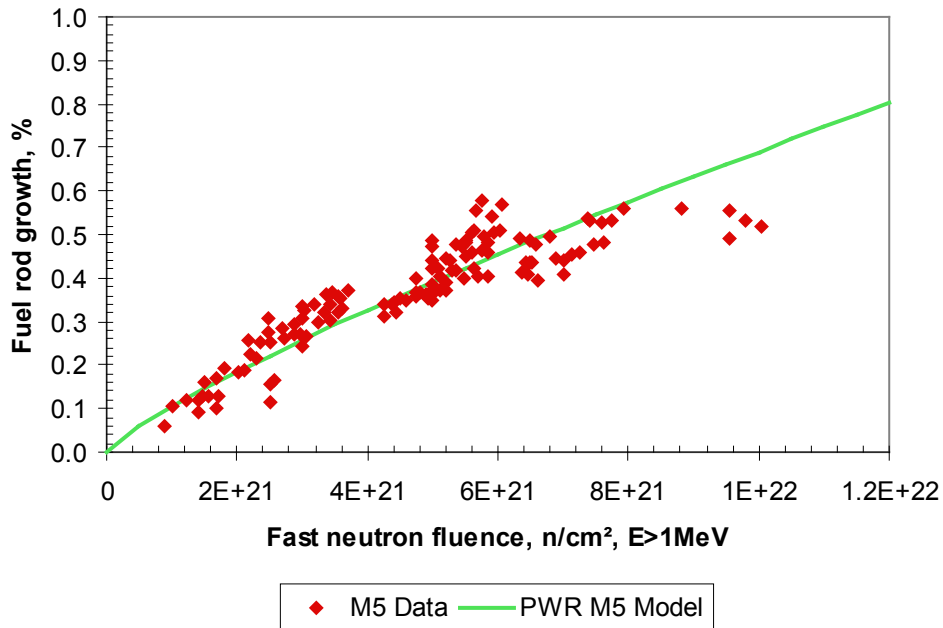


Figure 3.10. Model-to-Data Comparison for M5. M5 data was collected by Gilbon et al. (2000). The standard error of $\Delta L/L$ (%) is 0.05.

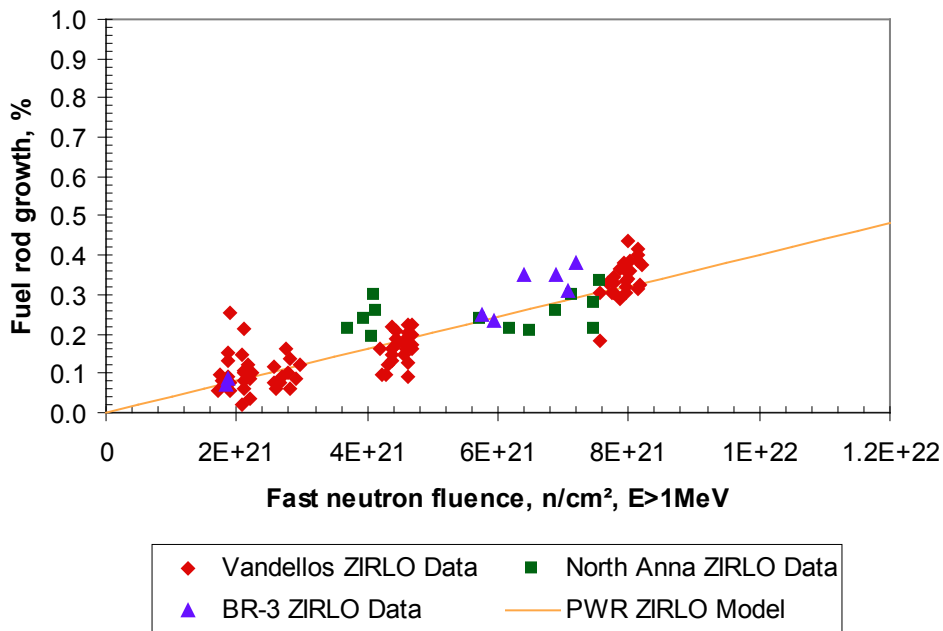


Figure 3.11. Model-to-Data Comparison for ZIRLO. Vandellos data was collected by Irisa (2000) while North Anna and BR-3 data was collected by Sabol (1994). The standard error of $\Delta L/L$ (%) is 0.05.

3.7.2 Applicability and Uncertainty

The CAGROW model in FRAPCON-4.0 is applicable over the temperature range from 700 to 900K for local burnups up to 65 GWd/MTU (or 12×10^{25} n/m² fluence, $E > 1\text{MeV}$). The absolute uncertainties for the growth strains predicted for stress-relief annealed Zr-4, M5, and ZIRLO are 0.11, 0.05, and 0.05%, respectively. The relative uncertainties are 22.3, 18.6, and 44.8%, respectively. These three alloys are typically used in PWRs, whereas RXA Zr-2 is typically used in BWRs. The absolute and relative uncertainties in growth strains for RXA Zr-2 are 0.07 and 20.3%, respectively. The relative uncertainty is used for each material except ZIRLO, which incorporates the absolute uncertainty.

It should be noted that these growth correlations should not be applied above the fluence levels of the data as accelerated growth has been observed in some zirconium alloys at fluences greater than seen at current U.S. NRC burnup limits. Furthermore, these models should only be used for fuel rods and not for other components that may have significantly different stress states (e.g., PWR guide tubes or BWR tie rods).

3.8 Creep Rate (CREPR)

The subcode Creep Rate (CREPR) is used by FRAPCON-4.0 to determine the cladding creep rate, accounting for both thermal and irradiation creep. The CREPR subcode was not used in MATPRO. Also, since creep is a time-dependent deformation process, CREPR is not used in FRAPTRAN-2.0, because creep occurs over much longer time intervals than those considered in FRAPTRAN-2.0 of a minute or less. The FRAPTRAN calculation of cladding ballooning as a result of a loss-of-coolant accident is handled with a separate subroutine named BALON2.

3.8.1 Model Development and Comparisons

The creep model used by FRAPCON-4.0 is based on the model given by Limbäck and Andersson (1996). This model uses a thermal creep model described by Matsuo (1987) and an empirical irradiation creep rate with tuned model parameters that were fit to data from Franklin et al. (1983). The Limbäck model was further modified by PNNL to use effective stress rather than hoop stress as an input so that the principal stresses could be included and account for the difference in creep behavior during tensile and compressive creep. Several of the fitting coefficients were consequently changed to accommodate this modification. In addition, a temperature-dependent term was added to the formula for irradiation creep strain rate to account for differences that were not explained by thermal creep. This model has different parameters for SRA and RXA cladding types, and provides much more reasonable creep strains in the LWR range of temperatures and cladding hoop stresses than the previous model used in FRAPCON-3.3.

The steady-state thermal and irradiation creep rates are given by Equations 3.47 and 3.48, respectively.

$$\dot{\epsilon}_{th} = A \frac{E}{T} \left(\sinh \frac{a_t \sigma_{eff}}{E} \right)^n \exp \left(\frac{-Q}{RT} \right) \quad (3.47)$$

$$\dot{\epsilon}_{irr} = C_o \cdot \varphi^{C_1} \cdot \sigma_{eff}^{C_2} \cdot f(T) \quad (3.48)$$

where

- $\dot{\epsilon}_{th}$ = thermal strain rate (in./in./hr)
- $\dot{\epsilon}_{irr}$ = irradiation strain rate (in./in./hr)
- T = temperature (K)
- σ_{eff} = effective stress (MPa)
- R = universal gas constant (0.008314 kJ/mol-K)
- ϕ = fast neutron flux (n/m²-s)

The variables A, E, a_i, n, -Q, C₀, C₁, C₂, and the function f(T) have different values depending on temperature, flux, and cladding type (SRA or RXA). The values for these variables under different conditions are presented in Table 3.4.

Table 3.4. Parameters for FRAPCON-4.0 Creep Equation for SRA and RXA Cladding

Parameter	Units	SRA Cladding	RXA Cladding
A*	K/MPa/hr	1.08x10 ⁹ *	5.47x10 ⁸ *
E	MPa	1.149x10 ⁵ -59.9*T	
a _i	MPa ⁻¹	650{1-0.56[1-exp(-1.4x10 ⁻²⁷ *Φ ^{1.3})]}	
		Φ=fast neutron fluence (n/cm ²)	
n	unitless	2.0	3.5
Q	kJ/mole	201	
C ₀	(n/m ² -s) ^{-C1} MPa ^{-C2}	4.0985x10 ⁻²⁴	1.87473x10 ⁻²⁴
C ₁	unitless	0.85	
C ₂	unitless	1.0	
f(T)*	unitless	T < 570 570 < T < 625 T > 625	0.7283 -7.0237+0.0136T 1.4763
			0.7994 -3.18562+0.00699132T 1.1840

*Parameters changed from original Limbäck equation.

The thermal and irradiation creep rates may be added together as shown in Equation 3.49 and used to calculate the saturated primary hoop strain, which is presented in Equation 3.50.

$$\dot{\epsilon}_{th+irr} = \dot{\epsilon}_{th} + \dot{\epsilon}_{irr} \quad (3.49)$$

$$\epsilon_p^s = 0.0216 \cdot \dot{\epsilon}_{th+irr}^{0.109} \left(2 - \tanh(35500 \cdot \dot{\epsilon}_{th+irr}) \right)^{-2.05} \quad (3.50)$$

The total thermal strain can then be calculated as a function of time, t (hours), as shown in Equation 3.51. However, in FRAPCON-4.0 the strain rate is used, which is obtained by taking the derivative of Equation 3.51. This derivative is presented in Equation 3.52, which relates the total thermal strain rate to the saturated primary hoop strain, the combined thermal and irradiation creep rates, and time, t, in hours.

$$\varepsilon_H = \varepsilon_p^s \left(1 - \exp\left(-52 \cdot \sqrt{\dot{\varepsilon}_{th+irr} \cdot t}\right) \right) + \dot{\varepsilon}_{th+irr} \cdot t \quad (3.51)$$

$$\dot{\varepsilon}_H = \frac{52 \cdot \varepsilon_p^s \cdot \dot{\varepsilon}_{th+irr}^{1/2}}{2 \cdot t^{1/2}} \exp\left(-52 \cdot \sqrt{\dot{\varepsilon}_{th+irr} \cdot t}\right) + \dot{\varepsilon}_{th+irr} \quad (3.52)$$

The effective stress in the cladding is found using the principal stresses at the mid-wall radius using the thick wall formula. The principle stresses can be determined with Equations 3.53 through 3.55.

$$\sigma_r = \frac{P_i r_i^2 - P_o r_o^2 + \frac{r_i^2 r_o^2 (P_o - P_i)}{r^2}}{r_o^2 - r_i^2} \quad (3.53)$$

$$\sigma_t = \frac{P_i r_i^2 - P_o r_o^2 - \frac{r_i^2 r_o^2 (P_o - P_i)}{r^2}}{r_o^2 - r_i^2} \quad (3.54)$$

$$\sigma_l = \frac{P_i r_i^2 - P_o r_o^2}{r_o^2 - r_i^2} \quad (3.55)$$

where

- P_i = inner pressure
- P_o = outer pressure
- r_i = inner radius
- r_o = outer radius
- r = radius within tube
- σ_r = radial stress
- σ_t = tangential stress
- σ_l = longitudinal stress

The effective stress can then be calculated by Equation 3.56.

$$\sigma_{eff} = \sqrt{0.5 \left((\sigma_l - \sigma_t)^2 + (\sigma_t - \sigma_r)^2 + (\sigma_r - \sigma_l)^2 \right)} \quad (3.56)$$

The subcode CREPR can be used for newer alloys like M5 and ZIRLO but not Optimized ZIRLO. Optimized ZIRLO is partially recrystallized, which can change creep characteristics. It has been found that the Zircaloy RXA model adequately describes the creep behavior of M5 (Gilbon et al. 2000; Soniak et al. 2002). The Zircaloy SRA model is used for ZIRLO with a reduction factor of 0.8. The reduction factor is the result of studies that have shown that ZIRLO exhibits about 80 percent of SRA Zircaloy-4 creepdown (Sabol et al. 1994).

Model-to-data comparisons are presented in Figure 3.12 and Figure 3.13 for SRA and RXA Zircaloy cladding. Creep data was obtained from irradiated SRA and RXA tube from Franklin (1983), Soniak et al. (2002), and Gilbon et al. (2000). The relative standard error for the predictions is 14.5 percent for SRA and 21.6 percent for RXA cladding.

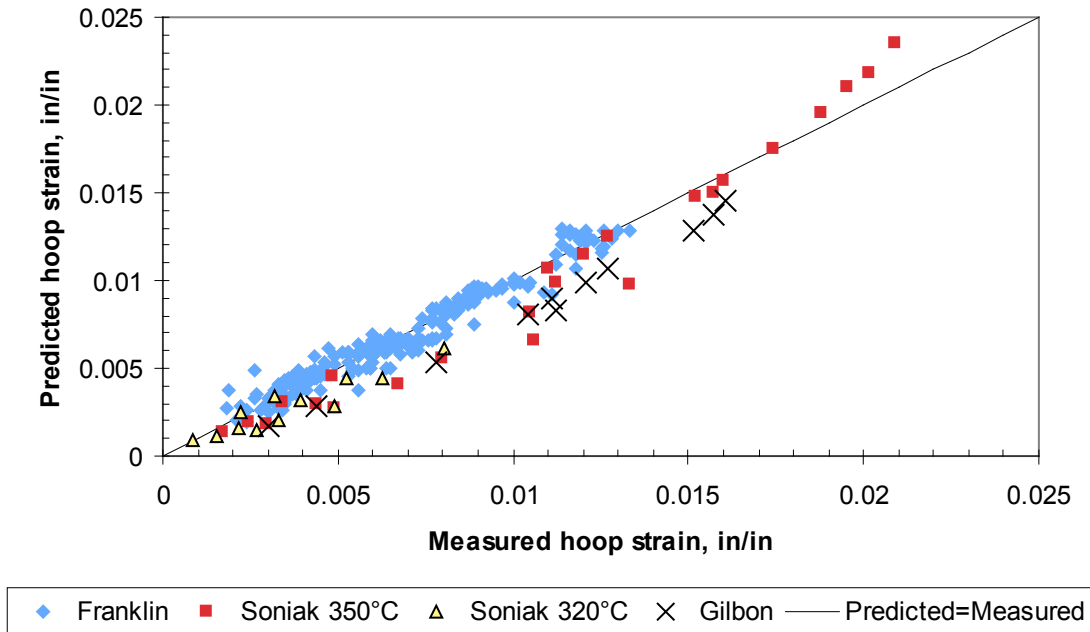


Figure 3.12. Predicted vs. Measured Hoop Strain for SRA Zircaloy Model

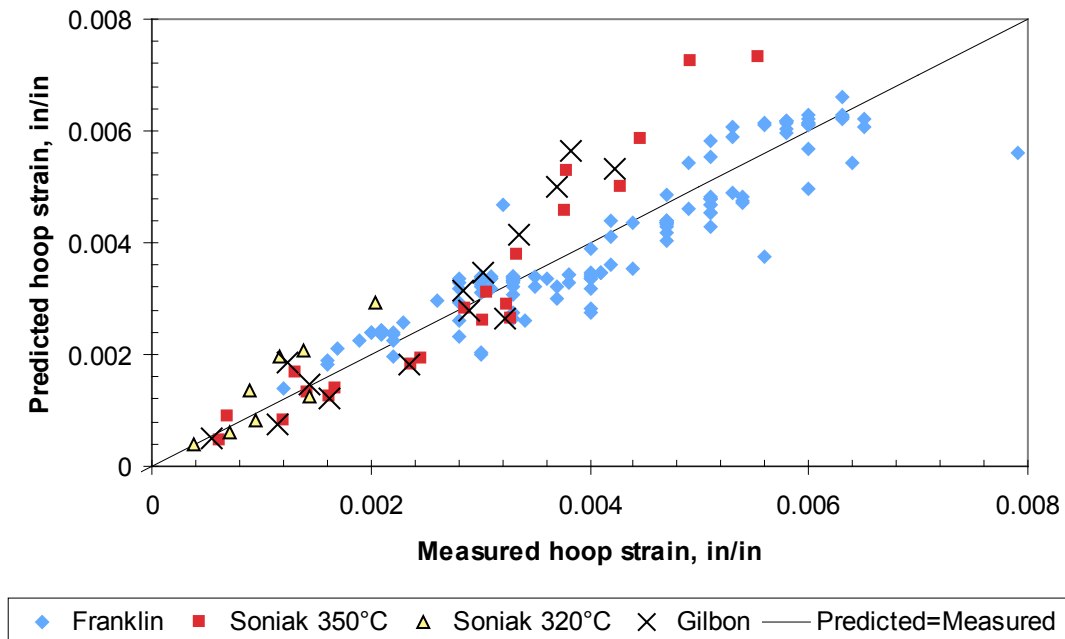


Figure 3.13. Predicted vs. Measured Hoop Strain for RXA Zircaloy Model

3.8.2 Applicability and Uncertainty

The subroutine CREPR is applicable over the range of conditions for which the data was collected. The database spans a temperature range of 570 to 625K, an effective stress range of 40 to 130 MPa, and a fast neutron flux range of 1×10^{17} to 2×10^{18} n/m²-s. This covers the nominal operating conditions for LWRs. The relative standard error for the predictions is 14.5 percent for SRA and 21.6 percent for RXA cladding. The uncertainty for predicting cladding creep in a fuel rod will most likely be greater than these values because there may be greater uncertainty in the estimate of fast neutron flux and cladding temperature than those from the creep data used to determine the creep model uncertainties.

3.9 Cladding Meyer Hardness (CMHARD)

The subroutine Cladding Meyer Hardness (CMHARD) calculates Meyer hardness (MH) as a function of cladding temperature. Hardness is one of the parameters required for calculating fuel-to-cladding contact conductance. As the contact pressure between the two surfaces increases, the points of contact enlarge due to localized plastic deformation and the solid-to-solid thermal conductance is improved. The MH is used by Ross and Stoute (1962) in their heat transfer correlation as an indication of the hardness of resistance to deformation of the softer (Zircaloy) material.

The same CMHARD subroutine is used in the MATPRO, FRAPCON-4.0, and FRAPTRAN-2.0 codes. However, FRAPTRAN-2.0 includes additional coding that ensures that the minimum hardness returned is 1.94×10^8 N/m² (the highest temperature data point) and includes provisions for ZrNb-1.

3.9.1 Model Development and Comparisons

In MATPRO, the MH number is a measure of indentation hardness and is defined in conjunction with Meyer's law, which is presented in Equation 3.57.

$$L = ad^n \quad (3.57)$$

where

- L = load
- d = the diameter of impression at the surface of a specimen in a static ball test
- n = the Meyer work hardening coefficient
- a = a material constant

The MH number is defined as $4L/\pi d^2$. Other hardness numbers are available (Brinell, Rockwell, etc.), and conversion from one to another is possible. However, the routine CMHARD was created to provide information required by the Ross and Stoute gap conductance model that includes a dependence on MH.

MH numbers for temperatures from 298 to 877K were taken from Peggs and Godin (1975). A regression analysis of the reciprocal of the MH values versus the log of temperature was used to obtain the analytical expression used in CMHARD. The correlation used is given by Equation 3.58.

$$MH = \exp \left\{ 2.6034 \times 10^1 + T \left\{ -2.6394 \times 10^{-2} + T \left[4.3502 \times 10^{-5} + T \left(2.5621 \times 10^{-8} \right) \right] \right\} \right\} \quad (3.58)$$

where

$$\begin{aligned} \text{MH} &= \text{Meyer hardness (N/m}^2\text{)} \\ T &= \text{temperature (K)} \end{aligned}$$

The MH decreased rapidly with increasing temperature, beginning at 2×10^9 MPa at room temperature and decreasing to 2×10^8 MPa at 875K. The hardness is presumed to continue its rapid rate of decrease at temperatures above 875K. The minimum MH number of Zircaloy cladding is 1.0×10^5 N/m².

A comparison between the CMHARD correlation and the data from which it was derived is presented in Figure 3.14.

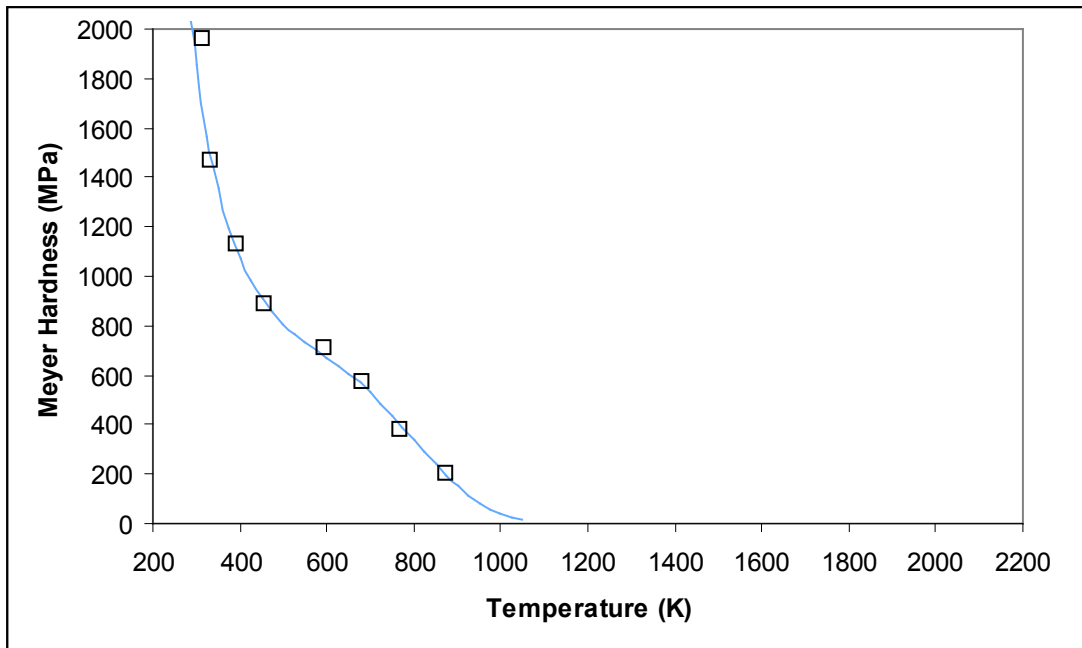


Figure 3.14. CMHARD Correlation as a Function of Temperature with Data from Peggs and Godin

3.9.2 Applicability and Uncertainty

The subroutine CMHARD is applicable for temperatures up to 875K. An estimate of the uncertainty has not been established for this correlation due to the limited data.

4.0 Gas Material Properties

This section describes material property correlations for gap gases. The functions used to determine the material correlation in either the FRAPCON/FRAPTRAN codes is given in parentheses in the heading of each subsection.

4.1 Gas Conductivity (GTHCON)

The function GTHCON calculates the gas thermal conductivity as a function of temperature and gas fraction for eight gases: helium (He), argon (Ar), krypton (Kr), xenon (Xe), hydrogen (H), nitrogen (N), air and water vapor (steam). The MATPRO, FRAPCON-4.0, and FRAPTRAN-2.0 codes use similar correlations to determine the gas thermal conductivity. However, FRAPCON-4.0 and FRAPTRAN-2.0 use updated fitting parameters to better estimate gas thermal conductivity at higher temperatures.

4.1.1 Model Development and Comparisons

The heat conductance of gas-filled gaps or pores is dependent on the thermal conductivity of the gas mixture when the dimensions of the gas-filled regions are large compared to the mean distance between gas molecule collisions (mean free path of the gas molecules). This section presents data and correlations for the thermal conductivities of the gases of interest in fuel rod analysis.

The correlations used for the gases of interest are all of the form presented in Equation (4.1).

$$K = AT^B \quad (4.1)$$

where

$$\begin{aligned} K &= \text{thermal conductivity (W/m-K)} \\ T &= \text{gas temperature (K)} \end{aligned}$$

The constants A and B are fitting parameters. The values for A and B used in MATPRO for each gas are given in Table 4.1 and the values used in FRAPCON-4.0 and FRAPTRAN-2.0 (FRAP) are given in Table 4.2.

Table 4.1. Constants Used in Gas Thermal Conductivity Correlations in MATPRO

Gas	A	B
He	2.639×10^{-3}	0.7085
Ar	2.986×10^{-4}	0.7224
Kr	8.247×10^{-5}	0.8363
Xe	4.351×10^{-5}	0.8616
H ₂	1.097×10^{-3}	0.8785
N ₂	5.314×10^{-4}	0.6898

Table 4.2. Constants Used in Gas Thermal Conductivity Correlations in FRAP

Gas	A	B
He	2.531×10^{-3}	0.7146
Ar	4.092×10^{-4}	0.6748
Kr	1.966×10^{-4}	0.7006
Xe	9.825×10^{-5}	0.7334
H ₂	1.349×10^{-3}	0.8408
N ₂	2.984×10^{-4}	0.7799
Air	1.945×10^{-4}	0.8586

The MATPRO steam correlation is also used in FRAPCON-4.0/FRAPTRAN-2.0 codes. For temperatures less than or equal to 973.15K, the correlation presented in Equation (4.2) is used. For temperatures greater than 973.15K, the correlation presented in Equation (4.3) is used to determine the thermal conductivity of steam. Temperature, T, is in kelvin and pressure, P, is in pascals.

$$k = 4.44 \times 10^{-6} * T^{1.45} + 9.45 \times 10^{-5} * (2.1668 \times 10^{-9} * \frac{P}{T})^{1.3} \quad (4.2)$$

$$k = \frac{P}{T} * (-2.8516 \times 10^{-8} + 9.424 \times 10^{-10} * T - 6.005 \times 10^{-14} * T^2) + 1.009$$

$$* \frac{P^2}{T^2 * (T - 273.15)^2} + [1.76 \times 10^{-3} + 5.87 \times 10^{-5} * (T - 273.15) + 1.08 \times 10^{-7} * (T - 273.15)^2 - 4.51 \times 10^{-11} * (T - 273.15)^3] \quad (4.3)$$

The thermal conductivity of gas mixtures is calculated with Equation (4.4).

$$k_{mix} = \sum_i^n \left(\frac{k_i x_i}{x_i + \sum_{j=1}^n (1 - \delta_{ij}) \Psi_{ij} x_j} \right) \quad (4.4)$$

where Ψ_{ij} is given in Equation (4.5)

$$\Psi_{ij} = \varphi_{ij} \left(1 + 2.41 \frac{(M_i - M_j)(M_i - 0.142 M_j)}{(M_i + M_j)^2} \right) \quad (4.5)$$

and φ_{ij} is given in Equation (4.6)

$$\varphi_{ij} = \frac{\left[1 + \left(\frac{k_i}{k_j} \right)^{1/2} \left(\frac{M_i}{M_j} \right)^{1/4} \right]^2}{2^{3/2} \left(1 + \frac{M_i}{M_j} \right)^{1/2}} \quad (4.6)$$

and

- δ_{ij} = Kronecker delta = 1 for $i = j$, 0 otherwise (unitless)
- n = number of components in mixture (unitless)
- M_i = molecular weight of component i (kg)
- x_i = mole fraction of component i (unitless)
- k_i = thermal conductivity of the component i (W/m-K)

Model-to-data comparisons for the gas conductivity models are presented in Figure 4.1 through Figure 4.7.

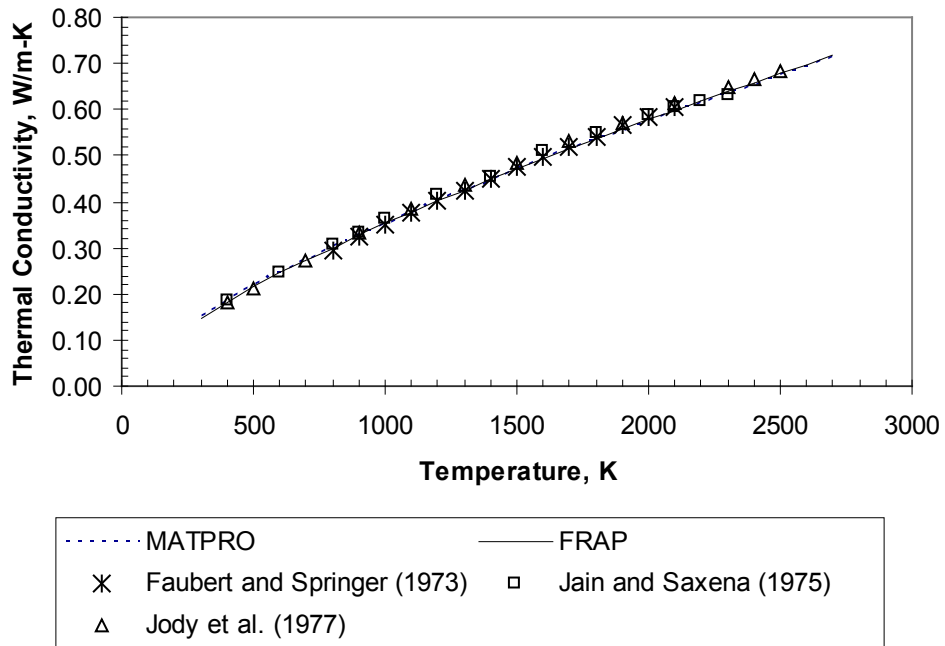


Figure 4.1. Model-to-Data Comparison for He Thermal Conductivity

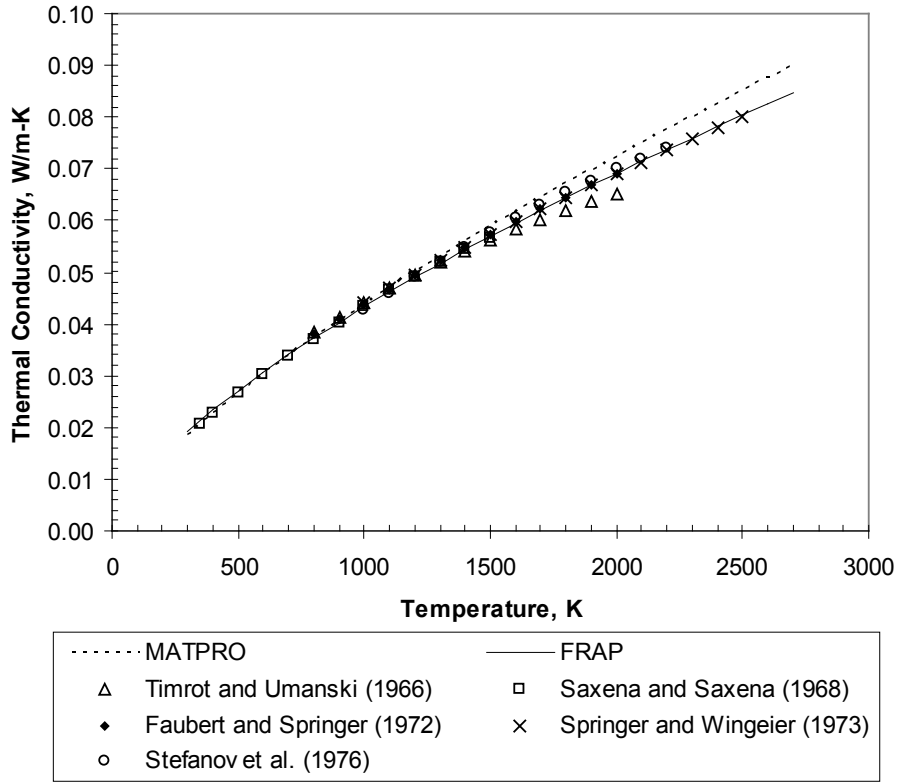


Figure 4.2. Model-to-Data Comparison for Ar Thermal Conductivity

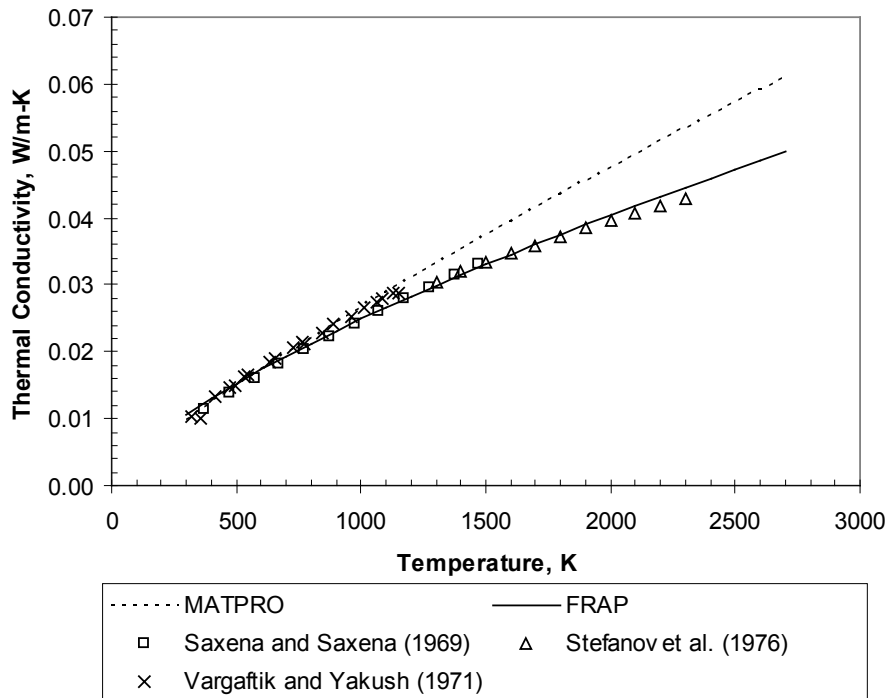


Figure 4.3. Model-to-Data Comparison for Kr Thermal Conductivity

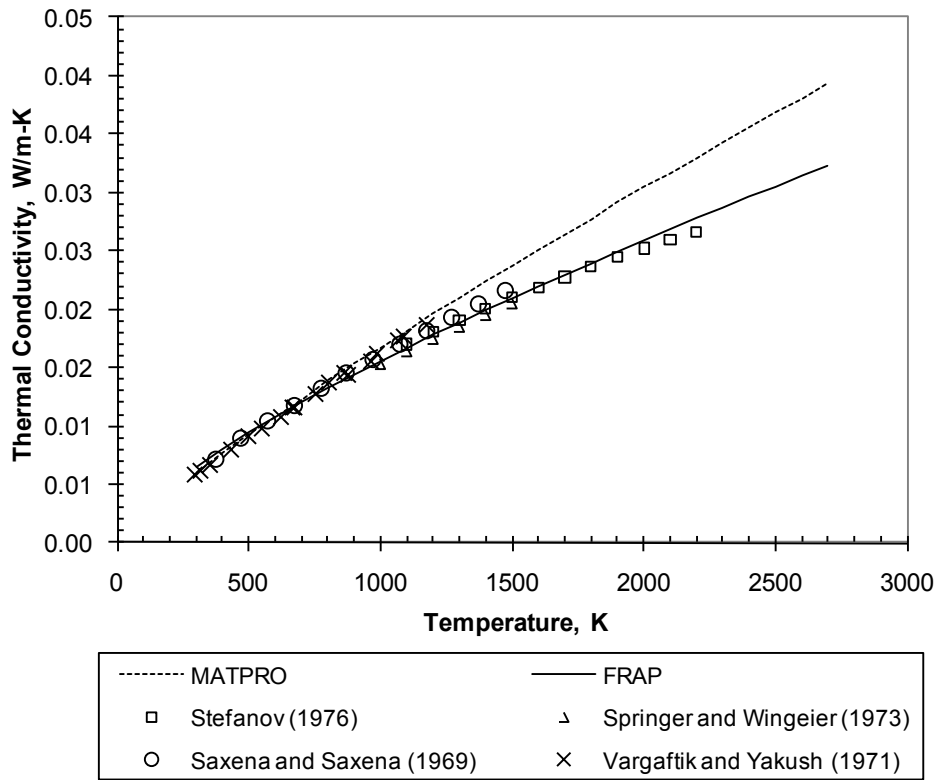


Figure 4.4. Model-to-Data Comparison for Xe Thermal Conductivity

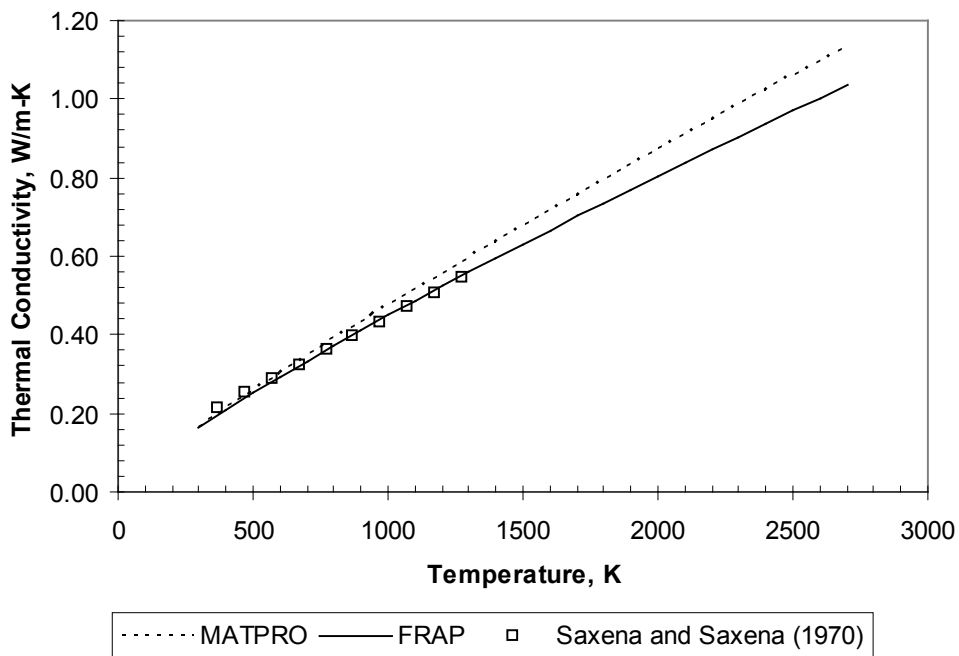


Figure 4.5. Model-to-Data Comparison for H₂ Thermal Conductivity

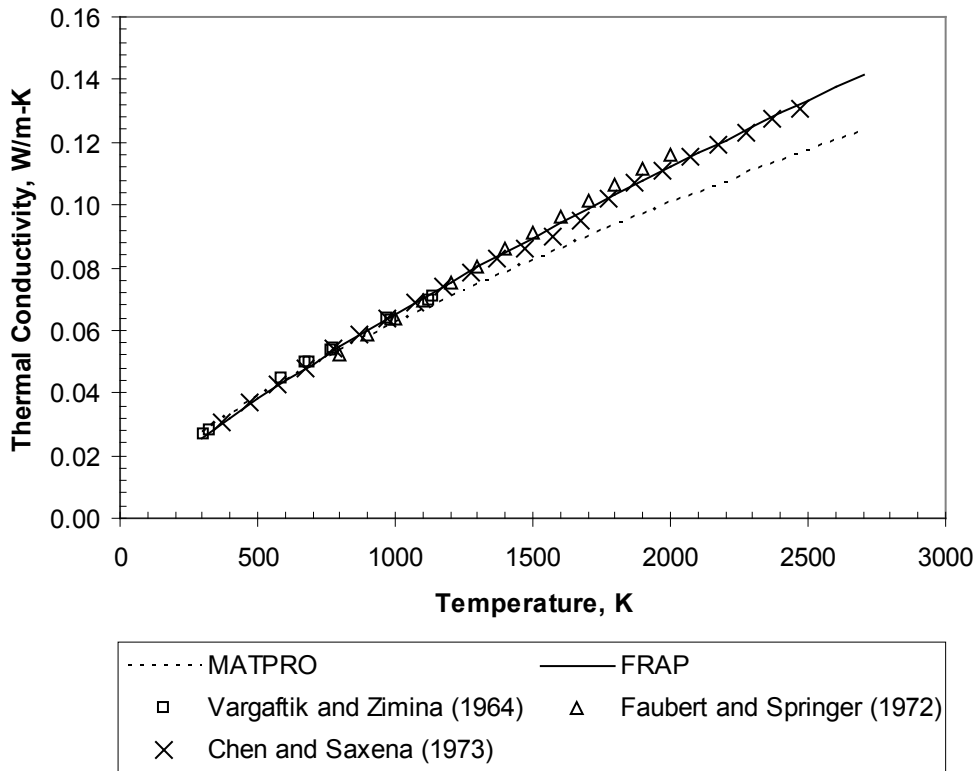


Figure 4.6. Model-to-Data Comparison for N₂ Thermal Conductivity

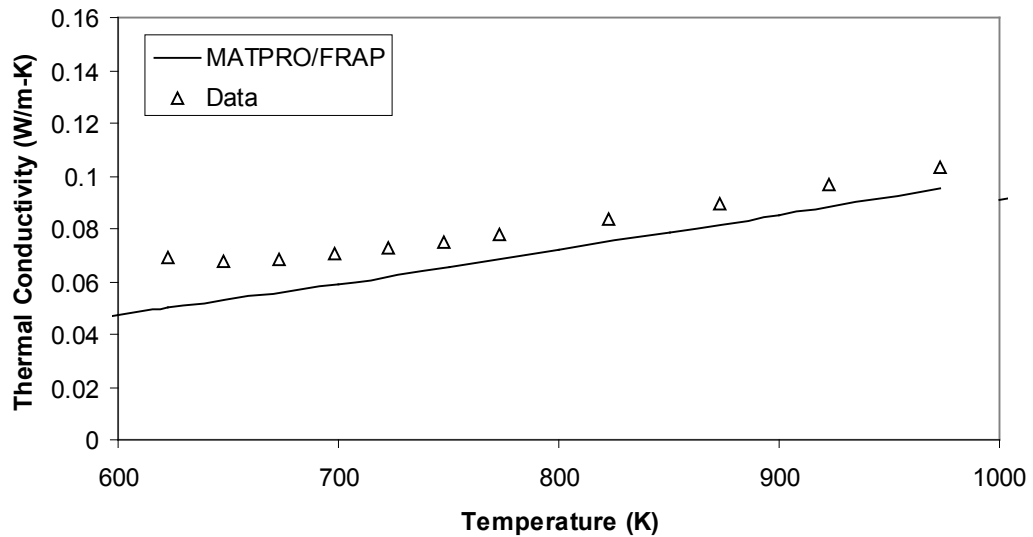


Figure 4.7. Model-to-Data Comparison for Steam Thermal Conductivity

4.1.2 Applicability and Uncertainty

The gas thermal conductivity correlations for used in GTHCON are applicable over the temperature range for which data was collected. The standard error for each correlation is given in Table 4.3.

Table 4.3. Standard Deviation of Gas Thermal Conductivity Correlations

Gas	Standard Deviation
He	8.99×10^{-3}
Ar	9.66×10^{-4}
Kr	8.86×10^{-4}
Xe	5.34×10^{-4}
H ₂	1.67×10^{-2}
N ₂	1.97×10^{-4}
Steam	1.69×10^{-3}

4.2 Gas Molecular Weight (GASMWT)

The function GASMTW calculates the molecular weight of the gas mixture. The correlation for the molecular weight is weighted based on the molar fraction of each individual gas species. The molecular weights of each of the gases modeled is given in Table 4.4.

Table 4.4. Molecular Weight of Gas Species

Gas	Molecular Weight (Grams/mol)
He	4.0026
Ar	39.94766
Kr	83.8
Xe	131.3
H ₂	2.01594
N ₂	28.01403
Air	28.9646 ¹
Steam	18.016

¹ – Air is calculated assuming a mixture of 78.084% N₂, 20.946% O₂, 0.934% Ar, 0.033% CO₂, 0.002% Ne and 0.001% He. The Molar Masses of O₂, CO₂ and Ne are 31.99874, 44.00989 and 20.17135, respectively

The molecular weight of the gas mixture (GasMWT) is expressed in Equation (4.7), where x is the molar fraction and MWt is the molecular weight of the individual gases.

$$GasMWTt = \sum_{i=1}^n MWt(i) * x(i) \quad (4.7)$$

4.3 Gas Density (GASRHO)

The function GASRHO calculates the density of the gas mixture. The mixture density is a function of the pressure applied to the mixture, the corresponding average temperature of the mixture and the ideal gas constant of the gas mixture. The gas constant of each of the gases modeled is given in Table 4.5.

Table 4.5. Ideal Gas Constant of Gas Species

Gas	Ideal Gas Constant (J/kg*K)
He	2077.235
Ar	208.129
Kr	99.216
Xe	63.323
H ₂	4124.299
N ₂	296.792
Air	287.052
Steam	461.4975

The density of the mixture is expressed in Equation (4.8)

$$\rho_{mix} = \frac{P}{R_{mix}T} \quad (4.8)$$

where

$$\begin{aligned} \rho_{mix} &= \text{Mixture density (kg/m}^3\text{)} \\ P &= \text{gas temperature (K)} \\ R_{mix} &= \text{Ideal gas constant of gas mixture} \\ T &= \text{gas temperature (K)} \end{aligned}$$

The ideal gas constant of the mixture is given by Equation (4.9)

$$R_{mix} = \sum_{i=1}^n R_i * x_i \quad (4.9)$$

4.4 Gas Viscosity (GVISCO)

The function GVISCO calculates the viscosity of the gas mixture. The gas viscosities are identical to those found in MATPRO.

Viscosity is modeled as a function of temperature, molecular weight, collision diameter and a fitting parameter, Ω . The viscosity of gas mixtures is calculated with Equation (4.4).

$$\mu_i = 2.6693 * 10^{-6} * \frac{\sqrt{M_i * T}}{cld^2 * \Omega} \quad (4.10)$$

Where

- μ_i = viscosity of the component i (kg/m-s)
- M_i = molecular weight of component i (g/mol)
- T = Gas temperature (K)
- cld = collision diameter (m)
- Ω = Fitting parameter

The gas collision diameter and ratio of maximum energy of attraction between a pair of molecules divided by Boltzmann's constant of each of the gases modeled are given in Table 4.6

Table 4.6. Viscosity Fits of Gas Species

Gas	Collision diameter	Energy of Attraction / Boltzmann's Constant
He	2.576	10.2
Ar	3.418	124.0
Kr	3.61	190.0
Xe	4.055	229.0
H ₂	2.915	38.0
N ₂	3.681	91.5
Air	3.617	97.0

The fitting parameter (Ω) is a look-up table based on the gas temperature divided by the ratio of maximum energy of attraction between a pair of molecules to Boltzmann's constant (eok). The parameter is shown graphically in Figure 4.8.

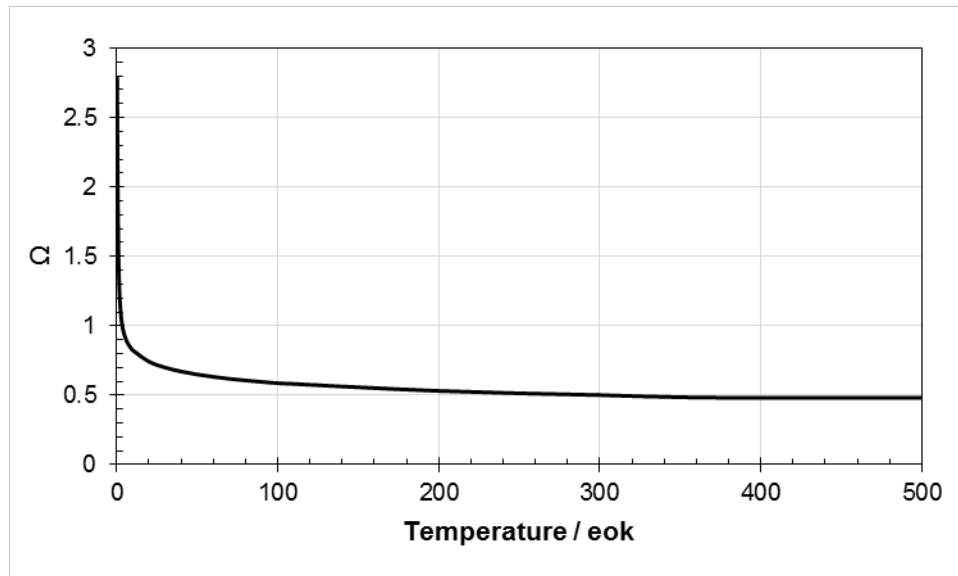


Figure 4.8. Fitting parameter (Ω) for calculating gas viscosity

The viscosity for steam is shown in Equation (4.11). The steam temperature (T) has a minimum allowable value of 75.61K.

$$\mu_{steam} = 1.0 * 10^{-7} * (0.407 * T - 30.77) \quad (4.11)$$

The viscosity of gas mixtures is calculated with Equation (4.4).

$$\mu_{mix} = \sum_i^n \left(\frac{\mu_i x_i}{x_i + \sum_{j=1}^n (1 - \delta_{ij}) \Psi_{ij} x_j} \right) \quad (4.12)$$

where Ψ_{ij} is given in Equation (4.5)

$$\Psi_{ij} = \frac{\left(1 + \left(\frac{\mu_i}{\mu_j} \right)^{0.5} * \left(\frac{M_j}{M_i} \right)^{0.25} \right)^2}{2^{3/2} * \left(1 + \frac{M_i}{M_j} \right)^{0.5}} \quad (4.13)$$

and

- δ_{ij} = Kronecker delta = 1 for $i = j$, 0 otherwise (unitless)
- n = number of components in mixture (unitless)
- M_i = molecular weight of component i (g/mol)
- x_i = mole fraction of component i (unitless)
- μ_i = viscosity of the component i (kg/m-s)

4.5 Gas Specific Heat (GASCP)

The function GASCP calculates the specific heat of the gas mixture. The specific heat is the sum of the specific heat of the individual gases, normalized by their molar fraction. Steam is modeled assuming it is also a non-condensable gas. If the temperature of the gas is below the minimum temperature threshold ($T_0 = 250K$ for all gases), the gas is assumed to have ideal specific heat behavior, shown in Equation (4.14).

$$C_v = c_0 \quad (4.14)$$

Otherwise,

$$C_v = c_0 + d_0 * (T - T_0) \quad (4.15)$$

Where

- C_v = Specific Heat at constant volume (J/kg*K)
- c_0 = constant parameter (J/kg*K)
- d_0 = linear temperature coefficient (J/kg*K²)
- T = gas temperature (K)

The fitting parameters of each of the gases modeled is given in Table 4.7.

Table 4.7. Fitting Parameters for Specific Heat of Gas Species

Gas	c_0	d_0
He	3115.839	3.455924×10^{-3}
Ar	312.192	3.517×10^{-3}
Kr	148.824	3.5×10^{-3}
Xe	94.9085	3.5×10^{-3}
H ₂	10310.75	5.22573×10^{-1}
N ₂	741.976	1.184518×10^{-1}
Air	715.0	1.0329037×10^{-1}

The specific heat of steam (J/kg*K) is modeled using Equation (4.9).

$$C_{p,steam} = C_1 + C_2 * T + \frac{(C_3 * P)}{(C_5 * T - C_6)^{2.4}} + \frac{(C_4 + P^3)}{(C_5 * T - C_6)^9} \quad (4.16)$$

Where T is the temperature (Kelvin) and P is the pressure (Pa). The temperature is required to be greater than 273.15K and the specific heat of the steam is limited to a maximum value of 4183.996 J/kg*K. The fitting parameters for the steam specific heat are given in Table 4.8.

Table 4.8. Fitting Parameters for Specific Heat of steam

C_1	1.68835968×10^3
C_2	0.6029856
C_3	482.0979623
C_4	2.95317905×10^7
C_5	1.8
C_6	460

The specific heat of the mixture is expressed in Equation (4.17), where x represents the molar fraction, R_i represents the ideal gas constant and $C_{v,i}$ represents the specific heat at constant volume of each gas species.

$$C_{p,mix} = \sum_i^n x_i * (C_{v,i} + R_i) \quad (4.17)$$

If steam is present, the specific heat of the mixture becomes

$$C_{p,mix} = C_{p,mix} + x_i * C_{p,steam} \quad (4.18)$$

5.0 References

- Adams M. 1954. "Thermal conductivity: III, prolate spheroidal envelope method." *Journal of the American Ceramic Society* 37:74-79.
- Adamson MG, EA Aitken, and RW Caputi. 1985. "Experimental and thermodynamic evaluation of the melting behavior of irradiated oxide fuels." *Journal of Nuclear Materials* 130:349-365.
- Affortit C and J Marcon. 1970. "Chaleur Specificque a Haute Temperature des Oxydes D'Uranium et de Plutonium." *Revue Internationale des Hautes Temperatures et des Refractaires* 7:236-241.
- Anderson WK, CJ Beck, AR Kephart, and JS Theilacker. 1962. *Zirconium Alloys*. Reactor Structural Materials: Engineering Properties as Affected by Nuclear Reactor Service, ASTM-STP-314, pp. 62-93, American Society for Testing and Materials, West Conshohocken, Pennsylvania.
- Armstrong PE and HL Brown. 1964. *Dynamic Young's Modulus Measurement above 1000°C on Some Pure Polycrystalline Metals and Commercial Graphites*. Transactions of the Metallurgical Society of AIME 230, pp. 962-966.
- Baldock PJ, WE Spindler, and TW Baker. 1966. "The x-ray thermal expansion of near-stoichiometric UO_2 ." *Journal of Nuclear Materials* 18(3):305-313. doi:10.1016/0022-3115(66)90171-1.
- Banks DA. 1974. "Some observations of density and porosity changes in UO_2 fuel irradiated in water-cooled reactors." *Journal of Nuclear Materials* 54:97-107.
- Bates JL, CA Hinman, and T Kawada. 1967. "Electrical conductivity of uranium dioxide." *Journal of the American Ceramic Society* 50:652-656.
- Bolmaro RE and F Povolo. 1988. "Anelastic behaviour of materials under multiaxial strains." *Journal of Materials Science* 23:371.
- Brassfield HC, JF White, L Sjudahl, and JT Bittel. 1968. *Recommended Property and Reactor Kinetics Data for Use in Evaluating a Light-Water-Coolant Reactor Loss-of-Coolant Incident Involving Zircaloy-4 or 304-SS-Clad UO_2* . Report GEMP-482, General Electric Company, Cincinnati, Ohio.
- Brett NH and LE Russel. 1960. "The Thermal Expansion of PuO_2 and Some Other Actinide Oxides Between Room Temperature and 1000°C." In *Proceedings of the Second International Conference on Plutonium Metallurgy*, pp. 397-410, April 19-22, 1, Grenoble, France.
- Brooks CR and EE Stansbury. 1966. "The specific heat of Zircaloy-2 from 50 to 700°C." *Journal of Nuclear Materials* 18:223.
- Bunnell LR, GB Mellinger, JL Bates, and CR Hann. 1977. *High Temperature Properties of Zircaloy Oxygen Alloys*. EPRI NP-524, Battelle Pacific Northwest Laboratory, Richland, Washington.
- Bunnell LR, JL Bates, and GB Mellinger. 1983. "Some high-temperature properties of Zircaloy-Oxygen alloys." *Journal of Nuclear Materials* 116(2-3):219-232.

- Burdick MD and HS Parker. 1956. "Effect of particle size on bulk density and strength properties of uranium dioxide Specimens." *Journal of the American Ceramic Society* 39:181-187.
- Busby CC. 1966. *Properties of Zircaloy-4 Tubing*. WAPD-TM-585, p. 65, Bettis Atomic Power Laboratory, Pittsburgh, Pennsylvania.
- Chen SHP and SC Saxena. 1973. "Experimental Determination of Thermal Conductivity of Nitrogen in the Temperature Range 100-2200°C." *High Temperature Science* 5(3):206-233.
- Chirigos, J.N., et al. 1961. "Development of Zircaloy-4," Fuel Element Fabrication, New York: Academic Press, pp. 19-55.
- Christensen JA. 1963. "Thermal expansion and change in volume of uranium dioxide on melting." *Journal of the American Ceramic Society* 46:607-608.
- Christensen, J.A. et al. 1964. "Uranium Dioxide Thermal Conductivity," Transactions of the American Nuclear Society, 7:391-392.
- Colombier V, MI Horvath, T Tverberg, and H Jenssen. 2010. *Comparative Study of the Gadolinia Experiments IFA-515.10, IFA-636, IFA-681.1, and IFA-676.1*. HWR-924, OECD Halden Reactor Project, Halden, Norway.
- Cabannes MMF, JP Stora, and J Tsakiris. 1967. "ORTIQUE-MOLECULAIRE-Fracteurs de re'flexion et d'e'mission de UO₂ a' haute Temperature." *C.R. Acad. SC. Paris*, 264.
- Coughlin JP and EG King. 1950. "High-temperature heat contents of some zirconium-containing substances." *Journal for the American Chemical Society* 72:2262.
- Cunningham ME, CE Beyer, FE Panisko, PG Medvedev, GA Berna, and HH Scott. 2001. *FRAPTRAN: Integral Assessment*, NUREG/CR-6739, Vol. 2, PNNL-13576, Pacific Northwest National Laboratory, Richland, Washington.
- Daniel RC. 1971. *In-Pile Dimensional Changes of Zircaloy-4 Tubing Having Low Hoop Stresses (LWBR Development Program)*, WAPD-TM-973, Bettis Atomic Power Laboratory, Pittsburgh, Pennsylvania.
- Daniel RC. 1972. "In-pile dimensional changes of zircaloy-4 tubing having stresses (light water breeder reactor development program)." *Nuclear Technology* 14:171-186.
- Deem HW and EA Eldridge. 1967. *Specific Heats of Transformation of Zirclaoy-2 and Low Nickel Zircaloy-2*. USAEC BM1-1803, Battelle Memorial Institute, Columbus, Ohio.
- Dideon, C.G., and G.M. Bain. 1983. Fuel Performance under Extended Burnup for the B&W 15x15 Design, DOE/ET-34212-38, Babcock and Wilcox, Lynchburg, VA.
- Duriez C, J-P Allesandri, T Gervais, and Y Philipponnea. 2000. "Thermal conductivity of hypostoichiometric low pu content (U,Pu)O_{2-x} mixed oxide." *Journal of Nuclear Materials* 277:143-158.

- Faubert FM and GS Springer. 1972. "Measurement of the thermal conductivity of argon, krypton, and nitrogen in the range 800-2000°K." *Journal of Chemical Physics* 57(6):2333-2340.
- Faubert FM and GS Springer. 1973. "Measurement of the thermal conductivity of helium up to 2100°K by the column method." *Journal of Chemical Physics* 58(10):4080-4083.
- Feith, A.D. 1966. Thermal Conductivity and Electrical Resistivity of Zircaloy-4, GEMP-669, October 1966, General Electric Company, Missile and Space Division, Cincinnati, OH.
- Fink JK. 2000. "Zircaloy Thermal Conductivity." International Nuclear Safety Center Material Properties Database (<http://www.insc.anl.gov/matprop/zircaloy/index.php>), Argonne National Laboratory, Argonne, Illinois.
- Fisher ES and CJ Renken. 1964. "Single – Crystal elastic moduli and the CHP-BCC transformation in Ti, Zr, and Hf." *Physical Review* 135(2A):A482-494.
- Franklin DG, GE Lucas, and AL Bement. 1983. *Creep of Zirconium Alloys in Nuclear Reactors*. ASTM-STP-815, American Society for Testing and Materials, West Conshohocken, Pennsylvania.
- Franklin DG. 1982. "Zircaloy Cladding Deformation during Power Reactor Irradiation." In *Proceedings of the Fifth International Symposium on Zirconium in the Nuclear Industry*, ASTM-STP-754, pp. 235-267, American Society of Testing and Materials, West Conshohocken, Pennsylvania.
- Freshley MD, DW Brite, JL Daniel, and PE Hart. 1976. "Irradiation-induced densification of UO₂ pellet fuel." *Journal of Nuclear Materials* 62:138-166.
- Freshley MD, DW Brite, JL Daniel, and PE Hart. 1978. "Irradiation-induced densification and PuO₂ particle behavior in mixed-oxide pellet fuel." *Journal of Nuclear Materials* 81:63-92.
- Garde, A.M. 1986. Hot Cell Examination of Extended Burnup Fuel from Fort Calhoun, DOE/ET-34030-11 (CEND-427), Combustion Engineering, Windsor, CT.
- Geelhood KJ, WG Luscher, PA Raynaud, IE Porter . 2015a. *FRAPCON-4.0: A Computer Code for the Calculation of Steady-State, Thermal-Mechanical Behavior of Oxide Fuel Rods for High Burnup*. PNNL-19418, Vol. 1 Rev. 2, Pacific Northwest National Laboratory, Richland, Washington.
- Geelhood KJ, WG Luscher, and JM Cuta. 2015b. *FRAPTRAN-2.0: A Computer Code for the Transient Analysis of Oxide Fuel Rods*. PNNL-19400, Vol. 1 Rev. 2, Pacific Northwest National Laboratory, Richland, Washington.
- Geelhood KJ, WG Luscher, and CE Beyer. 2008. *PNNL Stress/Strain Correlation for Zircaloy*. PNNL-17700, Pacific Northwest National Laboratory, Richland, Washington.
- Gibby RL, L Leibowitz, JF Kerrisk, and DG Clifton. 1974. "Analytical expressions for enthalpy and heat capacity for uranium-plutonium oxide." *Journal of Nuclear Materials* 50:155-161.
- Gibby, R.L. 1971. "The Effect of Plutonium Content on the Thermal Conductivity of (U,Pu)O₂ Solid Solutions," *Journal of Nuclear Materials*, 38:163-177.

Gilbon D, A Soniak, S Doriot, and JP Mardon. 2000. "Irradiation Creep and Growth Behavior, and Microstructural Evolution of Advanced Zr-Base Alloys." In *Zirconium in the Nuclear Industry: Twelfth International Symposium*, ASTM-STP-1354, pp. 51-73, eds. GP Sabol and GD Moan, American Society of Testing and Materials, West Conshohocken, Pennsylvania.

Gilchrist KE. 1976. "Thermal property measurements on zircaloy-2 and associated oxide layers up to 1200°C." *Journal of Nuclear Materials* 62:257-264.

Gilchrist KE. 1979. "Thermal conductivity of oxide deposited on zircaloy fuel tube material – A continuation of previous work." *Journal of Nuclear Materials* 82:193-194.

Godfrey, T.G., et al. 1964. Thermal Conductivity of Uranium Dioxide and Armco Iron by an Improved Radial Heat Flow Technique, ORNL-3556, Oak Ridge National Laboratory, Oak Ridge, TN.

Goldsmith, L.A., and J.A.M. Douglas. 1973. "Measurements of the Thermal Conductivity of Uranium Dioxide at 670-1270 K," *Journal of Nuclear Materials*, 47:31-42.

Gronvold F, NJ Kveseth, A Sveen, and J Tichý. 1970. "Thermodynamics of the UO_{2+x} phase I. Heat capacities of $UO_{2.017}$ and $UO_{2.254}$ from 300 to 1,000 K and electronic contributions." *Journal of Chemical Thermodynamics* 2:665-679, doi:10.1016/0021-9614(70)90042-X.

Gronvold F. 1955. "High temperature x-ray study of uranium oxides in the $UO_2-U_3O_8$ region." *Journal of Inorganic and Nuclear Chemistry* 1:357-370.

Hagrman DL, GA Reymann, and GE Mason. 1981. *A Handbook of Materials Properties for Use in the Analysis of Light Water Reactor Fuel Rod Behavior, MATPRO Version 11 (Revision 2)*, NUREG/CR-0479 (TREE-1280), prepared by EG&G Idaho, Inc., Idaho Falls, Idaho, for the U.S. Nuclear Regulatory Commission, Washington D.C.

Hamming RW. 1971. *Introduction to Applied Numerical Analysis*. New York: McGraw-Hill Book Company, Inc.

Harbottle JE. 1970. *The Temperature and Neutron Dose Dependence of Irradiation Growth in Zircaloy-2*. Irradiation Effect on Structural Alloys for Nuclear Reactor Applications, ASTM-STP-485, pp. 287-299, American Society of Testing and Materials, West Conshohocken, Pennsylvania.

Hein RA, LH Sjodahl, and R Swarc. 1968. "Heat content of uranium dioxide from 1,200 to 3,100 K." *Journal of Nuclear Materials* 25:99-102.

Held PC and DR Wilder. 1969. "High temperature hemispherical spectral emittance of uranium oxides at 0.65 and 0.70 μm ." *Journal of the American Ceramic Society* 52(4):182-185.

Hobson, I.C., R. Taylor, and J.B. Ainscough. 1974. "Effect of Porosity and Stoichiometry on the Thermal Conductivity of Uranium Dioxide," *Journal of Physics, Section D: Applied Physics*, 7:1003-1015.

Irisa Y, K Murai, K Goto, S Suzuki, R Sabate, and JM Alonso. 2000. "Segmented Fuel Rod Irradiation Programme on Advanced Materials for High Burnup." In *Proceedings of the 2000 Light Water Fuel Performance Meeting*, April 10-13, 2000, Park City, Utah.

- Jain PC and SC Saxena. 1975. "Transport properties of helium in the temperature range 400-2300K." *Chemical Physics Letters* 36(4):489-491.
- Jensen SE. 1969. *Parametric Studies of Fuel Pin Temperature Response*. IDO-17295, Philips Petroleum Company, Atomic Energy Division, Idaho Falls, Idaho.
- Jody BJ, SC Saxena, VPS Nain, and RA Aziz. 1977. "Thermal conductivity of helium: A problem for the repulsive wall of the interatomic potential." *Chemical Physics* 22:53-58.
- Jones JM and DG Murchison. 1965. "Optical properties of uranium oxides." *Nature* 205(4972):663-665.
- Kearns JJ. 1965. *Thermal Expansion and Preferred Orientation in Zircaloy*. WAPD-TM-472, pp. 17-18, Bettis Atomic Power Laboratory, Pittsburgh, Pennsylvania.
- Kempton, C.P., and R.E. Elliott. 1958. "Thermal Expansion of UN, UO₂, UO₂-ThO₂, and ThO₂." *Journal of Chemical Physics* 30:1524-1526.
- Kerrisk JF and DG Clifton. 1972. "Smoothed values for the enthalpy and heat capacity of UO₂." *Nuclear Technology* 16:531-535.
- Kingery WD, J Francl, RL Coble, and T Vasilos. 1954. "Thermal conductivity: X, data for several pure oxide materials corrected to zero porosity." *Journal of the American Ceramic Society* 37(2):107-100.
- Knuutila A. 2006. *Improvements on FRAPCON-3/FRAPTRAN Mechanical Modeling*. VTT-R-11337-06, VTT Technical Research Centre of Finland, Espoo, Finland.
- Komatsu J, T Tachibana, and K Konashi. 1988. "The melting temperature of irradiated oxide fuel." *Journal of Nuclear Materials* 154:38-44.
- Korber H and HE Unger. 1974. "Sensitivity study on core heatup and meltdown by variation of heat conductivity and thermal emissivity." *Transactions for the American Nuclear Society* 18:234-235.
- Krett, V., and J. Cleveland. 1997. *Thermophysical Properties of Materials for Water Cooled Reactors*, IAEA-TECDOC-949, pp. 67-84, International Atomic Energy Agency, Vienna, Austria.
- Kreyns, P.H., quoted by E. Duncombe et al. 1996. Comparison with Experiment of Calculated Changes and Failure Analysis of Irradiated Bulk Oxide Fuel Test Rods Using the CYGRO01 Computer Program, WAPD-TM-583, Bettis Atomic Power Laboratory, Pittsburgh, PA.
- Kruger OL and H Savage. 1968. "Heat capacity and thermodynamic properties of plutonium dioxide." *Journal of Chemical Physics* 45:4540-4544.
- Lanning DD and ER Bradley. 1984. *Irradiation History and Interim Postirradiation Data for IFA-432*, NUREG/CR-3071, Pacific Northwest Laboratory for the U.S. Nuclear Regulatory Commission, Washington D.C.

Lanning DD, CE Beyer, and CL Painter. 1997. *FRAPCON-3: Modifications to Fuel Rod Material Properties and Performance Models for High-Burnup Application*, NUREG/CR-6534, Vol. 1, Pacific Northwest National Laboratory for the U.S. Nuclear Regulatory Commission, Washington D.C.

Lanning DD, CE Beyer, and KG Geelhood. 2005. *FRAPCON-3 Updates, Including Mixed-Oxide Fuel Properties*, NUREG/CR-6534, Vol. 4, PNNL-11513, Pacific Northwest National Laboratory, Richland, Washington.

Lapshov VN and AV Bashkatov. 1973. "Thermal conductivity of coatings of zirconium dioxide applied by the plasma sputtering method." *Heat Transfer-Soviet Research* 5:19-22.

Leibowitz L, DF Fischer, and MG Chasanov. 1972. "Enthalpy of uranium plutonium oxides (U_{0.8}Pu_{0.2}) O_{1.07} from 2,350 to 3,000 K." *Journal of Nuclear Materials* 42:113-116.

Leibowitz L, LW Mishler, and MG Chasanov. 1969. "Enthalpy of solid uranium dioxide from 2,500 K to its melting point." *Journal of Nuclear Materials* 29:356-358.

Leibowitz, L., et al. 1971. "Enthalpy of Liquid Uranium Dioxide to 3500 K," *Journal of Nuclear Materials*, 39:115-116.

Limbäck M and T Andersson. 1996. "A Model for Analysis of the Effect of Final Annealing on the In- and Out-of-Reactor Creep Behavior of Zircaloy Cladding." In *Zirconium in the Nuclear Industry: Eleventh International Symposium*, ASTM STP 1295, pp. 448-468, eds. ER Bradley and GP Sabol, American Society for Testing and Materials, West Conshohocken, Pennsylvania.

Ljusternik, V.E., et al. 1993. "Experimental research of zirconium reactor materials thermal properties: 110-alloy." *M.J. Higher Temperature Thermal Physics* 31(4).

Lucks, C.F., and H.W. Deem. 1958. Progress Relating to Civilian Applications during June, 1958, R.W. Dayton and C.R. Tipton, Jr., eds., BMI-1273, pp. 7-9, Battelle Memorial Institute, Columbus, OH.

Lucuta PG, HS Matzke, and IJ Hastings. 1996. "A pragmatic approach to modeling thermal conductivity of irradiated UO₂ fuel: Review and recommendations." *Journal of Nuclear Materials* 232:166-180.

Luscher, W.G., and K.J. Geelhood. 2014. Material Property Correlations: Comparisons between FRAPCON-3.4, FRAPTRAN 1.4, and MATPRO, NUREG/CR-7024, PNNL-19417, Pacific Northwest National Laboratory, Richland, WA.

Lustman B and F Kerze. 1955. *The Metallurgy of Zirconium*, p. 355, McGraw-Hill Book Company, New York.

Lyon WF and WE Baily. 1967. "The solid liquid phase diagram for the UO₂-PuO₂ system." *Journal of Nuclear Materials* 22:332.

Maglic, K.D., N.L.j. Perovic, and A.M. Stanimirovic. 1994. "Calorimetric and Transport Properties of Zircalloy 2, Zircalloy 4, and Inconel 625," *International Journal of Thermophysics*, 15(4):741-755.

- Maki H. 1973. "Heat transfer characteristics of zircaloy-2 oxide film." *Journal of Nuclear Science and Technology* 10:107-175.
- Martin DG. 1988. "The thermal expansion of solid UO₂ and (U,Pu) mixed oxides – A review and recommendations." *Journal of Nuclear Materials* 152:94-101.
- Massih AR, S Persson, and Z Weiss. 1992. "Modeling of (U,Gd)O₂ Fuel Behavior in Boiling Water Reactors." In *Proceedings of Symposium E on Nuclear Materials for Fission Reactors of the 1991 E-MRS Fall Conference; Journal of Nuclear Materials* 188:323-330.
- Matsuo Y. 1987. "Thermal creep of zircaloy-4 cladding under internal pressure." *Journal of Nuclear Science and Technology* 24(2):111-119.
- Mehan RL and FW Wiesinger. 1961. *Mechanical Properties of Zircaloy-2*, KAPL-2110, pp. 11-12, General Electric Company, Knolls Atomic Power Laboratory, Schenectady, New York.
- Mehan, R.L. 1958. Modulus of Elasticity of Zircaloy-2 Between Room Temperature and 1,000°F, KAPL-M-RLM-16, General Electric Company, Knolls Atomic Power Laboratory, Schenectady, NY.
- Mogensen M, CT Walker, ILF Ray, and M Coquerelle. 1985. "Local fission gas release and swelling in water reactor fuel during slow power transients." *Journal of Nuclear Materials* 131:162-171.
- Momin AC, EB Mirza, and MD Mathews. 1991. "High temperature x-ray diffraction studies on the lattice thermal expansion behavior of UO₂, ThO₂, and (U_{0.2}Th_{0.8})O₂ doped with fission products." *Journal of Nuclear Materials* 185:308-310.
- Murabayashi, M., S. Tanaka, and Y. Takahashi. 1975. "Thermal Conductivity and Heat Capacity of Zircaloy-2, -4 and Unalloyed Zirconium," *Journal of Nuclear Science and Technology*, 12(10):661-662.
- Newman, L.W. 1986. The Hot Cell Examination of Oconee 1 Fuel Rods after Five Cycles of Irradiation, DOE/ET-34212-36, Babcock and Wilcox, Lynchburg, VA.
- Newman, L.W. 1986. The Hot Cell Examination of Oconee 1 Fuel Rods After Five Cycles of Irradiation, DOE/ET/34212-50, Babcock and Wilcox Company, Lynchburg, VA.
- Northwood, D.O., et al. 1975. "Elastic Constants of Zirconium Alloys," *Journal of Nuclear Materials*, 55:299-310.
- NRC – U.S. Nuclear Regulatory Commission. 1978. "An Acceptable Model and Related Statistical Methods for the Analysis of Fuel Densification." Regulatory Guide 1.126, Rev. 1, U.S. Nuclear Regulatory Commission, Washington D.C.
- Ohira K and N Itagaki. 1997. "Thermal Conductivity Measurements of High Burnup UO₂ Pellet and a Benchmark Calculation of Fuel Center Temperature." In *Proceedings of the ANS International Topical Meeting on LWR Fuel Performance*, pp. 541-549, March 2-6, 1997, Portland, Oregon.
- Padel A and A Groff. 1976. "Variation du Module de Young du Zirconium b en Fonction de la Temperature." *Journal of Nuclear Materials* 59:325-326.

Peggs and Bunnell. et al. (1983)

Peggs ID and DP Godin. 1975. "The yield strength-hot hardness relationship of zircaloy-4." *Journal of Nuclear Materials* 57:246-248.

Peggs, I.D., A.M. Stadnyk, and D.P. Godin. 1976. "Thermophysical Properties of Zirconium-Alloy Fuel Channel Components," *High Temperatures-High Pressures*, 8(4):441-450.

Popov SG, JJ Carbajo, VK Ivanov, and GL Yoder. 2000. *Thermophysical Properties of MOX and UO₂ Fuel Including the Effects for Irradiation*. ORNL/TM 2000/351, Oak Ridge National Laboratory, Oak Ridge, Tennessee.

Powers, A.E. 1961. Application of the Ewing Equation for Calculating Thermal Conductivity from Electrical Conductivity from Electrical Conductivity, KAPL-2146, Knolls Atomic Power Laboratory, General Electric Company, Schenectady, NY.

Rolstad, E., et al. 1974. "Measurements of the Length Changes of UO₂ Fuel Pellets During Irradiation," Enlarged HPG Meeting on Computer Control and Fuel Research, June 4-7, 1974.

Ronchi C, M Sheindlin, M Musella, and GJ Hyland. 1999. "Thermal conductivity of uranium dioxide up to 2900K from simultaneous measurement of the heat capacity and thermal diffusivity." *Journal of Applied Physics* 85(2):776-789.

Ronchi, C., M. Sheindlin, D. Staicu, and M. Kinoshita. 2004. "Effect of Burn-up on the Thermal Conductivity of Uranium Dioxide up to 100,000 MWdt-1," *Journal of Nuclear Materials*, 327:58-76.

Ross AM and RL Stoute. 1962. *Heat Transfer Coefficient Between UO₂ and Zircaloy-2*. AECL-1552, Atomic Energy of Canada, Ltd., Chalk River, Ontario.

Sabol GP, RJ Comstock, RA Weiner, P Larouere, and RN Stanutz. 1994. "In-Reactor Corrosion Performance of ZIRLO and Zircaloy-4." In *Zirconium in the Nuclear Industry: Tenth International Symposium*, ASTM-STP-1425, pp. 724-744, eds. AM Garde and ER Bradley. American Society for Testing and Materials, Philadelphia, Pennsylvania.

Saxena SC and VK Saxena. 1970. "Thermal conductivity data for hydrogen and deuterium in the range 100-1100°C." *Journal of Physics A*, 3(3):309-320.

Saxena, V.K., and S.C. Saxena. 1968. "Measurement of the Thermal Conductivity of Argon Using Hot-Wire Type Thermal Diffusion Columns," *Chemical Physics Letters*, 2(1):44-46.

Saxena VK and SC Saxena. 1969. "Thermal conductivity of krypton and xenon in the temperature range 350-1500K." *Journal of Chemical Physics* 51(8):3361-3368.

Scott DB. 1965. *Physical and Mechanical Properties of Zircaloy 2 and 4*, WCAP-3269-41, pp. 5, 9, Westinghouse Electric Corporation, Atomic Power Division, Pittsburgh, Pennsylvania.

Shestopalov A, K Lioutov, L Yegorova, G Abyshov, and K Mikitiouk. 1999. *Modification of USNRC's FRAP-T6 Fuel Rod Transient Code for High Burnup VVER Fuel*. NUREG/IA-0164, U.S. Nuclear Regulatory Commission, Washington D.C.

Shober FB, JA Van Echo, LL Marsh, Jr., and JR Keeler. 1957. *The Mechanical Properties of Zirconium and Zircaloy-2*. BMI-1168, Battelle Memorial Institute, Columbus, Ohio.

Siefken LJ, EW Coryell, EA Harvego, and JK Hohorst. 2001. *SCDAP/RELAP5/MOD 3.3 Code Manual MATPRO-A Library of Materials Properties for Light-Water-Reactor-Accident Analysis*. NUREG/CR-6150, Vol. 4, Rev. 2, INEL-96/0422, Idaho National Engineering and Environmental Laboratory, Idaho Falls, Idaho.

Small GJ. 1987. "Densification of uranium dioxide at low burn-up." *Journal of Nuclear Materials*, 148:302-315.

Smith, GP, R.C. Pirek, H.R. Freeburn, and D. Schrire. 1994. *The Evaluation and Demonstration of Methods for Improved Nuclear Fuel Utilization*, DOE/ET-34-013-15, Combustion Engineering, Windsor, CT.

Soniak A, NL Hullier, J-P Mardon, V Rebeyrolle, P Boffioux, and C Bernaudat. 2002. "Irradiation Creep Behavior of Zr-Base Alloys." *Zirconium in the Nuclear Industry: Thirteenth International Symposium*, ASTM STP 1423, eds GD Moan and P Rudling, pp.837-862, June 10-14, 2001, ASTM International, West Conshohocken, Pennsylvania.

Spasic, Z., et al. 1968. *Conference on the Use of Zirconium Alloys in Nuclear Reactors*, Marlanske Lanze, Czechoslovakia, USAEC CONF-681086, 1968, pp. 277-284.

Springer GS and EW Wingeier. 1973. "Thermal conductivity of neon, argon, and xenon at high temperatures." *Journal of Chemical Physics* 59(5):2747-2750.

Stefanov B, L Zarkova, and D Oliver. 1976. "Measurement of the thermal-conductivity coefficient of gases and vapors up to 2500°K." *High Temperature* 14(1):48-57.

Timrot DL and AS Umanskii. 1966. "Thermal conductivity of hydrogen and argon," *High Temperature* 3:285-287.

Tokar, M., and A.W. Nutt. 1972. "Thermal Expansion of PuO₂ from 25 to 1420°C," *Transactions of the American Nuclear Society*, 10:210-211.

Toyoaki Y, M Hideharu, and Y Masahiro. 1999. "Melting and measurements of solidification point of UO₂-Gd₂O₃ solid solutions under solar furnace." *Journal of High Temperature Study* 25(2):71-79.

Vargaftik, N.B., and L.V. Yakush. 1971. "Measurement of the thermal conductivities of neon, krypton, and xenon over a wide range of temperatures." *Journal of Engineering Physics* 21(3):1156-1161.

Vargaftik NB and NKh Zimina. 1964. "Thermal Conductivity of Nitrogen at High Temperatures." *High Temperature* 2(6):782-790.

Volkov BYu, VF Viktorov, PA Platonov, and A Rjazantzeva. 1989. *Library of Subprograms on Physical and Mechanical Properties of the N1-Alloy Fuel Rod Cladding Material*. Preprint IAE-4941/11, Institute of Automation and Electrometry, Moscow, Russia.

Volkov BYu, VF Viktorov, PA Platonov, and AV Ryazantseva. 1989. *Library of subprograms on physical-mechanical properties of H-1 alloy fuel element cladding*. IAE-4941-11, 24(02):16.

Weilbacher JC. 1972. "Diffusivite Thermique de l'Oxyde d'Uranium et de l'Oxyde de Thorium a Haute Temperature," *High Temperatures-High Pressure*, 4:431-438.

Whitmarsh CL. 1962. *Review of Zircaloy-2 and Zircaloy-4 Properties Relevant to N.S. Savannah Reactor Design*, ORNL-3281, Oak Ridge National Laboratory, Oak Ridge, Tennessee.

Wiesenack W and T Tverberg. 2000. "Thermal Performance of High Burnup Fuel – In-Pile Temperature Data and Analysis." In *Proceedings of the ANS International Topical Meeting on Light Water Reactor Fuel Performance*, pp. 730-737, April 2000, Park City, Utah.

Appendix A
Subroutine Source Codes

Appendix A

Subroutine Source Codes

A.1 Uranium Dioxide/Mixed Oxide Properties

A.1.1 Fuel Melting Temperature (PHYPRP)

FRAPCON-4.0: PHYPRP

```
*deck phyprp
  subroutine phyprp(gadoln)
c
c  phyprp returns uo2, (u,pu)o2, and zircaloy melting points
c  and heats of fusion, and zirconium and zircaloy alpha to beta
c  transition temperatures.
      common / phypro / ftmelt,fhefus,ctmelt,chefus,ctranb,
+           ctrane,ctranz,fdelta,bu,comp,deloxy
c  ftmelt = output uo2 or mixed oxide fuel melting points (k)
c  fhefus = output uo2 or mixed oxide fuel heat of fusion (j/kg)
c  ctmelt = output zr clad melting point (k)
c  chefus = output zr clad heat of fusion (j/kg).
c  ctranb = output start of zr-4 alpha-beta transus temperature (k)
c  ctrane = output end of zr-4 alpha-beta transus temperature (k)
c  ctranz = output zr isothermal alpha-beta transus temperature (k)
c  fdelta = output liquid-solid coexistence temperature range (k)
c  bu      = input burnup (mw-s/kg-u)
c  comp    = input puo2 content (wt%)
c  deloxy  = input oxygen concentration - oxygen concentration
c           of as received cladding (kg oxygen/kg zircaloy)
c  the uo2 and zr cladding melting points and heats of fusion are
c  taken from the following references. uo2 fuel melting point of
c  3113k from h.c.brassfield et al gemp-482. uo2 heat of fusion
c  of 17.7 kcal/mole from l.leibowitz et al, j.nuc.mat. 39 p 115
c  (1971). cladding melting point of 2098 k from m.l. picklesimer
c  private communication. cladding heat of fusion of 4.9 kcal/mol
c  from brassfield et al, gemp-482.
c  beginning and end of alpha-beta transus are from data in
c  figure iii.33 of anl-76-49
c  isothermal zirconium alpha-beta transus temperature is 1135 k
c  taken from b.lustman & f.kerze "the metallurgy of zirconium"
c  mcgraw-hill book co., new york, 1955
c  mixed oxide melting point was obtained from lyon et al, j. nuc.
c  mat., 22 (1967) p 332
c  phypro was coded by v.f. baston in may 1974
c  modified by c.s. olsen in feb. 1975
c  modified by b.w. burnham in nov. 1977
c  modified by d.l. hagrman in june 1979
c  burnup dependance for fuel melting temperature changed from 3.2K/GWd/tHM
c  to 0.5 K/GWd/tHM by K.J. Geelhood in June 2004 based on
c  S. G. Popov, et al., "Thermophysical Properties of MOX and UO2 Fuels
c  including the Effects of Irradiation," ORNL/TM-2000/351.
      include 'lacmdl.h'
      data      on      / 1 /,
+             off      / 2 /,
+             locidx   / 2   /
      sldus(c) = 2840.0-5.41395*c+7.468390e-3*c*c
      liqds(c) = 2840.0-3.21860*c-1.448518e-2*c*c
```

```

fbu = bu/86.4
if (comp.gt.0.0) go to 100
ftmelt = 3113.15-5.0*fbu/10000.0-4.8*gadln*100.0
fdelta = 1.0e-10
go to 110
100 c1 = comp
ftmelt = sldus(c1)+273.15-5.0*fbu/10000.0-4.8*gadln*100.0
fdelta = liqds(c1)-sldus(c1)-5.0*fbu/10000.0-4.8*gadln*100.0
110 fhefus = 27.4e+4
ctmelt = 2098.15
chefus = 22.5e+04
wfox = deloxy+0.0012
ctranb = 1094.+wfox*(-1.289e+03+wfox*7.914e+05)
if (wfox.lt.0.025) go to 120
ctranb = 1556.4+3.8281e+04*(wfox-0.025)
120 ctrane = 392.46*((100.*deloxy+0.1242807)**2+3.1417)
if (deloxy.lt.4.7308937e-03) go to 130
ctrane = (100.*deloxy+0.12)*491.157+1081.7413
130 continue
ctranz = 1135.15
return
end

```

FRAPTRAN-2.0: PHYPRP

```

*deck phyprp
c
c      subroutine phyprp (icm)
c
c      implicit real (a-h,o-z)
c
c      real liqds
c
c      This is a MATPRO-11, Rev. 2 routine modified by PNNL for use in FRAPT
c
c      phyprp returns uo2, (u,pu)o2, and zircaloy melting points
c      and heats of fusion, and zirconium and zircaloy alpha to beta
c      transition temperatures.
c
c      include 'phypro.h'
c
c      ftmelt = output uo2 or mixed oxide fuel melting points (k)
c      fhefus = output uo2 or mixed oxide fuel heat of fusion (j/kg)
c      ctmelt = output zr clad melting point (k)
c      chefus = output zr clad heat of fusion (j/kg).
c      ctranb = output start of zr-4 alpha-beta transus temperature (k)
c      ctrane = output end of zr-4 alpha-beta transus temperature (k)
c      ctranz = output zr isothermal alpha-beta transus temperature (k)
c      fdelta = output liquid-solid coexistence temperature range (k)
c
c      bumtp = input burnup (mw-s/kg-u)
c      compmt = input puo2 content (wt%)
c      deloxy = input oxygen concentration - oxygen concentration
c              of as received cladding (kg oxygen/kg zircaloy)
c
c      the uo2 and zr cladding melting points and heats of fusion are
c      taken from the following references. uo2 fuel melting point of
c      3113k from h.c.brassfield et al gemp-482. uo2 heat of fusion
c      of 17.7 kcal/mole from l.leibowitz et al, j.nuc.mat. 39 p 115
c      (1971). cladding melting point of 2098 k from m.l. picklesimer
c      private communication. cladding heat of fusion of 4.9 kcal/mol
c      from brassfield et al, gemp-482.
c
c      beginning and end of alpha-beta transus are from data in

```

```

c   figure iii.33 of anl-76-49
c   isothermal zirconium alpha-beta transus temperature is 1135 k
c   taken from b.lustman & f.kerze "the metallurgy of zirconium"
c   mcgraw-hill book co., new york, 1955
c
c   mixed oxide melting point was obtained from lyon et al, j. nuc.
c   mat., 22 (1967) p 332
c
c   phypro was coded by v.f. baston in may 1974
c   modified by c.s. olsen in feb. 1975
c   modified by b.w. burnham in nov. 1977
c   modified by d.l. hagrman in june 1979
c   Modified by PNNL, January 1997, to clean up coding and delete
c   sensitivity uncertainty analysis coding
c   burnup dependance for fuel melting temperature changed from
c   3.2 K/GWd/tHM to 0.5 K/GWd/tHM by K.J.Geelhood in June 2004 based on
c   S.G. Popov, et al., "Thermophysical Properties of MOX and UO2 Fuels
c   including the Effects of Irradiation," ORNL/TM-200/351
c
c
c   sldus(c)      = 2840.0d0 - 5.41395d0*c + 7.468390d-3*c*c
c   liq dus(c)    = 2840.0d0 - 3.21860d0*c - 1.448518d-2*c*c
c   fbu = bumtp/86.4d0
c   if (compmt .gt. 0.0d0) go to 10
c
c   ftmelt = 3113.15d0 - 5.0d0*fbu/10000.0d0
c   fdelta = 1.0d-10
c   go to 20
c
c   10 continue
c   c1      = compmt
c   ftmelt = sldus(c1) + 273.15d0 - 5.0d0*fbu/10000.0d0
c   fdelta = liq dus(c1) - sldus(c1) - 5.0d0*fbu/10000.0d0
c
c   20 continue
c   fhefus = 27.4d+4
c
c   go to (400,400,400,400,400,600,400,600,400,400)icm
c
c   400 continue
c   generic Zry properties
c   ctmelt = 2098.15d0
c   chefus = 22.5d+04
c   go to 50
c   600 continue
c   Zr-1%Nb properties from RRC-KI
c   ctmelt = 2133.d0
c   chefus = 21.0d+4
c   50 continue
c
c   5/7/03: ctranb, ctrane, ctranz phase transition temperatures
c   not currently used in FRAPTRAN; RRC-KI does have different
c   transition temperatures for Zr-1%Nb
c   wfox = deloxy + 0.0012d0
c   ctranb = 1094.d0 + wfox*(-1.289d+03 + wfox*7.914d+05)
c   if(wfox .lt. 0.025d0) go to 30
c   ctranb = 1556.4d0 + 3.8281d+04*(wfox - 0.025d0)
c   30 continue
c   ctrane = 392.46d0*((100.d0*deloxy + 0.1242807d0)**2 + 3.1417d0)
c   if(deloxy .lt. 4.7308937d-03) go to 40
c   ctrane = (100.d0*deloxy + 0.12d0)*491.157d0 + 1081.7413d0
c   40 continue
c   ctranz = 1135.15d0

```

```

c
      return
c

```

A.1.2 Fuel Specific Heat Capacity (FCP) and Fuel Enthalpy (FENTHL)

FRAPCON-4.0: FCP

```

*deck fcp
      function fcp (ftemp,facmot,fotmtl,gadoln)
c
c   the function fcp is used to calculate the specific heat capacity
c   of uo2, puo2, and (u,pu)o2 fuels as a function of temperature,
c   fraction of fuel which is molten, puo2 content, and oxygen-to-
c   metal ratio.
c   fcp      = output fuel specific heat capacity (j/(kg*K))
c   ftemp    = input fuel meshpoint temperature (K)
c   facmot   = input fuel fraction molten (unitless)
c   facmot   = 1.0 - fuel is all molten
c   facmot   = 0.0 - fuel is all solid
c   fotmtl   = input oxygen to metal ratio (unitless)
c   fotmtl   = (atoms oxygen)/(atoms metal) if not known,
c             enter 2.0
c   gadoln   = weight fraction of gadolinia in the fuel
c   ufcp     = estimated standard error for uo2 (j/(kg*K))
c             (not currently returned)
c   pufcp    = estimated standard error for puo2 (j/(kg*K))
c             (not currently returned)
c   the equations used in this function are based on data from;
c   (1) j.kerrisk and d.clifton, nuclear technology,16 (1972).
c   (2) o.kruger and h.savage, journal of chemical physics,45
c   (1968).
c   the effect of oxygen-to-metal ratio was estimated from
c   equations published by;
c   (3) c.affortit and j.marcon, revue internationale des hautes
c   temperatures et des refractaires,7 (1970).
c   the specific heat capacity of molten uo2 was taken from
c   (4) l.leibowitz et al, journal of nuclear materials,39 (1970)
c   fcp was originally coded by v.f.baston in march 1974.
c   last modified by g.a.reymann in may 1978.
c   Modification for gadolinia additions were made by DD Lanning
c   in 1996.
      common / phypro / ftmelt,fhefus,ctmelt,chefus,ctranb,
      +          ctrane,ctranz,fdelta,bu,comp,deloxy
c   the phypro common block is set by call to the subroutine
c   phypro which is part of the materials properties package
c   used at the inel.
c   quantities contained in it used in this subcode are;
c   ftmelt = fuel melting temperature (K)
c   fdelta = liquid-solid coexistence temperature (K)
c   comp   = puo2 content (wt.%)
c   when the function fcp is used alone, not as part of the
c   inel code, values for ftmelt, fdelta, and comp must be
c   input.
      data clu ,c2u ,c3u ,thu ,edu / 296.7 , 2.43e-02, 8.745e07,
      +          535.285, 1.577e05 /
      data clpu,c2pu,c3pu,thpu,edpu/ 347.4 , 3.95e-04, 3.860e07,
      +          571.0 , 1.967e05 /
      data clgd,c2gd,c3gd,thgd,edgd/ 315.86 , 4.044e-02 , 0.0,
      +          348.0 , 0.0 /
      cp(c1,c2,c3,th,ed,t,fotmtl) = c1*(th**2)*exp(th/t)/((t**2)*((exp(t
      +h/t)-1.)**2))+c2*t+(fotmtl/2.)*(c3*ed/(8.314*(t**2)))*exp(-ed/

```

```

      +(8.314*t))
      t = ftemp
      r = facmot
      tm = ftmelt
      fcomp = comp/100.0
      fcpmol = 503.0
c   fcpmol = specific heat capacity of molten fuel (j/(kg*K))
      if (t.gt.(tm+fdelta)) go to 100
      fcp = cp(c1u,c2u,c3u,thu,edu,t,fotmtl)*(1.0-fcomp)+cp(c1pu,c2pu,c3
+pu,thpu,edpu,t,fotmtl)*fcomp
      fcp = fcp*(1.0-gadoln) + gadoln*cp(c1gd,c2gd,c3gd,thgd,edgd,t,
+ fotmtl)
      if (t.lt.(tm-0.1)) go to 110
      fcp = (1.0-r)*fcp+r*fcpmol
      go to 110
100  fcp = fcpmol
      ufcpl = 2.0
      pufcp = 5.6
110  continue
      return
      end

```

FRAPTRAN-2.0: FCP

```

*deck fcp
      function fcp (ftemp,facmot,fotmtl,frden)
      implicit real (a-h,o-z)
c
c   This is a MATPRO-11, Rev. 2 routine modified by PNNL for use in FRAPT
c
c   the function fcp is used to calculate the specific heat capacity
c   of uo2, puo2, and (u,pu)o2 fuels as a function of temperature,
c   fraction of fuel which is molten, puo2 content, and oxygen-to-
c   metal ratio.
c
c   fcp      = output fuel specific heat capacity (j/(kg*k))
c
c   ftemp    = input fuel meshpoint temperature (k)
c   facmot   = input fuel fraction molten (unitless)
c             facmot = 1.0 - fuel is all molten
c             facmot = 0.0 - fuel is all solid
c   fotmtl   = input oxygen to metal ratio (unitless)
c             fotmtl = (atoms oxygen)/(atoms metal) if not known,
c             enter 2.0
c   ufcpl    = estimated standard error for uo2 (j/(kg*k))
c             (not currently returned)
c   pufcp    = estimated standard error for puo2 (j/(kg*k))
c             (not currently returned)
c
c   the equations used in this function are based on data from;
c   (1) j.kerrisk and d.clifton, nuclear technology,16 (1972).
c   (2) o.kruger and h.savage, journal of chemical physics,45
c       (1968).
c
c   the effect of oxygen-to-metal ratio was estimated from
c   equations published by;
c   (3) c.affortit and j.marcon, revue internationale des hautes
c       temperatures et des refractaires,7 (1970).
c   the specific heat capacity of molten uo2 was taken from
c   (4) l.leibowitz et al, journal of nuclear materials,39 (1970)
c
c   fcp was originally coded by v.f.baston in march 1974.
c   last modified by g.a.reymann in may 1978.
c   Modified by PNNL, January 1997, to clean up coding and delete lic

```

```

c      analysis and sensitivity uncertainty coding
c
c
c      include 'phypro.h'
c
c      the phypro common block is set by call to the subroutine
c      phypro which is part of the materials properties package
c      used at the inel.
c      quantities contained in it used in this subcode are;
c          ftmelt = fuel melting temperature (k)
c          fdelta = liquid-solid coexistence temperature (k)
c          compmt = puo2 content (wt.%)
c      when the function fcp is used alone, not as part of the
c      inel code, values for ftmelt, fdelta, and compmt must be
c      input.
c
c      data c1u ,c2u ,c3u ,thu ,edu / 296.7d0 , 2.43d-02, 8.745d07,
&          535.285d0, 1.577d05 /
c      data c1pu,c2pu,c3pu,thpu,edpu/ 347.4d0 , 3.95d-04, 3.860d07,
&          571.0d0 , 1.967d05 /
c
c      cp(c1,c2,c3,th,ed,t,fotmtl) =
&      c1*(th**2)*exp(th/t)/((t**2)*((exp(th/t)-1.d0)**2)) + c2*t
&      + (fotmtl/2.d0)*(c3*ed/(8.314d0*(t**2)))*exp(-ed/(8.314d0*t))
c
c      t      = ftemp
c      r      = facmot
c      tm     = ftmelt
c      fcomp  = compmt/100.0d0
c      fcpmol = 503.0d0
c      fcpmol = specific heat capacity of molten fuel (j/(kg*k))
c
c      if (t .gt. (tm+fdelta)) go to 50
c
c      fcp    = cp(c1u ,c2u ,c3u ,thu ,edu ,t,fotmtl)*(1.0d0 - fcomp) +
&          cp(c1pu,c2pu,c3pu,thpu,edpu,t,fotmtl)*fcomp
c
c      if (t .lt. (tm-0.1d0)) go to 100
c      fcp    = (1.0d0 - r)*fcp + r*fcpmol
c      go to 100
c
c      50 continue
c      fcp    = fcpmol
c      ufcf   = 2.0d0
c      pufcf  = 5.6d0
c
c      100 continue
c
c      return
c
c      end

```

FRAPCON-4.0: FENTHL

```

*deck fenthl
c
c      function fenthl (temp,fcomp,fotmtl,ftmelt,facmot,fhefus,gadoln)
c      implicit real * 8 (a-h,o-z)
c      *****
c      this function is called by subroutine energy and computes the
c      enthalpy of fuel at a point relative to zero degrees absolute
c      temperature
c      *****
c      input arguments

```

```

c *****
c facmot - fraction of molten fuel
c fcomp - puo2 fraction of the fuel
c fhefus - heat of fussion of the fuel (j/kg)
c fotmtl - fuel oxygen to metal ratio
c ftmelt - fuel melting temperature (K)
c gadoln - weight fraction of gadolinia in the fuel
c temp - local temperature (K)
c *****
c output
c *****
c fenth1 - local fuel enthalpy relative to zero degrees-K (j/kg)
c *****
c fcpmol = specific heat capacity of molten fuel ( j/(kg*K) )
c data fcpmol / 503.e0 /
c the following data statements contain constants from matpro-11 fcp
c data clu, c2u, c3u, thu, edu / 296.7 , 2.43e-02, 8.745e07,
c + 535.285, 1.577e05 /
c data clpu, c2pu, c3pu, thpu, edpu / 347.4 , 3.95e-04, 3.860e07,
c + 571.0 , 1.967e05 /
c data clgd, c2gd, c3gd, thgd, edgd / 315.86 , 4.044e-2, 0.0 ,
c + 348.0 , 0.0 /
c the following equation is the integral of the fuel specific heat
c with respect to temperature
c cpdt(cl,th,c2,otm,ed,t,c3) = c1*th*(1./(exp(th/t)-1.))+c2*t*t/2.e0
c ++c3*otm*exp(-ed/(t*8.314e0))/2.e0
c tx = temp
c if (tx.gt.ftmelt) tx = ftmelt
c fenth1 = cpdt(clu,thu,c2u,fotmtl,edu,tx,c3u)*(1.e0-fcomp)
c fenth1 = fenth1+cpdt(clpu,thpu,c2pu,fotmtl,edpu,tx,c3pu)*fcomp
c fenth1 = fenth1*(1-gadoln)+
c &gadoln*cpdt(clgd,thgd,c2gd,fotmtl,edgd,tx,c3gd)
c if (temp.le.ftmelt-2.e0) go to 100
c fenth1 = fenth1+fhefus*facmot
c if (temp.le.(ftmelt+2.)) go to 100
c fenth1 = fenth1+(temp-ftmelt)*fcpmol
100 continue
return
end

```

FRAPTRAN-2.0: FENTHL

```

*deck fenth1
c
c function fenth1 (temp, fcomp, fotmtl, ftmelt, facmot, fhefus)
c
c implicit real (a-h,o-z)
c
c *****
c this function is called by subroutine energy and computes the
c enthalpy of fuel at a point relative to zero degrees absolute
c temperature
c
c *****
c input arguments
c *****
c
c facmot - fraction of molten fuel
c fcomp - puo2 fraction of the fuel
c fhefus - heat of fussion of the fuel (j/kg)
c fotmtl - fuel oxygen to metal ratio
c ftmelt - fuel melting temperature (K)

```

```

c      temp      - local temperature (K)
c
c      *****
c                      output
c      *****
c
c      fenth1 - local fuel enthalpy relative to zero degrees-K (j/kg)
c
c      *****
c
c      fcpmol = specific heat capacity of molten fuel ( j/(kg*K) )
c
c      data  fcpmol / 503.d0 /
c
c      the following data statements contain constants from matpro-11 fcp
c
c      data  clu, c2u, c3u, thu, edu / 296.7d0 , 2.43d-02, 8.745d07,
&          535.285d0, 1.577d05 /
c      data  c1pu,c2pu,c3pu,thpu,edpu / 347.4d0 , 3.95d-04, 3.860d07,
&          571.0d0 , 1.967d05 /
c
c      the following equation is the integral of the fuel specific heat
c      with respect to temperature
c
c      cpdt(c1,th,c2,otm,ed,t,c3) =
&          c1*th * (      1.d0 / (exp(th/t)-1.d0))
&          + c2 * t * t / 2.d0
&          + c3 * otm * exp(-ed / (t * 8.314d0) )/2.d0
c
c      tx = temp
c      if(tx .gt. ftmelt) tx = ftmelt
c
c      fenth1 = cpdt(clu      ,thu      ,c2u      ,fotmt1      ,edu
&          ,tx      ,c3u      ) * ( 1.d0 - fcomp )
c
c      if( fcomp .gt. 0.d0 ) fenth1 = fenth1 + cpdt(c1pu ,thpu ,c2pu
&          ,fotmt1 ,edpu ,tx ,c3pu) * fcomp
c
c      if( temp .le. ftmelt - 2.d0 ) go to 100
c
c
c
c      fenth1 = fenth1 + fhefus * facmot
c
c      if(temp.le.(ftmelt+2.d0))go to 100
c
c
c      fenth1 = fenth1 + (temp - ftmelt) * fcpmol
100 continue
c
c      return
c      end

```

A.1.3 Fuel Thermal Conductivity (FTHCON)

FRAPCON-4.0: FTHCON

```

*deck fthcon
      subroutine fthcon (ftemp,fraden,fotmt1,con,burnup
+ ,gadoln,imox)
c
c      fthcon calculates the fuel thermal conductivity and its

```



```

c derivative with respect to temperature as a function of
c temperature, density, composition and burnup.
c
c UO2 Fuel (IMOX = 0)
c
c The equation used in this subroutine is that proposed by
c staff at NFI, Japan, at the May 1997 ANS Topical Meeting on
c Light Water Reactor Fuel performance in Portland, OR: (Ohira,
c K., and N.Itagaki, 1997. "Thermal Conductivity Measurements
c of High Burnup UO2 Pellet and a Benchmark Calculation of Fuel
c Center Temperature", proceedings pp. 541-549. Applies to UO2.
c
c MOX:
c
c Option number 1 (IMOX = 1)
c
c The 100% dense solid MOX fuel thermal conductivity formulation is based
c on a combination of the Duriez stoichiometry-dependent correlation,
c derived from diffusivity measurements on unirradiated fuel pellets
c (C.Duriez, et al, J.Nuclear Materials 277, 143-158 2000) and the burnup
c degradation contained in a modified version of the NFI fuel thermal
c conductivity model
c
c Option number 2 (IMOX = 2)
c
c The MOX fuel thermal conductivity formulation is based
c on the OECD Halden Reactor Project report "Thermal Performance of
c of High Burnup Fuel In-pile Temperature Data and Analysis"
c W.Wiesnack, T. Tverberg, Proceedings of the 2000 International
c Topical Meeting on LWR Fuel Performance
c
c
c burnup = current local burnup (MWd/MTU)
c con = output fuel thermal conductivity (W/(m*K))
c ftemp = current fuel ring temperature (K)
c fraden = input fuel density (ratio of actual density to
c theoretical density)
c fotmtl = input oxygen to metal ratio of fuel (atoms oxygen/
c atoms metal)
c gadoln = input weight fraction of gadolinia in the fuel
c
c the following inputs are by common block
c comp = input puo2 content of fuel (percent puo2
c in total fuel weight)
c bu = input burnup (mw-s/kg-u)
c emflag(12) = input switch for evaluation model. if this
c variable is equal to 1.0, the matpro model for
c fuel thermal conductivity is replaced by the
c subcode emfton
c
c common /uncert/sigftc, sigftex, sigfgr
c & ,sigswell ,sigcreep ,siggro ,sigcor ,sigh2
c common / phypro / ftmelt,fhefus,ctmelt,chefus,ctranb,
c + ctrane,ctranz,fdelta,bu,comp,deloxy
c
c include 'lacmdl.h'
c data on / 1 /,
c + off / 2 /,
c + locidx / 12 /
c
c find constants
c
c frpu = comp/100.

```

```

t = ftemp
c
c Burnup in GWd/MTU
c
c   bug = burnup/1000.0
c
c   if(imox.eq.0) then
c
c     NFI formula (Ohira & Itagaki, ANS LWR Fuel perf. Topical mtg. 1997)
c     MODIFIED in January 2002 to raise low-burnup thermal conductivity
c     at low temperature and lower thermal conductivity at very high temp.
c
c       h = 1/(1.0+396.0*exp(-6380.0/t))
c       rphonon= 1.0/(0.0452+0.000246*t + 1.0*0.00187*bug+1.1599*gadln
c       & + (1.0-0.9*exp(-0.04*bug))*0.038*bug**0.28*h)
c       elect = (3.50e9/t**2)*exp(-16361/t)
c       base = rphonon + elect
c
c     fm is the Lucuta porosity correction factor(applied to 100% TD fuel)
c
c       fm = fraden/(1.0 + 0.5*(1.0-fraden))
c
c     NFI base equation is for 95% TD fuel, so multiply by 1.079 to
c     raise to 100% TD fuel conductivity, then multiply by fm
c
c       con = base*fm*1.079
c
c     else if(imox.eq.1) then
c
c     Using the Duriez/NFI Mod correlation combination
c
c     base term for MOX
c     where X = deviation from stoichiometry (2-O/M)
c     fm = 1.0789*fraden/(1.0+0.5*(1.0-fraden))
c fm is multiplied by 1.0789 to account for 95% TD
c Porosity correction is Lucuta correction, not Maxwell-Euken
c as proposed by Duriez et al.
c     x = 2.0-fotmt1
c     ax=2.85*x+0.035
c     cx=(2.86-7.15*x)*1.0e-4
c
c     h = 1/(1.0+396.0*exp(-6380.0/t))
c     rphonon = 1.0/(ax + cx*t + 0.00187*bug+1.1599*gadln
c     &+ (1.0-0.9*exp(-0.04*bug))*0.038*bug**0.28*h)
c     elect = (1.50e9/t**2)*exp(-13520/t)
c     base = rphonon + elect
c     con = base*fm
c
c     else if(imox.eq.2) then
c
c     Using the Halden correlation
c
c     tc=t-273.15
c     tco=min(1650.0,tc)
c     buguo2=bug*0.8815
c     fm = 1.0789*fraden/(1.0+0.5*(1.0-fraden))
c     base=0.92/(0.1148+0.004*buguo2+1.1599*gadln+
c     & 2.475e-4*(1.0-0.00333*buguo2)*tco)+
c     & 0.0132*exp(0.00188*tc)
c     con=base*fm
c
c
c If IMOX.ne.0,1,2 then stop the calculations
c

```

```

else
stop 'fthcon - IMOX not within bounds'
end if

c
c find uncertainty
if(sigftc.gt.0.0) con = con*(1.0+sigftc*0.088)
if(sigftc.lt.0.0) con = con/(1.0-sigftc*0.088)

if(imox.eq.0) then
if(t.lt.ftmelt) then
ucon = 0.2*(1.0+abs(2.0-fotmtl)*10.)
else
ucon = con/2.0
endif
else
if(t.le.1800.0) then
ucon = 0.07*con
else
frac=(t-1800.0)/(3100.0-1800.0)*(0.20-0.07)+0.07
ucon=frac*con
endif
endif
if (emflag(locidx).eq.on) call emfton (ftemp,fraden,ftmelt,con)
return
end

```

FRAPTRAN-2.0: FTHCON

```
*deck fthcon
```

```

c
c      subroutine fthcon (ftemp, fraden, fotmtl, con, dkdt, burnup,
c      &                  gadoln, compmt)
c
c      implicit real (a-h, o-z)
c
c      FTHCON calculates the UO2 fuel thermal conductivity
c      as a function of temperature, density, composition and burnup.
c
c      The equation used in this subroutine is that proposed by
c      staff at NFI, Japan, at the May 1997 ANS Topical Meeting on
c      Light Water Reactor Fuel Performance in Portland, Oregon.
c      reference: Ohira and Itakaki, 1997. "Thermal Conductivity
c      Measurements of High Burnup UO2 Pellet and a Benchmark
c      Calculation of Fuel Center Temperature," proceedings pg. 541-549.
c
c      The NFI formula was modified in January 2002 by PNNL to raise
c      low-burnup thermal conductivity at low temperature and lower thermal
c      conductivity at very high temperature.
c      The PNNL reference is: Lanning and Beyer. 2002. "Revised UO2 Thermal
c      Conductivity for FRAPCON-3 NRC Fuel Performance Codes," in Proceedings of
c      ANS Annual Meeting, June 9-13, 2002, Hollywood, Florida.
c
c      This is the same formulation used in FRAPCON-3.2 (February 2003),
c      minus the formulations for MOX fuel.
c
c      burnup = current local burnup (MWd/MTU)
c      con    = output fue thermal conductivity (W/(m*K))
c      ftemp  = current fuel ring temperature (K)
c      fraden = input fuel density (ratio of actual to theoretical)
c      fotmtl = input oxygen to metal ratio of fuel
c              (atoms oxygen/atoms metal)
c      gadoln = input weight fraction of gadolinia in the fuel
c      compmt = input weight % of Pu in Pu and U

```

```

c
c convert burnup to Gwd/MTU
  bug = burnup/1.d3
  if(bug .lt. 1.d-10) bug = 0.001
c use modified NFI model for UO2 and Duriez/NFI Mod model for MOX
  if(compmt.gt.0.0) go to 100
c UO2 Model
c
c NFI formula (Ohira & Itagaki, ANS LWR Fuel perf. Topical mtg. 1997)
c MODIFIED in January 2002 to raise low-burnup thermal conductivity
c at low temperature and lower thermal conductivity at very high temp.
c
c calculate terms
c temperature dependence of annealing of irradiation effects
  h = 1.0/(1.0 + 396.0*exp(-6380.0/ftemp))
c phonon term
  rphonon = 1.0/(0.04520 + 0.000246*ftemp + 0.00187*bug
    & + (1.0 - 0.9*exp(-0.04*bug))*(0.038*bug**0.28)*h)
c electronic term
  elect = (3.50d9/ftemp**2)*exp(-16361./ftemp)
c base is conductivity before apply porosity correction
  base = rphonon + elect
c apply lucuta porosity correction factor (applied to 100% TD fuel)
  fm = fraden/(1.0 + 0.5*(1.0-fraden))
c NFI base equation is for 95% TD fuel, so multiply by 1.079 to
c raise to 100% TD fuel conductivity, then multiply by fm
  con = base*fm*1.079
  go to 200

c
c MOX Model
c
100 continue
c Using the Duriez/NFI Mod correlation combination
c
c base term for MOX
c where X = deviation from stoichiometry (2-O/M)
  fm = 1.0789*fraden/(1.0+0.5*(1.0-fraden))
c fm is multiplied by 1.0789 to account for 95% TD
c Porosity correction is Lucuta correction, not Maxwell-Euken
c as proposed by Duriez et al.
  x = 2.0-fotmt1
  ax=2.85*x+0.035
  cx=(2.86-7.15*x)*1.0e-4

c
  h = 1/(1.0+396.0*exp(-6380.0/ftemp))
  rphonon = 1.0/(ax + cx*ftemp + 0.00187*bug+1.1599*gadoln
&+ (1.0-0.9*exp(-0.04*bug))*0.038*bug**0.28*h)
  elect = (1.50e9/ftemp**2)*exp(-13520/ftemp)
  base = rphonon + elect
  con = base*fm

c
200 continue
  return
  end

```

A.1.4 Fuel Emissivity (FEMISS)

FRAPCON-4.0: FEMISS

```

*deck femiss
  function femiss (ftemp)

```

```

c
c femiss calculates fuel emissivity as a function of temperature.
c ftemp = input fuel temperature (k)
c femiss = output fuel emissivity (unitless)
c data used to develop the model are
c held and wilder, journ. amer. ceram. soc.
c vol. 52, (1969)
c cabannes, et at, c. r. acad. sci., paris, ser. b
c (1967)
c femiss was coded by r. e. mason in october 1978.
c femiss = 0.78557+1.5263e-05*ftemp
c the following calculations provide the upper and lower bounds.
c the upper and lower bounds are not an output unless the user
c desires to modify the subcode appropriately.
c femisu is the upper bound
c femisu = femiss*(1.+0.06796)
c femisl is the lower bound
c femisl = femiss*(1.-0.06796)
100 continue
return
end

```

FRAPTRAN-2.0: FEMISS

```

*deck femiss
function femiss (ftemp)
implicit real (a-h,o-z)
c
c This is a MATPRO-11, Rev. 2 routine modified by PNNL for use in FRAPT
c
c femiss calculates fuel emissivity as a function of temperature.
c
c ftemp = input fuel temperature (k)
c femiss = output fuel emissivity (unitless)
c
c data used to develop the model are
c held and wilder, journ. amer. ceram. soc.
c vol. 52, (1969)
c cabannes, et at, c. r. acad. sci., paris, ser. b
c (1967)
c
c femiss was coded by r. e. mason in october 1978.
c Modified by PNNL, January 1997, to clean up coding and delete lic
c analysis and sensitivity uncertainty coding
c
c femiss = 0.78557d0 + 1.5263d-05 * ftemp
c
c the following calculations provide the upper and lower bounds.
c the upper and lower bounds are not an output unless the user
c desires to modify the subcode appropriately.
c femisu is the upper bound
c femisu = femiss * (1.d0 + 0.06796d0)
c femisl is the lower bound
c femisl = femiss * (1.d0 - 0.06796d0)
c
c return
c
end

```

A.1.5 Fuel Thermal Expansion (FTHEXP)

FRAPCON-4.0: FTHEXP

```
*deck fthexp
      function fthexp (ftemp,facmot)
c
c   the subprogram fthexp is used to calculate the strain of the
c   fuel caused by thermal expansion.
c   thermal expansion strain is calculated for uo2,puo2, or (u,pu)O2
c   as a function of temperature, puo2 content, and fraction of
c   the fuel which is molten.
c   the correlations were derived with the assumption that the
c   thermal expansion strain is zero at 300k.
c   fthexp = output fuel strain due to thermal expansion (unitless)
c   ufthex = estimated standard error of fthexp (per cent)
c   (not currently returned).
c   ftemp = input fuel temperature (k)
c   facmot = input fuel fraction which is molten (unitless)
c   facmot = 1.0 - fuel is all molten
c   facmot = 0.0 - fuel is all solid
c   the correlations used in this subroutine are based on data from;
c   (1) p.j.baldock et al, journal of nuclear materials, 18 (1966)
c   (2) n.h.brett and l.e.russel, proceedings of the 2nd
c   international conference on plutonium metallurgy, grenoble,
c   france (1960) pp 397-410.
c   (3) m.d.burdock and h.s.parker, journal of the american
c   ceramic society,39 (1956) pp 181-187.
c   (4) j.a.christensen, journal of the american ceramic society,
c   46 (1963) pp 607-608.
c   (5) j.b.conway et al, transactions of the american nuclear
c   society,6 (1963).
c   (6) f.gronvold, journal of inorganic and nuclear chemistry,1
c   (1955) pp 357-370.
c   (7) m.hoch and a.c.momin, high temperatures-high pressures,1
c   (1969) pp 401-407.
c   (8) c.p.kempter and r.o.elliott, the journal of chemical
c   physics,30 (1958) pp 1524-1526.
c   (9) w.a.lambertson and j.h.handwerk, anl-5053 (1956).
c   (10)m.tokar et al, nuclear technology, 17 (1973) pp 147-152.
c   fthexp was originally coded by v.f.baston in march 1974
c   modified by c.s.olsen in feb. 1975
c   last modified by g.a.reymann in july 1978
      common /uncert/sigftc, sigftex, sigfgr
      & ,sigswell ,sigcreep ,siggro ,sigcor ,sigh2
      common / phypro / ftmelt,fhefus,ctmelt,chefus,ctranb,
      +
      +          ctrane,ctranz,fdelta,bu,comp,deloxy
c   the phypro common block is set by call to the subroutine
c   phypro which is part of the materials properties package
c   used at the inel.
c   quantities contained in it used in this subcode are;
c   comp = puo2 content (wt. :)
c   ftmelt = fuel melting temperature (k)
c   fdelta = liquid-solid coexistence temperature range (k)
c   when the function fthexp is used alone, not as part of
c   the inel code, values for comp, ftmelt, and fdelta must
c   be input.
c
c   clu, c2u, c3u, edu parameters updated by W.G. Luscher 10-17-07
c
      data clu ,c2u ,c3u ,edu / 9.8e-06, 2.61e-03, 3.16e-01, 1.32e-19 /
      data clpu,c2pu,c3pu,edpu/ 9.0e-06, 2.7e-03, 7.0e-02, 7.0e-20 /
      ftx(c1,c2,c3,ed,bk,t) = c1*t-c2+c3*exp(-ed/(bk*t))
```

```

t = ftemp
bk = 1.38e-23
c  bk      = boltzmann's constant (j/k)
  fcomp = comp/100.0
  if (t.gt.ftmelt) go to 100
  fthexp = ftx(c1u,c2u,c3u,edu,bk,t)*(1.0-fcomp)+ftx(c1pu,c2pu,c3pu,
+edpu,bk,t)*fcomp
  go to 120
100  fthexm = ftx(c1u,c2u,c3u,edu,bk,ftmelt)*(1.0-fcomp)+ftx(c1pu,c2pu,
+c3pu,edpu,bk,ftmelt)*(fcomp)
  if (t.ge.(ftmelt+fdelta)) go to 110
  fthexp = fthexm+.043*facmot
  go to 120
110  fthexp = fthexm+.043+3.6e-05*(t-(ftmelt+fdelta))
120  continue
c    add on uncertainty
  if(sigftex.gt.0.0) fthexp = fthexp*(1.0+sigftex*0.103)
  if(sigftex.lt.0.0) fthexp = fthexp/(1.0-sigftex*0.103)
  ufthex = 10.0
  return
  end

```

FRAPTRAN-2.0: FTHEXP

```

*deck fthexp
c
  function fthexp (ftemp, facmot)
c
  implicit real (a-h,o-z)
c
c  This is a MATPRO-11, Rev. 2 routine modified by PNNL for use in FRAPT
c
c  the subprogram fthexp is used to calculate the strain of the
c  fuel caused by thermal expansion.
c  thermal expansion strain is calculated for uo2,pu02, or (u,pu)02
c  as a function of temperature, puo2 content, and fraction of
c  the fuel which is molten.
c  the correlations were derived with the assumption that the
c  thermal expansion strain is zero at 300k.
c
c  fthexp = output fuel strain due to thermal expansion (unitless)
c  ftemp  = input fuel temperature (k)
c  facmot = input fuel fraction which is molten (unitless)
c          facmot = 1.0 - fuel is all molten
c          facmot = 0.0 - fuel is all solid
c
c  the correlations used in this subroutine are based on data from;
c  (1) p.j.baldock et al, journal of nuclear materials, 18 (1966)
c  (2) n.h.brett and l.e.russel, proceedings of the 2nd
c  international conference on plutonium metallurgy, grenoble,
c  france (1960) pp 397-410.
c  (3) m.d.burdock and h.s.parker, journal of the american
c  ceramic society,39 (1956) pp 181-187.
c  (4) j.a.christensen, journal of the american ceramic society,
c  46 (1963) pp 607-608.
c  (5) j.b.conway et al, transactions of the american nuclear
c  society,6 (1963).
c  (6) f.gronvold, journal of inorganic and nuclear chemistry,1
c  (1955) pp 357-370.
c  (7) m.hoch and a.c.momin, high temperatures-high pressures,1
c  (1969) pp 401-407.
c  (8) c.p.kempter and r.o.elliott, the journal of chemical
c  physics,30 (1958) pp 1524-1526.
c  (9) w.a.lambertson and j.h.handwerk, anl-5053 (1956).

```

```

c      (10)m.tokar et al, nuclear technology, 17 (1973) pp 147-152.
c
c      fthexp was originally coded by v.f.baston in march 1974
c      modified by c.s.olsen in feb. 1975
c      last modified by g.a.reymann in july 1978
c      Modified by PNNL, January 1997, to clean up coding and delete lic
c      analysis and sensitivity uncertainty coding
c
c      include 'phypro.h'
c
c      the phypro common block is set by call to the subroutine
c      phypro which is part of the materials properties package
c      used at the inel.
c      quantities contained in it used in this subcode are;
c      compmt = puo2 content (wt. :)
c      ftmelt = fuel melting temperature (k)
c      fdelta = liquid-solid coexistence temperature range (k)
c      when the function fthexp is used alone, not as part of
c      the inel code, values for compmt, ftmelt, and fdelta must
c      be input.
c
c      clu, c2u, c3u, and edu parameters updated by W.G. Luscher 10-17-07
c
c      data clu ,c2u ,c3u ,edu / 9.8d-06, 2.61d-03, 3.16d-01, 1.32d-19 /
c      data clpu,c2pu,c3pu,edpu/ 9.0d-06, 2.7d-03, 7.0d-02, 7.0d-20 /
c      bk is Boltzmann's constant (J/k)
c      data bk / 1.38d-23 /
c
c      ftx (c1,c2,c3,ed,bk,t) = c1 * t - c2 + c3 * exp(-ed/(bk * t))
c
c      t      = ftemp
c      fcomp  = compmt/100.0d0
c
c      if(t .gt. ftmelt) go to 25
c
c      fthexp = ftx(clu ,c2u ,c3u ,edu ,bk,t) * (1.0d0 - fcomp)
c      &      + ftx(clpu,c2pu,c3pu,edpu,bk,t) * fcomp
c      go to 100
c
c 25 continue
c      fthexm = ftx(clu ,c2u ,c3u ,edu ,bk,ftmelt) * (1.0d0 - fcomp)
c      &      + ftx(clpu,c2pu,c3pu,edpu,bk,ftmelt) * fcomp
c
c      if(t .ge. (ftmelt+fdelta)) go to 75
c
c      fthexp = fthexm + 0.043d0 * facmot
c      go to 100
c
c 75 continue
c      fthexp = fthexm + 0.043d0 + 3.6d-05 * (t- (ftmelt + fdelta))
c
c 100 continue
c
c      return
c      end

```


A.1.6 Fuel Densification (FUDENS)

FRAPCON-4.0: FUDENS

```
*deck fudens
      function fudens (ftemp,bu,fdens,rsntr,tsint,comp,prvden)
c
c   fudens calculates irradiation-induced densification.
c   fudens = output fuel dimensional change (%)
c   ftemp = input fuel temperature (k)
c   bu     = input burnup (mw-s/kg-u)
c   fdens  = input fuel density (kg/m**3)
c   rsntr  = input maximum density change determined by a resintering
c   test of 1973 k for 24 hours (kg/m**3)
c   tsint  = input fuel sintering temperature (k)
c   comp   = input plutonia content (weight percent)
c   prvden = input total densification from previous time step (%)
c   fudens was developed and programmed by c. s. olsen (january 1975).
c   updated and corrected by b. w. burnham (october 1975).
c   fudens was modified by r. e. mason (november 1978).
      dimension c(2),b(5)
      data c / 10.96, 11.46/
      data b / 3.0, 1.00, 3.0, 2.00, 35.00 /
      dlen2(alen,bu,abu) = -b(1)+alen+b(2)*exp(-b(3)*(bu+abu))+b(4)*exp(
+-b(5)*(bu+abu))
      dlen3(bu) = -b(2)*b(3)*exp(-b(3)*bu)-b(4)*b(5)*exp(-b(5)*bu)
      fbu = bu*1.157e-05
      ts = tsint-2.7315e02
c   if rsntr or tsint is not defined by user, the default value is
c   tsint = 1873 k.
      if (tsint.le.0.0) ts = 1600.0
      roth = c(1)*c(2)/(0.01*comp*c(1)+(1.0-0.01*comp)*c(2))
      de = fdens/(roth*10.0)
      if (rsntr.gt. 0.0) dlen1 = 100.0 * rsntr/(3.0 * fdens)
      if ((ftemp.ge.1000.).and.(rsntr.le.0.)) dlen1 = 66.6*(100.0-de)/(t
+s-1180.0)
      if ((ftemp.lt.1000.).and.(rsntr.le.0.)) dlen1 = 22.2*(100.0-de)/(t
+s-1180.0)
      x3 = 0.0
      x4 = 1.0
      a11 = dlen1
      a13 = 3.0-a11
      a14 = 0.0
      if (a13.le.4.27e-03) go to 130
      do 100 i=1,6
      y2 = dlen2(a13,x4,a14)
      y1 = dlen2(a13,x3,a14)
      if (y1*y2.le.0.) go to 110
      x3 = x4
      x4 = x4+1.0
      if (i.eq.6) go to 160
100   continue
110   continue
      x1 = x3
      do 120 j=1,50
      x = x1-dlen2(a13,x1,a14)/dlen3(x1)
      err = abs((x-x1)*100.0/x)
      if (err.le.2.0e-04) go to 140
      x1 = x
120   continue
130   a13 = 2.996
      a12 = 5.384
      go to 150
```

```

140  al2 = x
150  continue
      fuden = dlen2(al3,fbu,al2)
      if (bu.lt.1728) fuden = 0.0
      go to 170
160  print 180
      fuden = 0.0
170  continue
      if (abs(fuden).le.abs(prvden)) fudens = 0.0
      if (abs(fuden).gt.abs(prvden)) fudens = fuden-prvden
      return
180  format (1x,/' no roots found between 0 and 6000 mws/mt uo2')
      end

```

A.1.7 Fuel Swelling (FSWELL)

FRAPCON-4.0: FSWELL

```

*deck fswell
      subroutine fswell (fdens,comp,bu,bul,ftemp,soldsw,gadoln)
c
c  comp  = input plutonia content (weight percent)
c  fdens = input initial density of the fuel (kg/m**3)
c  ftemp = input temperature of the fuel ring (k)
c  bu    = input burnup to end of time step (mw-s/kg-u)
c  bul   = input burnup to end of last time step (mw-s/kg-u)
c  soldsw = output fuel swelling due to solid fission products
c         (fraction)
c  fswell was developed and programmed by r. e. mason - june 1978.
c  fswell was revised July 1995 by G. A. Berna per D. D. Lanning
c  recommendations in ltr to L. Siefken, May 4, 1995
c  fswell was revised October 2008 by K.J. Geelhood
c  - program -
      common /uncert/sigftc, sigftex, sigfgr
      & ,sigswell ,sigcreep ,siggro ,sigcor ,sigh2
      bus = fdens*2.974e+10*(bu-bul)
      soldsw = bus*(2.315e-23+sigswell*2.987e-24)
      if(bu.ge.6912000.0) soldsw = bus*(3.211e-23+sigswell*5.974e-24)
      if(gadoln.gt.0.0) soldsw=bus*(1.867e-23+sigswell*2.315e-24)
      return
      end

```

A.2 Cladding Material Properties

A.2.1 Cladding Specific Heat (CCP)

FRAPCON-4.0: CCP

```

*deck ccp
      function ccp (ctemp)
c
c  ccp calculates the specific heat at constant pressure
c  for zircaloys
c  ccp  = output cladding specific heat at constant
c  pressure (j/kg-k)
c  ctemp = input cladding temperature (k)
c  this code is based on data from
c  (1) c. r. brooks and e. e. stansbury, "the specific heat of
c  of zircaloy-2 from 50 to 700 c", journal of nuclear
c  materials 18 (1966) p 233

```

```

c (2) e. a. eldridge and h. w. deem, specific heats and heats
c of transformation of zircaloy-2 and low nickel zircaloy-2
c bmi-1803 (may 31, 1967)
c conversion from j/(kg*k) to cal/(gm*c) is
c 2.39006d-4 (cal/(gm*c))/(j/(kg*k))
c estimated standard error of the prediction of
c ccp for the specific heat of zircaloy cladding
c samples -- (sum of squared residuals/(number of
c residuals-degrees of freedom)**0.5 -- is
c (1) for temperature less than 1090 k, 10j/kg-k)
c (2) for temperature 1090 k to 1300 k, 25j/kg-k)
c (3) for temperature above 1300 k , 100j/kg-k)
c ccp coded by r. l. miller october 1974
c modified by d. l. hagrman may 1976
  include 'lacmdl.h'
  dimension cpdata(26)
  data cpdata/ 281., 300., 302., 400., 331.,640.,
+ 375.,1090., 502.,1093., 590.,1113., 615.,1133.,
+ 719.,1153., 816.,1173., 770.,1193., 619.,1213.,
+ 469.,1233., 356.,1248. /
  data npcpc, iu / 13,1/
  data on / 1 /,
+ off / 2 /,
+ locidx / 4 /
  if (emflag(locidx).eq.on) go to 110
  if (ctemp.ge.1248.0) go to 100
  ccp = polate(cpdata,ctemp,npcpc,iu)
  go to 120
100  ccp = 356.
  go to 120
110  ccp = emccp(ctemp)
120  continue
  return
  end

```

FRAPTRAN-2.0: CCP

```

*deck ccp
  function ccp (ctemp, icm)
  implicit real (a-h,o-z)
c
c This is a MATPRO-11, Rev. 2 routine modified by PNNL for use in FRAP
c
c ccp calculates the specific heat at constant pressure
c for zircaloys
c
c ccp = output cladding specific heat at constant
c pressure (j/kg-k)
c ctemp = input cladding temperature (k)
c
c this code is based on data from
c (1) c. r. brooks and e. e. stansbury, "the specific heat of
c of zircaloy-2 from 50 to 700 c", journal of nuclear
c materials 18 (1966) p 233
c (2) e. a. eldridge and h. w. deem, specific heats and heats
c of transformation of zircaloy-2 and low nickel zircaloy-2
c bmi-1803 (may 31, 1967)
c
c conversion from j/(kg*k) to cal/(gm*c) is
c 2.39006d-4 (cal/(gm*c))/(j/(kg*k))
c
c estimated standard error of the prediction of
c ccp for the specific heat of zircaloy cladding
c samples -- (sum of squared residuals/(number of

```

```

c      residuals=degrees of freedom)**0.5 -- is
c      (1) for temperature less than 1090 k, 10j/kg-k)
c      (2) for temperature 1090 k to 1300 k, 25j/kg-k)
c      (3) for temperature above 1300 k , 100j/kg-k)
c
c      ccp coded by r. l. miller october 1974
c      modified by d. l. hagrman may 1976
c      Modified by PNNL, January 1997, to clean up coding, including
c      removed licensing assistance coding and sensitivity uncertainty
c      coding
c
c      Zry properties
c      dimension cpdata(28)
c      data cpdata/279.d0,290.d0,
c      & 281.d0, 300.d0, 302.d0, 400.d0, 331.d0, 640.d0,
c      & 375.d0,1090.d0, 502.d0,1093.d0, 590.d0,1113.d0, 615.d0,1133.d0,
c      & 719.d0,1153.d0, 816.d0,1173.d0, 770.d0,1193.d0, 619.d0,1213.d0,
c      & 469.d0,1233.d0, 356.d0,1248.d0 /
c      data npcpc, iu / 14 , 1 /
c
c      Zr-1%Nb properties
c      low heat rate (<1000K/s)
c      dimension cpwrr(24)
c      data cpwrr/345.0d0,280.d0,
c      & 360.d0, 473.d0, 370.d0, 573.d0, 380.d0, 673.d0,
c      & 383.d0, 773.d0, 385.d0, 873.d0, 448.d0, 883.d0, 680.d0, 973.d0,
c      & 816.d0,1025.d0, 770.d0,1073.d0, 400.d0,1153.d0, 392.d0,1173.d0/
c      data npwr / 12 /
c      high heat rate (>1000K/s)
c      dimension cpwrr2(26)
c      data cpwrr2/412.6d0,1100.d0,
c      & 420.d0,1110.d0, 480.d0,1120.d0, 600.d0,1134.d0,
c      & 1000.d0,1142.d0, 1400.d0,1150.d0,1600.d0,1155.d0,1400.d0,1161.d0,
c      & 1000.d0,1168.d0, 600.d0,1177.d0, 400.d0,1180.d0, 360.d0,1190.d0,
c      & 348.d0,1200.d0/
c      data npw2 / 13 /
c
c      go to (400,400,400,400,400,600,400,600,400,400,400)icm
c
c      400 continue
c      generic Zry
c      ccp = 279.d0
c      if (ctemp.ge.290.d0 .and. ctemp.le.1248.d0)
c      & ccp = polate (cpdata, ctemp, npcpc, iu)
c      if (ctemp .ge. 1248.d0) ccp = 356.d0
c      return
c
c      600 continue
c      RRC-KI Zr-1%Nb property
c
c      This block calculates the specific heat at constant pressure for
c      H1-alloy cladding. If iwrr = 1 then data is derived from
c      Volkov B.Yu. et. al."Material property library for H1-alloy
c      cladding", Preprint IAE-4941/11, 1989. This property are induced
c      by low heating rate. If iwrr = 2 then data is derived from
c      Ljusternik V.E. et. al."Experimental research of zirconium reactor
c      materials thermal properties:110-alloy". M.,J. High Temperature
c      Thermal Physics." v.31 n.4, 1993. This property are induced by
c      high-rate heating>=1000 K/s.
c
c      5/5/03: default to iwrr=1 until can set this flag up
c      iwrr = 1
c      low heat rate

```

```

        if(iwwer.eq.2) go to 601
        if(ctemp .lt. 1173.d0) ccp = polate(cpwwer,ctemp,npww,iu)
        if(ctemp.ge.1173.d0) ccp = 392.d0
        return
c
c 601 continue
c high heat rate
        ccp = 237.5d0+15.91d-2*ctemp
        if(ctemp.ge.1100.d0 .and. ctemp.le.1200.d0)
&      ccp = polate(cpwwr2,ctemp,npw2,iu)
        if(ctemp.gt.1200.d0) ccp = 199.7d0+12.364d-2*ctemp
        return
c
        end

```

A.2.2 Cladding Thermal Conductivity (CTHCON)

FRAPCON-4.0: (CTHCON)

```

*deck cthcon
        subroutine cthcon (ctemp,time,flux,coldw,ccon)
c
c cthcon calculates cladding thermal conductivity as a function
c of temperature, time, flux, and cold work
c ccon = output thermal conductivity of zircaloy-4 (w/m-k)
c ctemp = input cladding meshpoint temperature (k)
c time = input time at temperature and flux (s)
c flux = input fast neutron flux ((neutrons/m**2)/s)
c coldw = input cold work (unitless ratio of areas)
c the equation used in this subcode is based on data from
c w.k. anderson, c.j. beck, a.r. kephart and j.s. theilacker
c astm-stp-314, 1962, pp 62 - 93
c j.n. chirigos, c. kass, w.s. kirk and g.j. salvaggio
c fuel element fabrication, academic press, 1961, pp 19 - 55
c a.d. feith, gemp-669 (oct 1966)
c c.f. lucks and h.w. deem, bmi-1273 (1958) pp 7-9
c a.e. powers, kapl-2146 (1961)
c d.b. scott, wcap-3269-41 (1965) pp 5-9
c this version of cthcon does not use time, flux or coldwork
c as parameters in calculation of zircaloy thermal conductivity
c one standard deviation of this function = 1.01 w/m-k
c this version of cthcon was developed by r.l. miller, dec 1975
c last modified by e.r. carlson in june 1978.
        include 'lacmdl.h'
        data      on      / 1 /,
+               off     / 2 /,
+               locidx  / 7 /
        if (emflag(locidx).eq.on) go to 100
        ccon = 7.511+ctemp*(2.088e-2+ctemp*(-1.450e-5+ctemp*7.668e-09))
        go to 110
100      call emcton (ctemp,time,flux,coldw,ccon)
110      continue
        return
        end

```

FRAPTRAN-2.0: (CTHCON)

```

*deck cthcon
        subroutine cthcon (ctemp, time, flux, coldw, ccon, cdkdt, icm)
        implicit real (a-h,o-z)
c
c This is a MATPRO-11, Rev. 2 routine modified by PNNL for use in FRAPT
c

```

```

c   cthcon calculates cladding thermal conductivity as a function
c   of temperature, time, flux, and cold work
c
c   ccon  = output thermal conductivity of zircaloy-4 (w/m-k)
c   cdkdt = output derivative of thermal conductivity with
c           respect to temperature
c
c   ctemp = input cladding meshpoint temperature (k)
c   time  = input time at temperature and flux (s)
c   flux  = input fast neutron flux ((neutrons/m**2)/s)
c   coldw = input cold work (unitless ratio of areas)
c
c   go to appropriate model for cladding type
c   go to (400,400,400,400,400,600,400,600,400,400) icm
c
c   400 continue
c   Generic Zircaloy property from MATPRO
c
c   the equation used in this subcode is based on data from
c   w.k. anderson, c.j. beck, a.r. kephart and j.s. theilacker
c   astm-stp-314, 1962, pp 62 - 93
c   j.n. chirigos, c. kass, w.s. kirk and g.j. salvaggio
c   fuel element fabrication, academic press, 1961, pp 19 - 55
c   a.d. feith, gemp-669 (oct 1966)
c   c.f. lucks and h.w. deem, bmi-1273 (1958) pp 7-9
c   a.e. powers, kapl-2146 (1961)
c   d.b. scott, wcap-3269-41 (1965) pp 5-9
c
c   this version of cthcon does not use time, flux or coldwork
c   as parameters in calculation of zircaloy thermal conductivity
c
c   one standard deviation of this function = 1.01 w/m-k
c
c   this version of cthcon was developed by r.l. miller, dec 1975
c   last modified by e.r. carlson in june 1978.
c   Modified by PNNL, January 1997, to clean up coding and delete
c   licencing analysis and sensitivity uncertainty coding
c
c   ccon = 7.511d0 + ctemp*(2.088d-2 + ctemp * (-1.450d-5 +
&       ctemp*7.668d-09))
c   cdkdt = 2.088d-2 + ctemp*(-2.9d-5 + ctemp*2.3d-8)
c   return
c
c   600 continue
c   E-110 property as coded by RRC-KI and provided to PNNL
c
c   This code block calculates thermal conductivity (w/(m*k)) and
c   derivative of thermal conductivity with respect to temperature
c   (w/(m*k*k)) of H1-alloy. Data is derived from:
c   Volkov B.Yu. et. al."Material property library for H1-alloy
c   cladding", Preprint IAE-4941/11, 1989.
c
c   if(ctemp.le.2133.0d0) then
c       ccon = dexp(0.000461843d0*ctemp)*15.0636d0
c       cdkdt = 0.006957018215d0*dexp(0.000461843d0*ctemp)
c   else
c       ccon = 36.d0
c       cdkdt = 0.d0
c   endif
c   return
c
c   end

```

A.2.3 Cladding Oxide Thermal Conductivity (ZOTCON)

FRAPCON-4.0: ZOTCON

```
*deck zotcon
      function zotcon (ctemp)
c
c   zotcon calculates zirconium dioxide thermal conductivity as a
c   function of temperature.
c   zotcon = output thermal conductivity of zro2 (w/m-k)
c   ctemp = input cladding meshpoint temperature (k)
c   the data used to generate this correlation were taken from:
c   w.d. kingery, j. francl, r.l. coble and t. vasilos
c   j. amer. ceram. soc., 37 no.i (1954) pp 107-110
c   zotcon was coded by r.l.miller in march 1974.
c   modified by r.l. miller may 1974
c   use caution above 1700k
      t = ctemp
      zotcon = 1.9599-t*(2.41e-4-t*(6.43e-7-t*1.946e-10))
      return
      end
```

FRAPTRAN-2.0: ZOTCON

```
*deck zotcon
      function zotcon (ctemp)
      implicit real (a-h,o-z)
c
c   zotcon calculates zirconium dioxide thermal conductivity as a
c   function of temperature.
c
c   zotcon = output thermal conductivity of zro2 (W/m-K)
c   ctemp = input cladding meshpoint temperature (K)
c
c   the data used to generate this correlation were taken from:
c   w.d. kingery, j. francl, r.l. coble and t. vasilos
c   j. amer. ceram. soc., 37 no.i (1954) pp 107-110
c
c   zotcon was coded by r.l.miller in march 1974.
c   modified by r.l. miller may 1974
c
c   use caution above 1700K
c
c   t      = ctemp
c   zotcon = 1.9599d0 - t*(2.41d-4 - t*(6.43d-7 - t*1.946d-10))
c
      return
      end
```

A.2.4 Cladding Oxide Emissivity (ZOEMIS)

FRAPCON-4.0: ZOEMIS

```
*deck zoemis
      subroutine zoemis (ctmax,zroxid,emissv)
c
c   zoemis calculates the emissivity of the cladding surface
c   as a function of maximum cladding temperature and
c   oxide thickness. expected standard error of the
c   calculated emissivity compared to in-reactor
c   data is also returned.
c   emissv = output cladding surface emissivity (unitless)
c   pueor = output positive standard error expected in emissv
```

```

c   when compared to in-reactor data (not currently returned)
c   uemis = output negative standard error expected in emissv
c   when compared to in-reactor data (not currently returned)
c   ctmax = input maximum cladding temperature (k)
c   zroxid = input oxide layer thickness (m)
c   the equations used in this subroutine are based on data from
c   (1) aec fuels and materials development program progress
c   report no. 76, usaec report gemp - 1008 (1968). section by
c   e. f. juenke and s. j. sjodahl, p 239
c   (2) t. b. burgoyne and a. garlick, paper presented at
c   specialists meeting on the behaviour of water reactor
c   fuel elements under accident conditions, spatind norway
c   (september 1976)
c   (3) e. v. murphy and f. havelock, emissivity of zirconium
c   alloys in air in the temperature range 100 - 400 c
c   j. nuc. mat., 60 (1976) pp 167-176
c   zoemis coded by r. l. miller sept 1974
c   modified by d. l. hagrman october 1976
c   model for temperatures below 1500k follows
      if (zroxid.ge.3.88e-06) go to 100
      emissv = 3.25e-01+1.246e05*zroxid
      go to 110
100  emissv = 8.08642e-01-5.00e01*zroxid
110  puemis = 0.1
      uemis = 0.1
      if (ctmax.le.1500.) go to 120
c   modification for maximum temperatures above 1500 k follows
      emissv = emissv*exp((1.50e03-ctmax)/3.00e02)
      if (emissv.lt.0.325) emissv = 0.325
      puemis = puemis/exp((1.50e03-ctmax)/3.00e02)
      uemis = puemis
c   standard error cut off at impossible values follows
      if (puemis.gt.(1.00-emissv)) puemis = 1.00-emissv
      if (uemis.gt.emissv) uemis = emissv
120  continue
      return
      end

```

FRAPTRAN-2.0: ZOEMIS

```

*deck zoemis
  subroutine zoemis (ctmax, zroxid, emissv)
    implicit real (a-h,o-z)
c
c   This is a MATPRO-11, Rev. 2 routine modified by PNNL for use in FRAPT
c
c   zoemis calculates the emissivity of the cladding surface
c   as a function of maximum cladding temperature and
c   oxide thickness. expected standard error of the
c   calculated emissivity compared to in-reactor
c   data is also returned.
c
c   emissv = output cladding surface emissivity (unitless)
c   puemis = output positive standard error expected in emissv
c           when compared to in-reactor data (not currently returned)
c   uemis = output negative standard error expected in emissv
c           when compared to in-reactor data (not currently returned)
c
c   ctmax = input maximum cladding temperature (k)
c   zroxid = input oxide layer thickness (m)
c
c   the equations used in this subroutine are based on data from
c   (1) aec fuels and materials development program progress
c   report no. 76, usaec report gemp - 1008 (1968). section by

```



```

c      e. f. juenke and s. j. sjodahl, p 239
c      (2) t. b. burgoyne and a. garlick, paper presented at
c      specialists meeting on the behaviour of water reactor
c      fuel elements under accident conditions, spatind norway
c      (september 1976)
c      (3) e. v. murphy and f. havelock, emissivity of zirconium
c      alloys in air in the temperature range 100 - 400 c
c      j. nuc. mat., 60 (1976) pp 167-176
c
c      zoemis coded by r. l. miller sept 1974
c      modified by d. l. hagrman october 1976
c      Modified by PNNL, January 1997, to clean up coding, delete sensiti
c      uncertainty coding, and correct error in PUEMIS for T > 1500K
c
c      model for temperatures below 1500K:
c      emissv = 3.25d-01 + 1.246d05*zroxid
c      if (zroxid .ge. 3.88d-06) emissv = 8.08642d-01 - 5.0d+01*zroxid
c      puemis = 0.1d0
c      uuemis = 0.1d0
c      if(ctmax .le. 1500.d0) go to 50
c
c      modification for maximum temperatures above 1500K:
c      emissv = emissv * exp((1.50d03 - ctmax)/3.00d02)
c      if(emissv .lt. 0.325d0) emissv = 0.325d0
c      puemis = puemis*exp((1.50d03 - ctmax)/3.00d02)
c      uuemis = puemis
c
c      standard error cut off at impossible values follows
c      if(puemis .gt. (1.00d0-emissv)) puemis = 1.00d0 - emissv
c      if(uuemis .gt. emissv)          uuemis = emissv
c
c      50 continue
c
c      return
c
c      end

```

A.2.5 Cladding Thermal Expansion (CTHEXP)

FRAPCON-4.0: CTHEXP

```

*deck cthexp
      subroutine cthexp (ctemp,cathex,cdthex)
c
c      cthexp calculates axial and diametral thermal expansion of
c      zircaloy lwr cladding.
c      cathex = output axial thermal expansion of zircaloy (m/m)
c      cdthex = output diametral thermal expansion of zircaloy (m/m)
c      ctemp = input cladding meshpoint temperature (k)
c      data for the correlation from room temperature to 1273k are
c      taken from r.l. mehan and f.w. wiesinger, "mechanical properties
c      of zircaloy-2", usaec report kapl-2110 (1961), d.b. scott,
c      "physical and mechanical properties of zircaloy-2 and -4",
c      wcap-3269-41 (1965), and j.j. kearns, "thermal expansion
c      and preferred orientation in zircaloy", wapd-tm-472 (1965)
c      above 1273k the coefficient of thermal expansion used is the
c      constant value 9.7e-06/k recommended by b. lustman and f. kerze,
c      "the metallurgy of zirconium", mc graw-hill book company, new
c      york (1955) page 355.
c      between 1073 and 1273k (approximately the alpha-beta transition
c      range for zircaloy) cthexp uses the linear interpolation routine
c      polate to find the thermal expansion.

```

```

c   cthexp was originally coded by r.l. miller in nov. 1974.
c   last updated by g.a. reymann in june 1978.
      dimension cathxd (44)
      dimension dthexp (44)
      data cathxd/
+    3.52774e-03,      1073.15 ,      3.53000e-03,      1083.15 ,
+    3.50000e-03,      1093.15 ,      3.46000e-03,      1103.15 ,
+    3.41000e-03,      1113.15 ,      3.33000e-03,      1123.15 ,
+    3.21000e-03,      1133.15 ,      3.07000e-03,      1143.15 ,
+    2.80000e-03,      1153.15 ,      2.50000e-03,      1163.15 ,
+    2.00000e-03,      1173.15 ,      1.50000e-03,      1183.15 ,
+    1.30000e-03,      1193.15 ,      1.16000e-03,      1203.15 ,
+    1.13000e-03,      1213.15 ,      1.10000e-03,      1223.15 ,
+    1.11000e-03,      1233.15 ,      1.13000e-03,      1243.15 ,
+    1.20000e-03,      1253.15 ,      1.30000e-03,      1263.15 ,
+    1.40000e-03,      1273.15 /
      data npcatx, iu / 22,1 /
      data dthexp/
+    5.1395e-03, 1073.15,  5.2200e-03, 1083.15,  5.2500e-03, 1093.15,
+    5.2800e-03, 1103.15,  5.2800e-03, 1113.15,  5.2400e-03, 1123.15,
+    5.2200e-03, 1133.15,  5.1500e-03, 1143.15,  5.0800e-03, 1153.15,
+    4.9000e-03, 1163.15,  4.7000e-03, 1173.15,  4.4500e-03, 1183.15,
+    4.1000e-03, 1193.15,  3.5000e-03, 1203.15,  3.1300e-03, 1213.15,
+    2.9700e-03, 1223.15,  2.9200e-03, 1233.15,  2.8700e-03, 1243.15,
+    2.8600e-03, 1253.15,  2.8800e-03, 1263.15,  2.9000e-03, 1273.15/
      data npdexp / 22 /
      if (ctemp.le.1073.15) go to 100
      if (ctemp.ge.1273.15) go to 110
      cathex = polate(cathxd,ctemp,npcatx,iu)
      cdthex = polate(dthexp,ctemp,npdexp,iu)
      go to 120
100  cathex = -2.5060e-05+(ctemp-273.15)*4.4410e-06
      cdthex = -2.3730e-04+(ctemp-273.15)*6.7210e-06
      go to 120
110  cathex = -8.300e-03+(ctemp-273.15)*9.70e-06
      cdthex = -6.800e-03+(ctemp-273.15)*9.70e-06
120  continue
      return
      end

```

FRAPTRAN-2.0: CTHEXP

```

*deck cthexp
      subroutine cthexp (ctemp, cathex, cdthex, icm)
      implicit real (a-h,o-z)

c
c   cthexp calculates axial and diametral thermal expansion of
c   zircaloy lwr cladding.
c
c   cathex = output axial thermal expansion of zircaloy (m/m)
c   cdthex = output diametral thermal expansion of zircaloy (m/m)
c
c   ctemp  = input cladding meshpoint temperature (k)
c
c   data for the correlation from room temperature to 1273k are
c   taken from r.l. mehan and f.w. wiesinger, "mechanical properties
c   of zircaloy-2", usaec report kapl-2110 (1961), d.b. scott,
c   "physical and mechanical properties of zircaloy-2 and -4",
c   wcap-3269-41 (1965), and j.j. kearns, "thermal expansion
c   and preferred orientation in zircaloy", wapd-tm-472 (1965)
c
c   above 1273k the coefficient of thermal expansion used is the

```

```

c      constant value 9.7e-06/k recommended by b. lustman and f. kerze,
c      "the metallurgy of zirconium", mc graw-hill book company, new
c      york (1955) page 355.
c
c      between 1073 and 1273k (approximately the alpha-beta transition
c      range for zircaloy) cthexp uses the linear interpolation routine
c      polate to find the thermal expansion.
c
c      cthexp was originally coded by r.l. miller in nov. 1974.
c      last updated by g.a. reymann in june 1978.
c      Licensing analysis coding deleted 9/23/97 by ME Cunningham, PNNL
c
c generic Zry
c   dimension cathxd (44)
c   dimension dthexp (44)
c   data cathxd/ 0.0d0,293.15d0, 3.52774d-03,1073.15d0,
c   & 3.5300d-03,1083.15d0, 3.5000d-03,1093.15d0, 3.460d-03,1103.15d0,
c   & 3.4100d-03,1113.15d0, 3.3300d-03,1123.15d0, 3.210d-03,1133.15d0,
c   & 3.0700d-03,1143.15d0, 2.8000d-03,1153.15d0, 2.500d-03,1163.15d0,
c   & 2.0000d-03,1173.15d0, 1.5000d-03,1183.15d0, 1.300d-03,1193.15d0,
c   & 1.1600d-03,1203.15d0, 1.1300d-03,1213.15d0, 1.100d-03,1223.15d0,
c   & 1.1100d-03,1233.15d0, 1.1300d-03,1243.15d0, 1.200d-03,1253.15d0,
c   & 1.3000d-03,1263.15d0, 1.4000d-03,1273.15d0/
c   data npcats /22/
c   data dthexp/ 4.3480d-04,373.15d0,
c   & 5.1395d-03,1073.15d0, 5.2200d-03,1083.15d0, 5.2500d-03,1093.15d0,
c   & 5.2800d-03,1103.15d0, 5.2800d-03,1113.15d0, 5.2400d-03,1123.15d0,
c   & 5.2200d-03,1133.15d0, 5.1500d-03,1143.15d0, 5.0800d-03,1153.15d0,
c   & 4.9000d-03,1163.15d0, 4.7000d-03,1173.15d0, 4.4500d-03,1183.15d0,
c   & 4.1000d-03,1193.15d0, 3.5000d-03,1203.15d0, 3.1300d-03,1213.15d0,
c   & 2.9700d-03,1223.15d0, 2.9200d-03,1233.15d0, 2.8700d-03,1243.15d0,
c   & 2.8600d-03,1253.15d0, 2.8800d-03,1263.15d0, 2.9000d-03,1273.15d0/
c   data npdexp, iu /22, 1/
c
c      go to (400,400,400,400,400,600,400,600,400,400,400) icm
c
c 400 continue
c generic Zircaloy thermal expansion
c   if(ctemp .le. 1073.15d0) go to 401
c   if(ctemp .ge. 1273.15d0) go to 402
c
c   cathex = polate(cathxd,ctemp,npcats,iu)
c   cdthex = polate(dthexp,ctemp, npdexp,iu)
c   return
c
c 401 continue
c   cathex = -2.5060d-05 + (ctemp-273.15d0)*4.4410d-06
c   cdthex = -2.3730d-04 + (ctemp-273.15d0)*6.7210d-06
c   return
c
c 402 continue
c   cathex = -8.300d-03 + (ctemp-273.15d0)*9.70d-06
c   cdthex = -6.800d-03 + (ctemp-273.15d0)*9.70d-06
c   return
c
c 600 continue
c RRC-KI thermal expansion
c
c   if(ctemp .ge. 2133.d0) then
c     cathex=1.0582459d-2
c     cdthex=1.3133600d-2
c
c   else if(ctemp .gt.1153.d0) then

```

```

        cathex=1.076459d-3+9.7d-6*(ctemp-1153.d0)
        cdthex=3.627600d-3+9.7d-6*(ctemp-1153.d0)
c
    else if(ctemp .gt. 883.d0)then
        cathex=3.0465577d-3+2.312d-8*(ctemp-883.d0)
&        -7.358d-8*(ctemp-883.d0)**2+1.7211d-10*(ctemp-883.d0)**3
        cdthex=5.5977000d-3+2.312d-8*(ctemp-883.d0)
&        -7.358d-8*(ctemp-883.d0)**2+1.7211d-10*(ctemp-883.d0)**3
c
    else if(ctemp .gt. 573.d0) then
        cathex=0.13725577d-2+5.4d-6*(ctemp-573.d0)
        cdthex=0.3336985d-8*ctemp**2+5.65390d-6*ctemp-0.199649865d-2
c
    else
        cathex=0.1338985d-8*ctemp**2+3.85875d-6*ctemp-0.127813365d-2
        cdthex=0.3336985d-8*ctemp**2+5.65390d-6*ctemp-0.199649865d-2
    endif
c
    return
end

```

A.2.6 Cladding Elastic Modulus (CELMOD) and Shear Modulus (CSHEAR)

FRAPCON-4.0: CELMOD

```

*deck celmod
    function celmod (ctemp,fnck,cwkf,deloxy)
c
c    celmod calculates cladding young's modulus as a function
c    of temperature, fast neutron fluence, cold work, and average
c    oxygen concentration. grain orientation is assumed random.
c    the expected standard error is computed but not returned
c    (ucelmd).
c    celmod = output young's modulus for zircaloy 2 and 4
c    with random texture (pa)
c    ucelmd = output standard error expected in celmod (pa)
c    (not currently returned)
c    ctemp = input cladding temperature (k)
c    fnck = input effective fast fluence (neutrons/(m**2))
c    cwkf = input effective cold work (unitless ratio of areas)
c    deloxy = input average oxygen concentration excluding
c    oxide layer - average oxygen concentration of
c    as-received cladding (kg oxygen/kg zircaloy)
c    the young's modulus calculated by this function is based on
c    data from the following references
c    (1) l. r. bunnell, g. b. mellinger and j. l. bates, high
c    temperature properties of zircaloy - oxygen alloys, epri
c    report np - 524 (1977).
c    (2) e. s. fisher and c. j. renken, physical review 135 2a
c    (20 july 1964) pp a482 - 494.
c    (3) p. e. armstrong and h. l. brown, transactions of the
c    metallurgical society of aime 230 (august 1964)
c    pp 962 - 966
c    (4) a. padel and a. groff, journal of nuclear materials 59
c    (1976) pp 325-326
c    (5) w. r. smalley, saxton core ii fuel performance evaluation.
c    part i: materials, wcap-3385-56 (september 1971)
c    the expected standard error was derived using additional
c    data from the following references
c    (1) c. c. busby and c.r. woods (eds.) "properties of zircaloy-4
c    tubing", usaec report wcapd-tm-585 (december 1966) p 65
c    (2) z. spasic, m. pavlovic and g. simis, conference on

```

```

c the use of zirconium alloys in nuclear reactors, marianske
c lanze, czech. conf-681086 (1968) pp 277 - 284
c (3) r. l. mehan, modulus of elasticity of zircaloy-2 between
c room temperature and 1000 f, kapl-m-rlm-16 (july 1958)
c (4) d. o. northwood, i. m london, and l. e. bahen, journal
c of nuclear materials 55 (1975) pp 299-310
c (5) f. r. shober, j. a. van echo, l. l. marsh jr. and
c j. r. keeler, the mechanical properties of zirconium and
c zircaloy-2, bmi-1168 (1957)
c celmod was coded by r. l. miller in march 1974.
c updated and corrected by b. w. burnham in october 1975
c modified by b. w. burnham october 1977
c modified by d. l. hagrman december 1977
  include 'lacmdl.h'
  data      on      / 1 /,
+          off      / 2 /,
+          locidx   / 5 /
  if (emflag(locidx).eq.on) go to 130
c best estimate model young's modulus
  c1 = (1.16e+11+ctemp*1.037e+08)*5.7015
  c2 = 1.0
  if (fnck.gt.1.0e+22) c2 = 0.88*(1.0-exp(-fnck/1.0e+25))+exp(-fnck/
+1.0e+25)
  c3 = -2.6e+10
  celmod = (1.088e+11-5.475e+07*ctemp+c1*deloxy+c3*cwkf)/c2
  if (ctemp.lt.1090.) go to 140
c calculate a to a + b and a + b to b boundaries
  wfox = deloxy+0.0012
  taab = 1094.+wfox*(-1.289e+03+wfox*7.914e+05)
  if (wfox.lt.0.025) go to 100
  taab = 1556.4+3.8281e+04*(wfox-0.025)
100  tabb = 392.46*((100*deloxy+0.1242807)**2+3.1417)
  if (deloxy.lt.4.7308937e-03) go to 110
  tabb = (100*deloxy+0.12)*491.157+1081.7413
110  continue
  if (ctemp.lt.taab) go to 140
  if (ctemp.gt.tabb) go to 120
  amodl = (1.088e+11-5.475e+07*taab+c1*deloxy+c3*cwkf)/c2
  amodr = 9.21e+10-tabb*4.05e+07
  celmod = amodl+(ctemp-taab)*(amodr-amodl)/(tabb-taab)
  go to 140
120  celmod = 9.21e+10-ctemp*4.05e+07
  go to 140
c em model young's modulus
130  celmod = emclem(ctemp)
140  continue
  if (celmod.lt.1.0) celmod = 1.0
  ucelmd = 6.4e+09
  return
  end

```

FRAPTRAN1.5: CELMOD

```

*deck celmod
c
  function celmod (ctemp, fnck, cwkf, deloxy, icm)
c
  implicit real (a-h,o-z)
c
c This is a MATPRO-11, Rev. 2 routine modified by PNNL for use in FRAPT
c
c celmod calculates cladding young's modulus as a function
c of temperature, fast neutron fluence, cold work, and average
c oxygen concentration. grain orientation is assumed random.

```

```

c      celmod = output young's modulus for zircaloy 2 and 4
c              with random texture (pa)
c      ctemp  = input cladding temperature (k)
c      fnck   = input effective fast fluence (neutrons/(m**2))
c      cwkf   = input effective cold work (unitless ratio of areas)
c      deloxy = input average oxygen concentration excluding
c              oxide layer - average oxygen concentration of
c              as-received cladding (kg oxygen/kg zircaloy)
c
c      the young's modulus calculated by this function is based on
c      data from the following references
c      (1) l. r. bunnell, g. b. mellinger and j. l. bates, high
c          temperature properties of zircaloy - oxygen alloys, epri
c          report np - 524 (1977).
c      (2) e. s. fisher and c. j. renken, physical review 135 2a
c          (20 july 1964) pp a482 - 494.
c      (3) p. e. armstrong and h. l. brown, transactions of the
c          metallurgical society of aime 230 (august 1964)
c          pp 962 - 966
c      (4) a. padel and a. groff, journal of nuclear materials 59
c          (1976) pp 325-326
c      (5) w. r. smalley, saxton core ii fuel performance evaluation.
c          part i: materials, wcap-3385-56 (september 1971)
c
c      the expected standard error was derived using additional
c      data from the following references
c      (1) c. c. busby and c.r. woods (eds.) "properties of zircaloy-4
c          tubing", usaec report wapd-tm-585 (december 1966) p 65
c      (2) z. spasic, m. pavlovic and g. simis, conference on
c          the use of zirconium alloys in nuclear reactors, marianske
c          lanze, czech. conf-681086 (1968) pp 277 - 284
c      (3) r. l. mehan, modulus of elasticity of zircaloy-2 between
c          room temperature and 1000 f, kapl-m-rlm-16 (july 1958)
c      (4) d. o. northwood, i. m london, and l. e. bahen, journal
c          of nuclear materials 55 (1975) pp 299-310
c      (5) f. r. shober, j. a. van echo, l. l. marsh jr. and
c          j. r. keeler, the mechanical properties of zirconium and
c          zircaloy-2, bmi-1168 (1957)
c
c      celmod was coded by r. l. miller in march 1974.
c      updated and corrected by b. w. burnham in october 1975
c      modified by b. w. burnham october 1977
c      modified by d. l. hagrman december 1977
c      Modified by PNNL, January 1997, to clean up coding, delete licensi
c          analysis and sensitivity analysis coding
c
c      go to (400,400,400,400,400,600,400,600,400,400,400)icm
c
c 400 continue
c generic Zry model
c best estimate model young's modulus
c1 = (1.16d+11 + ctemp * 1.037d+08) * 5.7015d0
c2 = 1.0d0
if(fnck .gt. 1.0d+22) c2 = 0.88d0 * (1.0d0 - exp(-fnck/1.0d+25))
&                    + exp(-fnck/1.0d+25)
c3 = -2.6d+10
celmod = (1.088d+11 - 5.475d+07 * ctemp + c1 * deloxy + c3 * cwkf)
&        /c2
if(ctemp .lt. 1090.d0) go to 401
c
c calculate a to a + b and a + b to b boundaries
wfox = deloxy + 0.0012d0
taab = 1094.d0 + wfox * (-1.289d+03 + wfox * 7.914d+05)

```

```

        if (wfox .lt. 0.025d0) go to 415
        taab = 1556.4d0 + 3.8281d+04 * (wfox - 0.025d0)
415 continue
        tabb = 392.46d0 * ((100 * deloxy + 0.1242807d0)**2 + 3.1417d0)
        if (deloxy .lt. 4.7308937d-03) go to 425
        tabb = (100 * deloxy + 0.12d0) * 491.157d0 + 1081.7413d0
425 continue
c
        if (ctemp .lt. taab) go to 401
        if (ctemp .gt. tabb) go to 435
        amodl = (1.088d+11 - 5.475d+07 * taab + c1 * deloxy + c3 * cwkf)
&          /c2
        amodr = 9.21d+10 - tabb * 4.05d+07
        celmod = amodl + (ctemp - taab) * (amodr - amodl)/(tabb - taab)
        go to 401
c
435 continue
        celmod = 9.21d+10 - ctemp * 4.05d+07
c
401 continue
        if(celmod .lt. 1.0d0) celmod = 1.0d0
        return
c
600 continue
c Zr-1%Nb model from RRC-KI
c
c This code block calculates cladding Young's modulus as
c a function of temperature ; data is derived from
c Volkov B.Yu. et.al."Material property library for
c H1-alloy cladding", Preprint IAE-4941/11, 1989.
c Fedorov et.al."Influence of oxygen content and gamma
c -irradiation on the elastic module and internal
c friction pure zirconium" Metal Physics vol.32(3)
c p.621, 1971
c
        if(ctemp .gt. 1073.0d0) go to 601
        celmod = 1.121d11 - 6.438d07*ctemp
        celmod = celmod + 3.021d12*deloxy
        go to 602
601 continue
        celmod = 9.129d10 - 4.5d07*ctemp
602 continue
        if(celmod .lt. 1.0d0) celmod = 1.0d0
        return
c
        end

```

FRAPCON-4.0: CSHEAR

```

*deck cshear
        function cshear (ctemp,fnck,cwkf,deloxy)
c
c cshear calculates the shear modulus of zircaloy-2 and -4
c as a function of temperature, fast neutron fluence,
c cold work, and average oxygen concentration. grain
c orientation is assumed random.
c the expected standard error is computed but not returned
c (ucsher)
c cshear = output shear modulus for zircaloy-2 and -4
c with random texture (pa)
c ucsher = output standard error expected in cshear (pa)
c (not currently returned)
c ctemp = input cladding temperature (k)
c fnck = input effective fast fluence (neutrons/(m**2))

```

```

c   cwkf   = input effective cold work (unitless ratio of areas)
c   deloxy = input average oxygen concentration excluding
c   oxide layer - average oxygen concentration of
c   as-received cladding (kg oxygen/kg zircaloy)
c   the shear modulus calculated by this function is based on
c   data from the following references
c   (1) l. r. bunnell, g. b. mellinger and j. l. bates, high
c   temperature properties of zircaloy - oxygen alloys, epri
c   report np - 524 (1977)
c   (2) e. s. fisher and c. j. renken, physical review 135 2a
c   (20 july 1964) pp a482 - 494.
c   (3) p. e. armstrong and h. l. brown, transactions of the
c   metallurgical society of aime 230 (august 1964)
c   pp 962 - 966
c   (4) a. padel and a. groff, journal of nuclear materials 59
c   (1976) pp 325 - 326.
c   (5) w. r. smalley, saxton core ii fuel performance evaluation.
c   part i: materials, wcap-3385-56 (september 1971)
c   cshear was coded by r. l. miller, june 1974
c   modified by d. l. hagrman december 1977
      c1 = 7.07e+11-ctemp*2.315e+08
      c2 = 1.0
      if (fnck.gt.1.0e+22) c2 = 0.88*(1.0-exp(-fnck/1.0e+25))+exp(-fnck/
+1.0e+25)
      c3 = -.867e+10
      cshear = (4.04e+10-2.168e+07*ctemp+c1*deloxy+c3*cwkf)/c2
      if (ctemp.lt.1090.) go to 130
c   calculate a to a + b and a + b to b boundaries
      wfox = deloxy+0.0012
      taab = 1094.+wfox*(-1.289e+03+wfox*7.914e+05)
      if (wfox.lt.0.025) go to 100
      taab = 1556.4+3.8281e+04*(wfox-0.025)
100   tabb = 392.46*((100*deloxy+0.1242807)**2+3.1417)
      if (deloxy.lt.4.7308937e-03) go to 110
      tabb = (100*deloxy+0.12)*491.157+1081.7413
110   continue
      if (ctemp.lt.taab) go to 130
      if (ctemp.gt.tabb) go to 120
      amodl = (4.04e+10-2.168e+07*taab+c1*deloxy+c3*cwkf)/c2
      amodr = 3.49e+10-tabb*1.66e+07
      cshear = amodl+(ctemp-taab)*(amodr-amodl)/(tabb-taab)
      go to 130
120   cshear = 3.49e+10-ctemp*1.66e+07
130   continue
      if (cshear.lt.1.0) cshear = 1.0
      ucsher = 9.0e+09
      return
      end

```

FRAPTRAN-2.0: CSHEAR

```

*deck cshear
c
      function cshear (ctemp, fnck, cwkf, deloxy, icm)
c
      implicit real (a-h,o-z)
c
c   This is a MATPRO-11, Rev. 1 routine modified by PNNL for use in FRAPT
c
c   cshear calculates the shear modulus of zircaloy-2 and -4
c   as a function of temperature, fast neutron fluence,
c   cold work, and average oxygen concentration. grain
c   orientation is assumed random.
c   cshear = output shear modulus for zircaloy-2 and -4

```



```

c          with random texture (pa)
c      ctemp = input cladding temperature (k)
c      fnck  = input effective fast fluence (neutrons/(m**2))
c      cwkf  = input effective cold work (unitless ratio of areas)
c      deloxy = input average oxygen concentration excluding
c              oxide layer - average oxygen concentration of
c              as-received cladding (kg oxygen/kg zircaloy)
c
c      the shear modulus calculated by this function is based on
c      data from the following references
c
c      (1) l. r. bunnell, g. b. mellinger and j. l. bates, high
c          temperature properties of zircaloy - oxygen alloys, epri
c          report np - 524 (1977)
c      (2) e. s. fisher and c. j. renken, physical review 135 2a
c          (20 july 1964) pp a482 - 494.
c      (3) p. e. armstrong and h. l. brown, transactions of the
c          metallurgical society of aime 230 (august 1964)
c          pp 962 - 966
c      (4) a. padel and a. groff, journal of nuclear materials 59
c          (1976) pp 325 - 326.
c      (5) w. r. smalley, saxton core ii fuel performance evaluation.
c          part i: materials, wcap-3385-56 (september 1971)
c
c      cshear was coded by r. l. miller, june 1974
c      modified by d. l. hagrman december 1977
c      Modified by PNNL, January 1997, to clean up coding and delete
c          sensitivity uncertainty analysis coding
c
c      go to (400,400,400,400,400,600,400,600,400,400)icm
c
400 continue
c generic Zry properties
c      c1 = 7.07d+11 - ctemp * 2.315d+08
c      c2 = 1.0d0
c      if(fnck .gt. 1.0d+22) c2 = 0.88d0 * (1.0d0 - exp(-fnck/1.0d+25))
c      &
c          + exp(-fnck/1.0d+25)
c      c3 = -0.867d+10
c      cshear = (4.04d+10 - 2.168d+07 * ctemp + c1 * deloxy + c3*cwkf)/c2
c      if(ctemp .lt. 1090.d0) go to 401
c
c      calculate a to a + b and a + b to b boundaries
c      wfox = deloxy + 0.0012d0
c      taab = 1094.d0 + wfox * (-1.289d+03 + wfox * 7.914d+05)
c      if(wfox .lt. 0.025d0) go to 415
c      taab = 1556.4d0 + 3.8281d+04 * (wfox - 0.025d0)
415 continue
c      tabb = 392.46d0 * ((100 * deloxy + 0.1242807d0)**2 + 3.1417d0)
c      if(deloxy .lt. 4.7308937d-03) go to 425
c      tabb = (100 * deloxy + 0.12d0) * 491.157d0 + 1081.7413d0
425 continue
c
c      if(ctemp .lt. taab) go to 401
c      if(ctemp .gt. tabb) go to 435
c      amodl = (4.04d+10 - 2.168d+07 * taab + c1 * deloxy + c3*cwkf)/c2
c      amodr = 3.49d+10 - tabb * 1.66d+07
c      cshear = amodl + (ctemp - taab) * (amodr - amodl)/(tabb - taab)
c      go to 401
435 continue
c      cshear = 3.49d+10 - ctemp * 1.66d+07
401 continue
c      if(cshear .lt. 1.0d0) cshear = 1.0d0
c      return

```

```

c
c 600 continue
c Zr-1%Nb from RRC-KI
c
c This code block calculates cladding young's modulus and
c poisson's ratio as a function of temperature ; data is
c derived from Volkov B.Yu. et.al."Material property library
c for H1-alloy cladding", Preprint IAE-4941/11, 1989.
c
c elastic modulus
c ey = celmod (ctemp, fnck, cwkf, deloxy, CladType)
c
c poisson's ratio:
c xnu = 0.42628d0 - 5.556d-5*ctemp
c
c shear modulus
c cshear = 0.5d0*ey/(1.d0+xnu)
c if(cshear .lt. 1.0d0) cshear = 1.0d0
c return
c
c end

```

A.2.7 Cladding Axial Growth (CAGROW)

FRAPCON-4.0: CAGROW

```

*deck cagrow
function cagrow (flux,fluenc,icm,dtime)
common /uncert/sigftc, sigftex, sigfgr
& ,sigswell ,sigcreep ,siggro ,sigcor ,sigh2
c
c cagrow calculates axial cladding growth strain increment as a functi
c flux = input fast neutron flux ((neutrons/m**2)/s)
c fluenc = input fast neutron fluence (neutrons/m**2)
c dtime = input time increment at temperature (s)
c icm = input cladding material index:2 - Zircaloy 2
c 4 - Zircaloy 4
c 5 - M5
c 6 - ZIRLO
c 7 - Optimized ZIRLO
c cagrow = output axial cladding growth straini increment (m/m)
c cagrow coded by D. L. Hagrman, August 1975
c revised April, 1995 by D. D. Lanning and K. J. Geelhood
c to conform to EPRI model by D. G. Franklin, "Zircaloy-4
c Cladding Deformation During Power Reactor Irradiation,"
c ASTM STP 754, 1982, pp.235-267.
c f2=fluenc/10000.
c f1=(fluenc-flux*dtime)/10000.
c ax1=2.18e-21*f1**0.845
c ax2=2.18e-21*f2**0.845
c if(icm.eq.5) then
c ax1=7.013e-21*f1**0.81787
c ax2=7.013e-21*f2**0.81787
c elseif(icm.eq.6.or.icm.eq.7) then
c ax1=9.7893e-25*f1**0.98239
c ax2=9.7893e-25*f2**0.98239
c endif
c cagrow = ax2-ax1
c if( icm .lt. 4.0 ) cagrow = cagrow * 0.5
c
c add on uncertainty
c PWR cladding
c Zircaloy-4

```

```

        if(siggro.gt.0.0.and.icm.eq.4)
&cagrow = cagrow*(1.0+siggro*0.223)
        if(siggro.lt.0.0.and.icm.eq.4)
&cagrow = cagrow/(1.0-siggro*0.223)
c      M5
        if(siggro.gt.0.0.and.icm.eq.5)
&cagrow = cagrow*(1.0+siggro*0.186)
        if(siggro.lt.0.0.and.icm.eq.5)
&cagrow = cagrow/(1.0-siggro*0.186)
c      ZIRLO and Optimized ZIRLO
        if(icm.ge.6)
&cagrow = max(0.0,cagrow+siggro*0.0005)
c      BWR cladding
        if(siggro.gt.0.0.and.icm.lt.4)
&cagrow = cagrow*(1.0+siggro*0.203)
        if(siggro.lt.0.0.and.icm.lt.4)
&cagrow = cagrow/(1.0-siggro*0.203)
        return
        end

```

A.2.8 Cladding Creep Rate (CREPR)

FRAPCON-4.0: CREPR

```

*deck crepr
c
      subroutine crepr(sig,edot,phi,fluence,cldwks,CladAveTemp
&,GapPress,CoolantPress,rci,rco, ProblemTime)
c
      common /cladtype/ icm
      common /uncert/sigftc, sigftex, sigfgr
&,sigswell,sigcreep,siggro,sigcor,sigh2
c      implicit real*8 (a-h,o-z)
c      *****
c      crepr is called from cladf.
c      crepr computes (transverse) cladding creep strain rate
c      as a function of effective stress,temperature, fast
c      neutron flux and accumulated total creep strain
c      *****
c      input arguments
c      *****
c      CreepStrain - total accumulated creep strain (dimensionless)
c      phi - flux (neutrons/m**2/sec)
c      ProblemTime - time to end of power step (hr)
c      CladAveTemp - cladding average temperature (F)
c      sig - cladding hoop stress per node (psi)
c      *****
c      output arguments
c      *****
c      edot - creep strain rate (1/hr)
c      *****
c
c      NEW MODEL
c      New model uses a modified version of the Limback and Andersson equation
c      ASTM STP 1295 pp. 448-468
c      calculate stress in each direction
      sr=(GapPress*rci**2-CoolantPress*rco**2
&+rci**2*rco**2*(CoolantPress-GapPress)/((rco+rci)/2.0)**2)
&/(rco**2-rci**2)
      st=(GapPress*rci**2-CoolantPress*rco**2
&-rci**2*rco**2*(CoolantPress-GapPress)/((rco+rci)/2.0)**2)
&/(rco**2-rci**2)

```

```

    sl=(GapPress*rci**2-CoolantPress*rco**2)/(rco**2-rci**2)
c   sag is effective stress in MPa
c
c   sag = sig*6894.7573/1.0E6
    sag=0.707*sqrt((sl-st)**2+(st-sr)**2+(sr-sl)**2)*6894.7573/1.0E6
    tcak = (CladAveTemp+459.67)/1.8
    fluenceLimback = fluence/10000.0
c
c   Thermal Creep Rate
c
    A = 1.08E9
    if(cldwks.eq.0.0.or.icm.eq.5) A = 5.47E8
    an = 2.0
    if(cldwks.eq.0.0.or.icm.eq.5) an = 3.5
    E = 1.148E5 - 59.9*tcak
    Q = 201000.0
    R = 8.314
    ai = 650.0*(1.0-0.56*(1.0-exp(-1.4e-27*fluenceLimback**1.3)))
    edottherm = A*(E/tcak)*(sinh(ai*abs(sag)/E))**an*exp(-Q/(R*tcak))
c
c   Irradiation Creep Rate
c
    c0SR = 4.0985E-24
    c0RXA = 1.87473E-24
    c0 = C0SR
    if(cldwks.eq.0.0) c0 = c0RXA
    c1 = 0.85
    c2 = 1.0
    tmod=tcak
    if(tcak.lt.570.0) tmod=570.0
    if(tcak.gt.625.0) tmod=625.0
    ctemp=-7.0237+0.0136*tmod
    if(cldwks.eq.0.0) ctemp=-3.18562+0.00699132*tmod
    edotirr = c0*phi**c1*(abs(sag))**c2*ctemp
c
c   Primary Creep Rate
c
    if(ProblemTime.ge.0.1) then
    esat=0.0216*(edottherm+edotirr)**0.109*
&(2.0-tanh(3.55e4*(edottherm+edotirr)))**-2.05
    edotprimary=
&0.5*esat*52.0*(edottherm+edotirr)**0.5/((ProblemTime)**0.5)*
&exp(-52.0*(edottherm+edotirr)**0.5*(ProblemTime)**0.5)
    edottherm=edottherm+edotprimary
    endif
c
    edot = edottherm + edotirr
    edot = edot*1.1547
    if(icm.eq.6) edot = edot*0.8
100 continue
c   add on uncertainty
c   SRA cladding
    if(sigcreep.gt.0.0.and.cldwks.ne.0.0)
&edot = edot*(1.0+sigcreep*0.145)
    if(sigcreep.lt.0.0.and.cldwks.ne.0.0)
&edot = edot/(1.0-sigcreep*0.145)
c   RXA cladding
    if(sigcreep.gt.0.0.and.cldwks.eq.0.0)
&edot = edot*(1.0+sigcreep*0.216)
    if(sigcreep.lt.0.0.and.cldwks.eq.0.0)
&edot = edot/(1.0-sigcreep*0.216)
    return
end

```

A.2.9 Cladding Meyer Hardness (CMHARD)

FRAPCON-4.0: CMHARD

```
*deck cmhard
      function cmhard (ctemp)
c
c   the routine cmhard calculates meyer hardness as a function of
c   cladding temperature.
c   cmhard = output meyer hardness of zircaloy cladding (n/m**2)
c   ctemp = input cladding temperature (k)
c   the equations used in this function are based on data from
c   (1) a. m. ross and r. l. stoute, heat transfer coefficient
c   between uo2 and zircaloy - 2, aecl - 1552 (june 1962)
c   (2) i. d. peggs and d. p. godin, the yield strength - hot
c   hardness relationship of zircaloy - 4, journal of nuclear
c   materials 57 pp 246 - 248 (1975)
c   cmhard was coded by v.f.baston in may 1974.
c   modified by m. a. morgan june 1978
      t = ctemp
      cmhard = exp(2.6034e01-2.6394e-02*t+4.3502e-05*t**2-2.5621e-08*t**
+3)
      return
      end
```

FRAPTRAN-2.0: CMHARD

```
*deck cmhard
      function cmhard (ctemp, icm)
      implicit real (a-h,o-z)
c
c   This is a MATPRO-11, Rev. 2 routine modified by PNNL for use in FRAPT
c
c   the routine cmhard calculates meyer hardness as a function of
c   cladding temperature.
c
c   cmhard = output meyer hardness of zircaloy cladding (n/m**2)
c
c   ctemp = input cladding temperature (k)
c
c   the equations used in this function are based on data from
c   (1) a. m. ross and r. l. stoute, heat transfer coefficient
c   between uo2 and zircaloy - 2, aecl - 1552 (june 1962)
c   (2) i. d. peggs and d. p. godin, the yield strength - hot
c   hardness relationship of zircaloy - 4, journal of nuclear
c   materials 57 pp 246 - 248 (1975)
c
c   cmhard was coded by v.f.baston in may 1974.
c   modified by m. a. morgan june 1978
c   Modified by PNNL, January 1997, to clean up coding, delete sensiti
c   uncertainty coding
c
c   go to (400,400,400,400,400,600,400,600,400,400)icm
c
400 continue
c   generic Zry property
      cmhard = exp(2.6034d+01 - 2.6394d-02*ctemp + 4.3502d-05*ctemp**2
&
- 2.5621d-08*ctemp**3)
      if (cmhard .lt. 1.94d+08) cmhard = 1.94d+08
      return
c
600 continue
c   Zr-1%Nb from RRC-KI
      if(ctemp .lt. 800.d0) cmhard=1.d6*(2172.1d0 - 10.7055d0*ctemp
```

```

& + 0.02765d0*ctemp**2 - 3.278d-5*ctemp**3 + 1.423d-8*ctemp**4)
  if(ctemp .ge. 800.d0) cmhard=exp(26.034d0 - 2.6394d-2*ctemp
& + 4.3502d-5*ctemp**2 - 2.5621d-8*ctemp**3)
  if (cmhard .lt. 1.0d+05) cmhard = 1.0d+05
c
end

```

A.3 Gas Material Properties

A.3.1 Gas Thermal Conductivity (GTHCON)

FRAPCON-4.0

```

*deck gthcon
  function gthcon (gmix,gtemp,gpres,gpthk)
c
c  gthcon calculates gas thermal conductivity as a function of
c  temperature and gas fraction for seven gases:
c  gthcon = output gas thermal conductivity (w/m-k).
c  gmix(i) = input mole fractions of the gas mixture
c  the seven elements of gmix must sum to 1.0
c  constituent gas number key
c  1 helium
c  2 argon
c  3 krypton
c  4 xenon
c  5 hydrogen
c  6 nitrogen
c  7 water vapor
c  gtemp = input gas temperature (k)
c  gpres = input gas pressure (pa)
c  used for knudsen domain correction and for steam
c  not used if 0.
c  gpthk = input effective gap thickness for knudsen domain (m)
c  (maximum of gap dimension or surface roughness)
c  not used if 0.
c  formula for gas mixtures is from r.s.brokaw, report nasa tr r-81
c  (1960). conductivity of rare gases is based on j.m.gandhi and
c  s.c.saxena, jour. chem. and eng. data, vol.13, no.3 (1968)
c  also: wisconsin electric power co., docket no. 50-301 (jan 1973)
c  the accommodation factor is from r.a.dean, cvna-127 (1962)
c  steam equation is from meyer, et.al., "thermodynamic and
c  transport properties of steam", the american society of
c  mechanical engineers (1967)
c  gthcon coded by r.c.young march 1975
c  adapted from routine cmix by p.e.macdonald
  include 'lacmdl.h'
  dimension gmix(7), a(7), c(7), r(7), aa(6), bb(6)
  data a /4.003 , 39.944 ,83.80 ,131.30 , 2.016 ,28.8 ,
+ 18.016 /
c  r = sqrt(a)
  data r /2.00075 , 6.3201 , 9.1542 ,11.4586 , 1.41986 ,
+ 5.3666 , 4.2445 /
c
c  The "aa" and "bb" parameters are from MATPRO-11 Rev. 1, 1981
c  "aa" and "bb" parameters updated by W.G. Luscher 10-17-07
c
  data aa/2.531e-3,4.092e-4,1.966e-4,9.825e-5,1.349e-3,2.984e-4/
  data bb/0.7146, 0.6748, 0.7006, 0.7334, 0.8408, 0.7799/
c
c

```

```

data eps/1.e-9 /
data      on      / 1 /,
+         off     / 2 /,
+         locidx / 16 /
if (emflag(locidx).eq.on) gthcon = emgton(gmix,gtemp,gpres,gpthk)
if (emflag(locidx).eq.on) go to 170
if (gtemp.gt.5555.) go to 100
if (gtemp.gt.0.0000) go to 110
100 write (6,180) gtemp,gmix
stop
110 l = 0
c
do 120 i=1,6
if (gmix(i).le.eps) go to 120
l = i
c(i) = aa(i)*gtemp**bb(i)
120 continue
if (gmix(7).le.eps) go to 140
l = 7
c steam
c c(7) defination updated by W.G. Luscher 10-17-07
tc = gtemp - 273.15d0
if (gtemp.le.973.15d0)
& c(7) = gpres/gtemp*(-2.8516d-08 + 9.424d-10*gtemp
& -6.005d-14*gtemp**2) + 1.009d0*gpres**2/gtemp**2
& / (tc)**4.2d0 + (17.6d-4 + 5.87d-5*(tc)
& + 1.08d-7*(tc)**2 - 4.51d-11*(tc)**3)
if (gtemp.gt.973.15d0)
& c(7) = 4.44d-6*gtemp**1.45d0 + 9.45d0-05*(2.1668d-09*gpres
& /gtemp)**1.3d0
140 if (l.le.0) go to 100
gthcon = 0.
do 160 i=1,l
if (gmix(i).le.eps) go to 160
sum = 0.
do 150 j=1,l
if (j.eq.i) go to 150
if (gmix(j).le.eps) go to 150
rc = c(i)/c(j)
ra = a(i)/a(j)
fij = 1.+2.41*(ra-1.)*(ra-.142)/(1.+ra)**2
gij = (1.+sqrt(rc*r(i)/r(j)))**2/sqrt(8.*(1.+ra))
sum = sum+fij*gij*gmix(j)
150 continue
gthcon = gthcon+c(i)*gmix(i)/(gmix(i)+sum)
160 continue
170 continue
return
180 format ('lgthcon input bad. gtemp=',1pe12.4,' k',/'0fractions',(
+10e12.4))
end

```

FRAPTRAN-2.0

```

*deck gthcon
function gthcon (gmix,gtemp,gpres,gpthk)
implicit real (a-h, o-z)
c
c gthcon calculates gas thermal conductivity as a function of
c temperature and gas fraction for seven gases:
c
c gthcon = output gas thermal conductivity (w/m-K).
c gmix(i) = input mole fractions of the gas mixture
c the seven elements of gmix must sum to 1.0

```

```

c constituent gas number key
c 1 helium
c 2 argon
c 3 krypton
c 4 xenon
c 5 hydrogen
c 6 nitrogen
c 7 water vapor
c
c gtemp = input gas temperature (K)
c gpres = input gas pressure (pa)
c used for knudsen domain correction and for steam
c not used if 0.
c gpthk = input effective gap thickness for knudsen domain (m)
c (maximum of gap dimension or surface roughness)
c not used if 0.
c
c formula for gas mixtures is from r.s.brokaw, report nasa tr r-81
c (1960). conductivity of rare gases is based on j.m.gandhi and
c s.c.saxena, jour. chem. and eng. data, vol.13, no.3 (1968)
c also: wisconsin electric power co., docket no. 50-301 (jan 1973)
c the accommodation factor is from r.a.dean, cvna-127 (1962)
c steam equation is from meyer, et.al., "thermodynamic and
c transport properties of steam", the american society of
c mechanical engineers (1967)
c
c gthcon coded by r.c.young march 1975
c adapted from routine cmix by p.e.macdonald
c
c dimension gmix(7), a(7), c(7), r(7), aa(6), bb(6)
c data a /4.003d0, 39.944d0, 83.80d0, 131.30d0, 2.016d0,
c & 28.02d0, 18.02d0/
c r = sqrt(a)
c data r /2.00075d0, 6.3201d0, 9.1542d0, 11.4586d0, 1.41986d0,
c & 5.3666d0, 4.2445d0 /
c
c The "aa" and "bb" parameters are from MATPRO-11 Rev. 2, 8/1981
c "aa" and "bb" parameters updated by W.G. Luscher 10-17-07
c
c data aa/2.531d-3,4.092d-4,1.966d-4,9.825d-5,1.349d-3,2.984d-4/
c data bb/0.7146d0,0.6748d0,0.7006d0,0.7334d0,0.8408d0,0.7799d0/
c data eps/1.d-9 /
c
c if (gtemp.gt.5555.d0) go to 100
c if (gtemp.gt.0.0000d0) go to 110
100 continue
c write (6,180) gtemp,gmix
c stop
c
110 continue
c l = 0
c
c do 120 i=1,6
c if (gmix(i).le.eps) go to 120
c l = i
c c(i) = aa(i)*gtemp**bb(i)
120 continue
c
c if (gmix(7).le.eps) go to 140
c l = 7
c steam (from MATPRO-11, Rev. 2)
c c(7) definition updated by W.G. Luscher 10-17-07
c tc = gtemp -273.15d0

```



```

      if (gtemp .le. 973.15d0)
&   c(7) = gpres/gtemp*(-2.8516d-08 + 9.424d-10*gtemp
&         - 6.005d-14*gtemp**2) + 1.009d0*gpres**2/gtemp**2
&         /(gtemp-273.15d0)**4.2d0 + (17.6d-4 + 5.87d-5*(tc)
&         + 1.08d-7*(tc)**2 - 4.51d-11*(tc)**3)
      if (gtemp .gt. 973.15d0)
&   c(7) = 4.44d-06*gtemp**1.45d0 + 9.45d-05*(2.1668d-09*gpres
&         /gtemp)**1.3d0
c     c(7) = 17.6e-3+tc*(5.87e-5+tc*(1.04e-7-4.51e-11*tc))
140 continue
      if (1.le.0) go to 100
      gthcon = 0.d0
c
      do 160 i=1,1
      if (gmix(i).le.eps) go to 160
      sum = 0.d0
      do 150 j=1,1
      if (j.eq.i) go to 150
      if (gmix(j).le.eps) go to 150
      rc = c(i)/c(j)
      ra = a(i)/a(j)
      fij = 1.d0+2.41d0*(ra-1.d0)*(ra-.142d0)/(1.d0+ra)**2
      gij = (1.d0+sqrt(rc*r(i)/r(j)))**2/sqrt(8.d0*(1.d0+ra))
      sum = sum+fij*gij*gmix(j)
150 continue
      gthcon = gthcon+c(i)*gmix(i)/(gmix(i)+sum)
160 continue
c
      return
c
180 format ('gthcon input bad. gtemp= ',1pe12.4,' K','/' fractions',
&         (10e12.4))
      end

```



Pacific Northwest
NATIONAL LABORATORY

*Proudly Operated by **Battelle** Since 1965*

902 Battelle Boulevard
P.O. Box 999
Richland, WA 99352
1-888-375-PNNL (7665)

U.S. DEPARTMENT OF
ENERGY

www.pnnl.gov